PREDICTING ERODIBILITY OF COHESIVE STREAMBEDS AND STREAMBANKS DUE TO FLUVIAL AND SEEPAGE FORCES

By

ABDUL-SAHIB TAUFEEQ AL-MADHHACHI

Bachelor of Science in Water Resources Engineering
Baghdad University
Baghdad, Iraq
1996

Master of Science in Water Resources Engineering
Baghdad University
Baghdad, Iraq
1999

Submitted to the Faculty of the
Graduate College of the
Oklahoma State University
in partial fulfillment of
the requirements for
the Degree of
DOCTOR OF PHILOSOPHY
December, 2012

PREDICTING ERODIBILITY OF COHESIVE STREAMBEDS AND STREAMBANKS DUE TO FLUVIAL AND SEEPAGE FORCES

Dissertation Approved:

Dr. Avdhesh K. Tyagi

Dissertation Co-Adviser

Dr. Garey A. Fox

Dissertation Co-Adviser

Dr. Rifat Bulut

Dr. Gregory J. Hanson

ACKNOWLEDGEMENTS

The National Science Foundation (under Grant No. 0943491) is gratefully acknowledged for funding this project. The Iraqi Ministry of Higher Education and Scientific Research is also gratefully acknowledged for providing a full scholarship to perform my Ph.D. program at Oklahoma State University. Credit is due to the faculty, staff, and students in both the Civil and Environmental Engineering Department and Biosystems and Agricultural Engineering Department, who were a pleasure to work with. I am especially grateful for my co-advisors, Dr. Avdhesh K. Tyagi and Dr. Garey A. Fox, for their constant mentoring and encouragement. Other Ph.D. committee members included Dr. Gregory J. Hanson, who provided valuable guidance and direction to perform Jet Erosion Tests and flume tests and helped to develop a mechanistic fundamental detachment rate model that is proposed in this study; and Dr. Rifat Bulut, who was an outstanding teacher of the soil mechanic class. I am especially grateful for the Oklahoma State University undergraduate students, Mohammad Rahi and David Criswell, for their assistance to perform the flume experiments. I appreciated many hours of field work with Taber Midgley, Aaron Mittelstet, Dr. Ron Miller, and many others. The staff in the USDA-Hydraulic Lab, in addition to Wayne Kiner and his staff in the BAE Lab were contributory in fabricating, repairing, and maintaining the equipment used in this research.

Several people contributed indirectly to the success of this effort. From an early age my parents instilled in me a deep sense of the importance of education. I am appreciative of my children, Rusel, Daniyah, and Yousif, who could always put a smile on my face after a long week of laboratory research. A special thank you goes to my wife, Resha Al-Ttaee, whose love, encouragement, and support are invaluable to me. Most of all, I thank my God, who daily provides me the successful way, strength, and purpose to do my mission in the best way.

Name: ABDUL-SAHIB TAUFEEQ AL-MADHHACHI

Date of Degree: DECEMBER, 2012

Title of Study: PREDICTING ERODIBILITY OF COHESIVE STREAMBEDS AND STREAMBANKS DUE TO FLUVIAL AND SEEPAGE FORCES

Major Field: CIVIL AND ENVIRONMENTAL ENGINEERING

Abstract: Scientists and engineers need to predict the erosion rate of cohesive soils due to fluvial and seepage forces. However, currently mechanistic approaches are unavailable for incorporating seepage forces into the commonly used excess shear stress model. A more mechanistically based detachment model, the "Wilson Model," is proposed in this research for modeling the erosion rate of soils using the hydraulic analysis of a Jet Erosion Test (JET). Seepage forces were incorporated into a mechanistic fundamental detachment rate model to improve predictions of the erosion rate of cohesive soils. A new miniature version of the JET device ("mini" JET) and flume tests were conducted on two cohesive soils (silty sand and clayey sand) to derive the "Modified Wilson Model" parameters (b_0 and b_1) in order to investigate the influence of seepage on the soil erodibility. The "mini" JETs were also performed on a horizontal experimental setup to mimic a streambank case.

The "mini" JET established equivalent predictions of the soil erodibility to the larger original laboratory JET for the two cohesive soils. The original and "mini' JETs can provide equivalent results to flume experiments for deriving the "Wilson Model" parameters b_0 and b_1 as well as to the excess shear stress parameter, k_d. Seepage forces had a non-uniform influence on the derived parameters (b_0 and b_1) as functions of the hydraulic gradient and dry density. The influence of seepage forces can be predicted using JET techniques by incorporating the known seepage gradients into the "Modified Wilson Model" parameters (b_0 and b_1) from performed JETs without seepage on streambeds and streambanks. The "Wilson Model" and/or "Modified Wilson Model" is advantageous in being a more mechanistic, fundamentally based erosion model as compared to the excess shear stress model; the proposed model can be used in the place of the excess shear stress model with parameters that can be estimated using existing JET techniques; proposed model can be used to predict and account for additional forces or factors such as turbulence, roughness, seepage forces, material soil orientation (i.e. streambed versus streambank), root effects, negative pore water pressure effects, etc.

TABLE OF CONTENTS

Chapter Page

Chapter Page

LIST OF TABLES

Table Page

Table Page

LIST OF FIGURES

Figure Page

Figure Page

Figure Page

Figure Page

CHAPTER I

INTRODUCTION

1.1. A LITRATURE OF REVIEW

Quantifying soil erodibility is an important challenge for many engineers and scientists because erosion is one of the major water resource issues in the world. One indication of the importance of quantifying the erodibility of soil materials is the sheer number of methods that have recently been developed to measure it in the laboratory and the field (Hanson, 1990b; Briaud et al., 2001; Hanson and Cook, 2004; Wan and Fell, 2004; Mazurek, 2010; Marot et al., 2011). Quantifying erodibility of soil materials has implications for predicting the erosion of disturbed and undisturbed landscapes, riparian areas, streambanks and beds, bridge pier and abutment scour, dams, and levees. Many factors influence the soil erodibility, such as texture, structure, unit weight, water content, swell, clay mineralogy, pore water chemistry, etc. Normally the erosion rate of soils is approximated using an excess shear stress model, dependent on the hydraulic boundary shear stress (τ, Pa) and two major soil parameters: the critical shear stress (τ_c, Pa) and the erodibility coefficient (k_d, $cm^3/N\ s$). The τ_c represents the flow condition where stress

is great enough to begin soil detachment, while the k_d is the rate of soil detachment when the boundary shear stress is greater than τ_c (Hanson and Cook, 2004). The erosion rate is typically expressed as (Partheniades, 1965; Hanson, 1990a, 1990b):

$$\varepsilon_r = k_d(\tau - \tau_c)^a \tag{1.1}$$

where ε_r is the erosion rate (cm/s) and a is an empirical exponent usually assumed to be unity (Hanson, 1990a, 1990b; Hanson and Cook, 1997).

Numerous studies have measured τ_c and k_d for soils using different techniques; large flumes (Hanson, 1990a; Hanson and Cook, 2004), small flumes (Briaud et al., 2001), laboratory hole erosion test (Wan and Fell, 2004), a submerged jet (Hanson and Cook, 2004; Mazurek, 2010; Marot et al., 2011). The submerged jet test (JET - Jet Erosion Test) apparatus is one of these methods for measuring these parameters in situ as well as in the laboratory (Hanson, 1990b; Hanson and Cook, 1997; Hanson and Simon, 2001; Hanson et al., 2002a, 2002b; Hanson and Cook, 2004; Wynn and Mostaghimi, 2006; Clark and Wynn, 2007; Hanson and Hunt, 2007; Shugar et al., 2007; Regazzoni, 2008; Wynn et al., 2008; Thoman and Niezgoda, 2008; Simon et al., 2010).

The original JET was first used and developed by Hanson (1990b) to measure soil erodibility in situ. Seven tests were performed for four soil types and the results were calibrated with those measured from flume tests by Hanson (1990a). Hanson (1990b) developed a linear model based on Reynolds number of the jet and the time factor. A jet index was studied in JET device for non –cohesive and cohesive soils and related to the soil erodibility in earthen spillway (Hanson, 1991). The same four soils were tested for a range of jet velocity from 166 to 731 cm/sec. Hanson (1991) developed a relationship between k_d and the jet index for soils. He found that jet index provided a common method to deal with erosion resistance of soils. The analytical

methods for JET were developed by Hanson and Cook (1997) to directly measure τ_c and k_d based on diffusion principles using an Excel spreadsheet.

Hanson and Simon (2001) measured the soil erodibility of streambeds in Midwestern USA. They employed the original JET device to measure τ_c and k_d. About 83 JETs were performed in cohesive streambeds for several streams in South – eastern Nebraska, South-Western Iowa, and the Yalobusha River Basin in North central Mississippi. They observed an inverse relationship between τ_c and k_d:

$$k_d = 0.2\tau_c^{-0.5} \tag{1.2}$$

Hanson and Simon (2001) found that generally soils have high erodibility when critical shear was low and that soils had low erodibility when critical shear was high (Figure 1.1). The erosion rate was measured for all test locations and for different boundary shear stresses (Hanson and Simon, 2001). Hanson (2001) presents the development procedure and analytical methodology for a submerged jet test to study the properties of erosion in cohesive soil materials. Hanson and Cook (2004) presented a description of jet apparatus, step by step testing methodology, and of analytical procedures to measure soil erodibility in situ. They calculated the average erosion rate by using JET results and compared the results with the measured average erosion in the earthen open channel flow tests.

Furthermore, a non – vertical (multi-angle) JET was used by numerous studies to measure k_d for cohesive streambank materials (Hanson et. al., 2002b, Wynn and Mostaghimi, 2006; Clark and Wynn, 2007; Wynn et al., 2008; Simon et al., 2010). Hanson et al. (2002b) provided details, methods, and analysis procedures for measuring soil erodibility in cohesive streambank materials. The schemata of Non-vertical JET apparatus is shown in Figure (1.2). The jet apparatus consisted of the following parts: jet submerged tank, lid, pin, adjustable head tank,

gage point, head tank mast, pressure gage, pump, and hoses. The non- vertical jet test apparatus was developed to perform tests at multiple angles for streambanks including vertical angle.

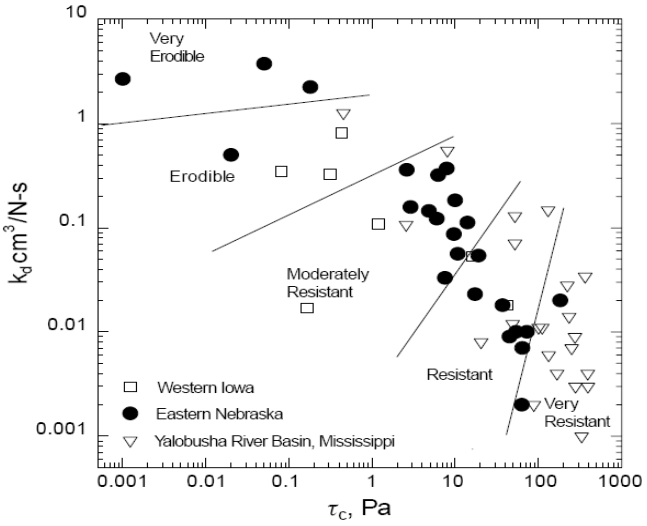

Figure 1.1. The critical shear stress versus the erdibility coefficient for cohesive streambed tests (Hanson and Simon, 2001).

In addition, Shugar et al. (2007) showed the importance of using JET apparatus to measure erosion resistance of Halton Till streambeds in Fletcher's creek. They performed ten JETs in this Till. They plotted τ_c versus k_d and found that their classification ranges from very erodible to moderately resistance for stream beds and banks. They recommended that during testing gravels could be removed at each 2 minutes interval instead of 5 to 10 minutes in soil with large cobbles. Thoman and Niezgoda (2008) found the significant erosion from cohesive channels in the Powder River Basin of Wyoming due to continuous discharge of coal bed natural gas (GBNG). The JET was used in their study to measure τ_c and k_d for 25 test sites in ephemeral, vegetated, cohesive channels of this river. Thoman and Niezgoda (2008) developed a relationship between cohesive soil characteristics and τ_c. They observed an inverse relationship between τ_c and k_d similar to Hanson and Simon (2001). Their results showed that there is a strong relationship between erosion parameters and cohesive soil properties.

Other researchers have focused on the impact of soil parameters on the measured soil erodibility. The influence of water content, soil texture, bulk density, soil compaction, and vegetation effect on measuring soil erodibility were investigated in numerous studies using the JET apparatus (Hanson, 2001; Wynn and Mostaghimi, 2006; Clark and Wynn, 2006; Hanson and Hunt, 2007; Regazzoni et al., 2008; Wynn et al., 2008). Hanson and Robinson (1993) utilized two types of soils (lean clay and silty clay) to measure soil erodibility relative to soil compaction and moisture content in earthen spillways using the JET device. Their results showed that water content, compaction, and density of soil had a considerable impact on the measured τ_c and k_d parameters.

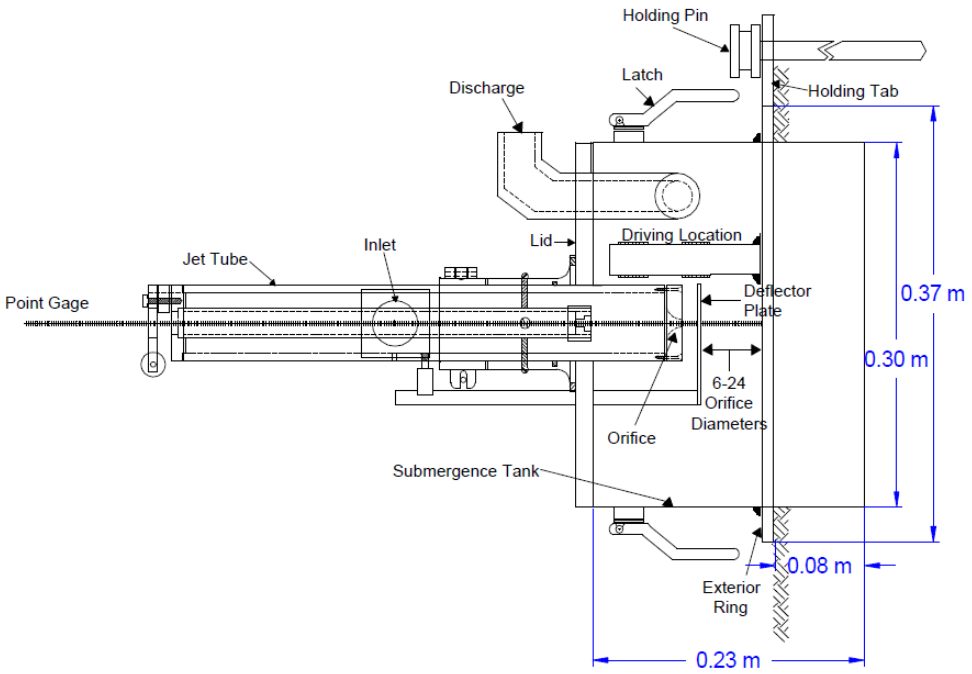

Figure 1.2. Non-vertical JET apparatus schematic (Hanson et. al., 2002b).

Wynn and Mostaghimi (2006) provided the first study on the effect of vegetation on streambank erosion. They examined the effective vegetation, soil physic, freeze/thaw cycle, and chemical properties on streambank erosion in southwest Virginia. The multi-angle JET was used

to measure τ_c and k_d in 25 field sites along streams near Blacksburg Town, southwest Virginia. They tested the lower and upper banks at each site to determine the impact of vegetation on τ_c and k_d. They found that bulk density, soil texture, soil moisture content, and the density of roots have a significant effect on soil erodibility coefficient and critical shear stress, and the measured k_d is decreasing when there is an increase in bulk density or the density of roots.

Additionally, Clark and Wynn (2006) measured τ_c and k_d of fine grained soil streambank materials in situ by using the multi-angle JET and compared the measured data with different empirical equations. They tested the same 25 field sites in southwest Virginia by Wynn and Mostaghimi (2006). The measured data of τ_c were compared with five methods: shield's diagram, soil percent clay, plasticity index, mean particle size, and percent silt-clay while the measured data of k_d were compared with two empirical equations developed by: Hanson and Simon (2001) (equation 1.2) and Osman and Thorne (1988). The erosion rate was determined based on an existing USGS gage stations using the excess shear stress equation and assuming a rectangular cross-section for stream channel. They found that the measured τ_c and k_d are higher than those predicted by empirical equations and suggested that the parameters τ_c and k_d should be measured in situ. Wynn et al. (2008) examined the temporally changes of measuring τ_c and k_d in streambanks due to surface weathering. Six multi-angle JETs were used in six different sites (one per site) to measure soil erodibility from February 2005 to January 2006 in the Stroubles Creek watershed, Blacksburg Town, Virginia. Soil moisture, temperature, bulk density, air temperature, and stream stage were measured in these sites. Their results showed that the measured k_d of streambanks in the winter was more than 2 to 3 times of values in the summer and spring, respectively. They concluded that freeze-thaw cycles, bulk density, and moisture water content have a significant influence for the measuring k_d of streambanks.

A laboratory version of the original JET device (Figure 1.3) was employed to examine the influence of soil compaction on measured k_d by Hanson and Hunt (2007). They utilized a soil sample of 944 cm^3 packed at different compaction water contents with a variety of compaction energies. They found that the resistance of erosion increased (decreased k_d) when soil compaction reached optimum water content and maximum dry density. Regazzoni et al. (2008) also demonstrated the impact of water content and different compaction energies on the measured erosion rate parameters (τ_c and k_d) using the laboratory original JET apparatus. Their results confirmed the previous findings by Hanson and Hunt (2007) that the k_d of clay soil was dependent on the water content at different compaction energies.

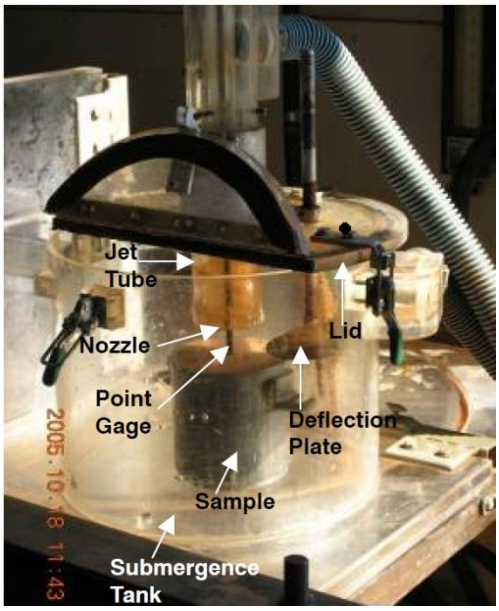

Figure 1.3. A Laboratory original JET apparatus (Hanson and Hunt, 2007).

Several flume studies have been conducted to measure the erosion of cohesive soils in order to verify the use of the original JET (Hanson, 1990a; Hanson and Cook, 1999; Hanson, 2001; Hanson and Cook, 2004). Hanson (1990a) measured soil erodibility in large outdoor

channels with soil material placed throughout the entire length of the channel beds. Six channels were constructed (0.91 m wide and 30.5 m long) with different slopes: 0.5, 1.5, and 3%. Hanson (1990b) empirically related JET index values determined from the three soils to the soil erodibility values determined from the flume studies of Hanson (1990a). Hanson and Cook (1999) performed two open channel flow tests in a large outdoor open channel (1.8 m wide and 29 m long with 2.4 m sidewalls) on compacted samples of lean clay and silty clay. The τ_c and k_d determined from the flume tests verified the use of in-situ and laboratory JET experiments. Hanson (2001) presented the development, procedure, analytical method, and use of JET apparatus to measure cohesive soil erodibility for different soil parameters in channel bed. Hanson (2001) measured τ_c and k_d with different amount of clay soils (lean clay and silty clay) and different soil parameters. He found that water content and density of soil had a major effect on measured τ_c and k_d. A comparison for the results in open channel and JETs was performed as shown in Figure (1.4). This study as well as other studies (Hanson et al. 2002a, Hanson and Cook, 2004, Hanson and Hunt 2007, and Hanson et al., 2011) have verified the use of the original JET to predict the rates of erosion for headcut migration, impinging jet scour, and embankment breach formation and widening.

In addition to the original JET, a new miniature version of the JET device, which is referred to as the "mini" JET, has been recently developed. The "mini" JET device is smaller and lighter than the original JET device and thus can be more easily handled in the field as well as in laboratory. The "mini" JET requires a smaller water supply in the field resulting in less effort transporting the required volume of water compared to the original JET. The "mini" JET device was first used by Simon et al. (2010) in the field, where they performed 279 tests using the "mini" JET to measure τ_c and k_d. They compared the "mini" JET results with the original JET device at 35 sites in the Tualatin River Basin, Oregon. They observed good agreement in measured values of τ_c, but observed differences in k_d and the τ_c - k_d relationships between the two JET devices.

Simon et al. (2010) hypothesized that these differences may be due to differences in the size of both submergence cans for these JET devices. These tests were conducted in-situ at side by side locations, but results may have been influenced by in situ heterogeneity and possible differences in methodology and set-up.

Silty Clay Soil

Lean Clay Soil

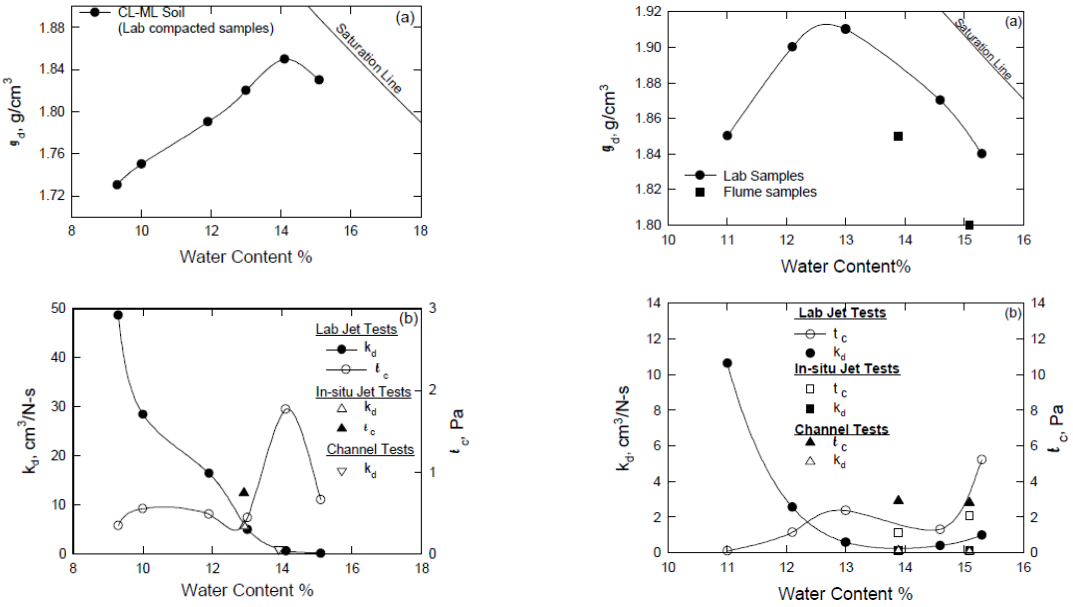

Figure 1.4. (a) Water content versus dry unit weight relationship and (b) Water content versus k_d and τ_c relationship for tested material (Hanson, 2001).

When quantifying fluvial erosion rates, the interaction between the fluvial forces and adjacent near-surface groundwater forces are generally neglected (Fox and Wilson, 2010). Recent studies have demonstrated the importance of ground water seepage on erosion and bank or hillslope failure (Fox et al., 2007; Wilson et al., 2007; Fox and Wilson, 2010). Several studies have investigated erosion specifically due to seepage, including the development of empirical sediment transport models for this process (Owoputi and Stolte, 2001; Rockwell, 2002; Lobkovsky et. al., 2004; Fox et. al., 2006a; Fox et. al., 2007; Wilson et. al., 2007; Chu-Agor et. al., 2008; Chu-Agor et. al., 2009; Midgley et al., 2012a). Owoputi and Stolte (2001) employed a

laboratory experiment to examine the role of seepage in the cohesionless soil under the effect of rainfall. Their results showed that seepage alone has little effect on erosion rates but erosion is increased by rainfall when seepage is present. Rockwell (2002) conducted soil erosion laboratory flume tests to examine the influence of ground water on processes of surface flow erosion during a rainstorm. He found that ground water influenced erosion processes originally by increasing unsaturated pore water pressures and reducing soil shear strength in surface rainflow.

Lobkovsky et al. (2004) presented a quantitative analysis of three modes of sediment mobilization: surface erosion, fluidization, and slumping in a non-cohesive soil. They studied the onset of erosion with shear stresses created by surface and subsurface flow. They derived a critical slope equation with the rationale that slopes greater than the critical were unstable to erosion with seepage. Fox et al. (2006a) developed an empirical sediment transport model for seepage erosion of non-cohesive streambank materials. They performed two-dimensional soil lysimeter experiments with three different soil layers to simulate seepage erosion occurring at Little Topashaw Creek, Northern Mississippi. Their model depended on a dimensionless sediment discharge and dimensional seepage flow shear stress. Fox et al. (2007) reported relationships between erosion rate and seepage discharge mimicking excess stress formulations from field measurements of seepage erosion at Goodwin Creek. Chu-Agor et al. (2008) investigated the underlying mechanisms of hillslope instability by seepage in three-dimensional laboratory soil blocks. Chu-Agor et al. (2009) developed a methodology for simulating seepage erosion undercutting in streambanks through an empirical sediment transport function based on an excess gradient for cohesive soils. The intricate linkage between seepage and fluvial forces has recently been emphasized in field seepage experiments (Midgley et al., 2012a).

In addition to the excess shear stress model, several other models have been proposed to predict the erosion rate of cohesive soils including numerous models based on excess shear stress formulations, some of which include the bulk density of beds (Parchure and Mehta, 1985;

Sanford and Maa, 2001), and turbulent burst erosion models (Cleaver and Yates, 1973; Nearing, 1991; Sharif and Atkinson, 2012). Turbulent burst erosion models have been developed for cohesive beds based on the average area of the turbulent burst acting on the bed, the mass of sediment eroded, probability distributions of fluid forces and resistive forces, and a turbulent burst time period. Cleaver and Yates (1973) and Nearing (1991) applied a turbulent burst erosion model to the detachment of aggregates from the surface of a bed. Sharif and Atkinson (2012) developed an aggregate size distribution relationship as function of the bed bulk density and the concept of self-similar growth of aggregates in the turbulent burst erosion model.

Even though the excess shear stress and turbulent burst erosion models provide a method of characterizing the erodibility of soil materials and predicting erosion rates, the disadvantage of these models are the lack of mechanistic predictions of its parameters for specific soil and hydraulic conditions such as when considering multiple forces (such as fluvial and seepage). A more fundamentally based detachment model using the mechanics of particle and/or aggregate motion would be preferred for modeling the range of environmental conditions experienced during fluvial erosion. For example, recent research on seepage processes on hillslopes and streambanks suggest these forces may be important, even during fluvial erosion, in increasing the erodibility of cohesive soils (Fox and Wilson, 2010; Midgley et al., 2012a). A mechanistic detachment model has the advantage of allowing a more in depth accounting and evaluation of the impact of factors such as turbulence, roughness, seepage forces, material soil orientation (i.e. streambed versus streambank), root effects, negative pore water pressure effects, etc.

Wilson (1993a, 1993b) developed a fundamental mechanistic detachment model to provide a general framework for studying soil and fluid characteristics and their impact on cohesive soil erodibility. The model was developed based on a simple two-dimensional representation of particles. However, the detachment model is not restricted to a single particle and can be applied for aggregates. The model was evaluated using erosion rate data for cohesive

soils. The model was calibrated to the observed data based on two dimensional parameters b_0 and b_1. The model represented the observed data as well as or better than the excess shear stress model. However, the parameters can only be derived from observed erosion data from flumes or open channels which limits its applicability at the time of development.

No studies or research until now measured or predicted the erodibility of cohesive soil materials due to fluvial and seepage forces at the same time. This research investigated the prediction of erodibility in cohesive soil materials influenced by seepage forces with respect to fluvial erosion using "mini" JETs and flume tests. A mechanistic fundamental based detachment model was developed to predict the soil erodibility due to fluvial and seepage forces using JET techniques.

1.2. OBJECTIVES

The main objectives of this research were 1) to predict the erodibility of cohesive streambeds and streambanks due to fluvial and seepage forces, and 2) to develop a mechanistic fundamental-based detachment model to predict the soil erodibility due to fluvial and seepage forces using JET techniques.

To achieve the main objectives, this research was divided into several subjectives. A series of laboratory "mini" JET and a laboratory original JETs were performed on two cohesive soils (silty sand and clayey sand) in order to investigate if the "mini" JET could be used to provide equivalent soil erodibility in comparison to the original JET as proposed in **Chapter II**. The development methods of analysis of the JET to determine the "Wilson Model" parameters (b_0 and b_1), in a fashion similar to the methodology developed by Wilson (1993a, 1993b) for open channel flow, and a comparison of the excess shear stress model parameter k_d and the "Wilson Model" parameters (b_0 and b_1) determined from flume and JETs on the two soils were investigated in **Chapter III**. The development and incorporation of seepage forces into the

fundamental detachment model with the new model referred to as the "Modified Wilson Model" and the prediction of the influence of seepage gradient forces on the model parameters (b_0 and b_1) from flume tests and "mini" JETs on the two cohesive soils were investigated in **Chapters IV** and **V**. A modification to the "Modified Wilson Model" parameters (b_0 and b_1) to predict the influence of seepage on the erodibility of cohesive streambanks of the two soils from laboratory experiments and filed data using "mini" JETs was investigated in **Chapter VI**.

CHAPTER II

MEASURING SOIL ERODIBILITY USING A LABORATORY "MINI" JET[1]

2.1. ABSTRACT

Typically soil erodibility is quantified using an excess shear stress equation, dependent on two major soil parameters: the critical shear stress (τ_c) and the erodibility coefficient (k_d). A submerged jet test (JET – Jet Erosion Test) is one method that has been developed and methodology of use established in the literature for measuring these parameters. In this study, a new miniature version of the JET device ("mini" JET), with the advantage of being easier to use in the field, was used to measure τ_c and k_d for two soils (silty sand and clayey sand) and results were compared to the larger original laboratory JET. The objective of this research was to determine if the "mini" JET measured equivalent values for τ_c and k_d compared to the original JET device. In-order to compare the performance and repeatability of both JET devices, tests were performed on paired samples prepared in the same way and tested at the same time. Samples of the soils tested were prepared at different water contents with a standard compaction

[1] In review in *Transactions of the ASABE*
Al-Madhhachi, A.T., G.J. Hanson, G.A. Fox, A.K. Tyagi, and R. Bulut. 2012a. Measuring erodibility of cohesive soils using laboratory "mini" JET. T. ASABE.

effort of 600 kN-m/m^3 (ASTM). Some variability in measuring τ_c and k_d was observed between paired samples due to variability in the soil texture of the soil samples and differences in soil moisture levels. The k_d values measured by the two JET devices for both soils were not significantly different. The τ_c values measured by the "mini" JET were consistently lower than those measured by the original JET. This was hypothesized to be due to the structure of the soil sample due to the compaction method and the procedure utilized to determine τ_c. Adjustment of the equilibrium depth of the "mini" JET resulted in small differences in the estimated τ_c between both JET devices. Both JET devices also demonstrated consistent performance in measuring τ_c - k_d relationships, which were compared with those observed in previous field research.

2.2. INTRODUCTION

Quantifying soil erodibility is an important challenge for many engineers and scientists because erosion is one of the major water resources issues in the world. One indication of the importance of quantifying the erodibility of soil materials is the sheer number of methods that have recently been developed to measure it in the laboratory and the field (Hanson, 1990b; Briaud et al., 2001; Hanson and Cook, 2004; Wan and Fell, 2004; Mazurek, 2010; Marot et al., 2011). Quantifying erodibility of soil materials has implications for predicting the erosion of disturbed and undisturbed landscapes, riparian areas, streambanks and beds, bridge pier and abutment scour, dams, and levees. Many factors influence the soil erodibility, such as texture, structure, unit weight, water content, swell, clay mineralogy, pore water chemistry, etc. Normally the erosion rate of soils is approximated using an excess shear stress equation, dependent on the hydraulic boundary shear stress (τ, Pa) and two major soil parameters: the critical shear stress (τ_c, Pa) and the erodibility coefficient (k_d, m^3/N s). The τ_c represents the flow condition where stress is great enough to begin soil detachment, while the k_d is the rate of soil detachment when the

boundary shear stress is greater than τ_c (Hanson and Cook, 2004). The erosion rate is typically expressed as (Partheniades, 1965; Hanson, 1990a, 1990b):

$$\varepsilon_r = k_d(\tau - \tau_c)^a \tag{2.1}$$

where ε_r is the erosion rate (m/s) and a is an empirical exponent usually assumed to be unity (Hanson, 1990a, 1990b; Hanson and Cook, 1997).

Numerous studies have measured τ_c and k_d for soils using different techniques; large flumes (Hanson, 1990a; Hanson and Cook, 2004), small flumes (Briaud et al., 2001), laboratory hole erosion test (Wan and Fell, 2004), and a submerged jet (Hanson and Cook, 2004; Mazurek, 2010; Marot et al., 2011). The submerged jet test (JET - Jet Erosion Test) apparatus is one method for measuring these parameters in situ as well as in the laboratory (Hanson, 1990b; Hanson and Cook, 1997; Hanson and Simon, 2001; Hanson et al., 2002a, 2002b; Hanson and Cook, 2004; Hanson and Hunt, 2007) and is the focus of the study reported in this chapter.

A description of JET, step by step testing methodology, and development of analytical procedure were presented in numerous studies (Hanson and Cook, 1997; Hanson and Simon, 2001; Hanson et al., 2002a; Hanson and Cook, 2004). Hanson (1990b) performed seven tests on four types of soils using the JET device and the results were calibrated with those measured in a large open channel in another study by Hanson (1990a). Hanson and Cook (1997) and Hanson et al. (2002a) developed the analytical methods to directly measure τ_c and k_d based on diffusion principles using an Excel spreadsheet. Hanson and Simon (2001) measured the soil erodibility of streambeds in the Midwestern United States. They employed the JET apparatus to measure τ_c and k_d and observed an inverse relationship between the two parameters.

Other research has focused on the impact of soil parameters, such as the influence of water content, soil texture, bulk density, and soil compaction, on measuring soil erodibility using

the JET apparatus (Hanson and Robinson, 1993; Hanson and Hunt, 2007; Regazzoni et al., 2008). Hanson and Robinson (1993) utilized two types of soils (lean clay and silty clay) to measure soil erodibility relative to soil compaction and moisture content in earthen spillways using the JET device. Their results showed that water content, compaction, and density of soil had a considerable effect on the measured τ_c and k_d parameters. A laboratory version of the JET device (referred to as an original JET in this study) was employed to examine the influence of soil compaction on measured k_d by Hanson and Hunt (2007). They utilized a soil sample of 944 cm^3 packed at different compaction water contents with a variety of compaction energies. They found that the resistance of erosion increased (decreased k_d) when soil compaction reached optimum water content and maximum dry density. Regazzoni et al. (2008) also demonstrated the impact of water content and different compaction energies on the measured erosion rate parameters (τ_c and k_d) using the laboratory original JET apparatus. Their results confirmed the previous findings by Hanson and Hunt (2007) that the k_d of clay soil was dependent on the water content at different compaction energies.

A new miniature version of the JET device, which is referred to as the "mini" JET, has been developed. The "mini" JET device is smaller and lighter than the original JET device and thus can be more easily handled in the field as well as in laboratory. The "mini" JET requires a smaller water supply in field resulting in less effort transporting the required volume of water compared to the original JET. The "mini" JET device was first used by Simon et al. (2010) in the field, where they performed 279 tests using the "mini" JET to measure τ_c and k_d. They compared the "mini" JET results with the original JET device at 35 sites in the Tualatin River Basin, Oregon. They observed good agreement in measured values of τ_c, but observed differences in k_d and the τ_c -k_d relationships between the two JET devices. Simon et al. (2010) hypothesized that these differences may be due to differences in the size of both submergence cans for these JET

devices. These tests were conducted in-situ at side by side locations, but results may have been influenced by in situ heterogeneity and possible differences in methodology and set-up.

The objective of this research was to determine if the "mini" JET device established equivalent values for τ_c and k_d compared to the original JET device under controlled laboratory conditions without the influence of heterogeneity. The laboratory submerged jet test device, which was used by Hanson and Hunt (2007), was used as the original JET device in this study. Two types of soils were employed in this study: silty sand and clayey sand. The τ_c-k_d relationships were derived and compared with previous study for both JET devices.

2.3. MATERIALS AND METHODS

2.3.1. Laboratory JET Devices

2.3.1.1 Original JET device

The original JET device used in this study was the same as that used by Hanson and Hunt (2007). This laboratory JET apparatus consists of the following parts: jet tube, adjustable head tank, point gage, nozzle, deflection plate (deflector), jet submergence tank, lid, and hoses as shown in Figure (2.1a). The jet tube had a 50 mm inner diameter with 6.4 mm wall thickness and an 89 mm diameter orifice plate with a nozzle at the center of this plate. The nozzle was 6.4 mm in diameter. The adjustable head tank was 910 mm in height with a 50 mm inner diameter and was utilized to provide a desired water head upstream of the nozzle. Scour readings were taken using the point gage, which was passed through the jet nozzle and extended to the soil surface. The point gage diameter was equivalent to the jet nozzle diameter; therefore, the water jet was shut off during scour readings. The deflection plate (deflector) was used to prevent the water jet from impinging on the soil sample at the beginning of the test and at each scour reading. During the first filling of the jet tube, the air relief valve was used to remove air from the jet tube.

(a) Original JET Device

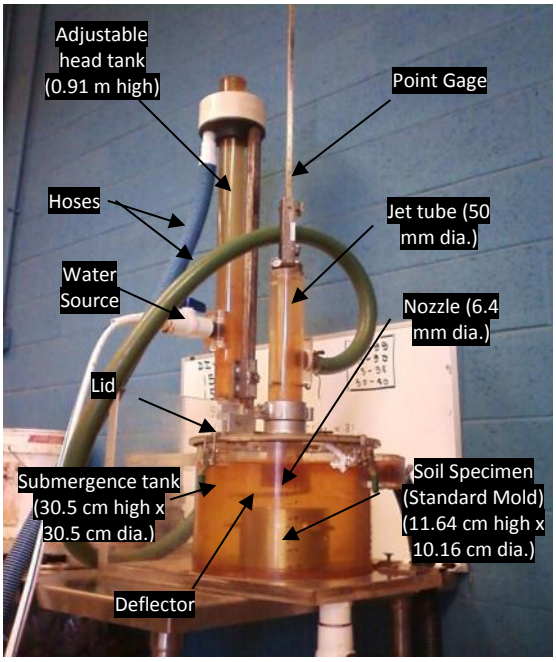

(b) "Mini" JET Device

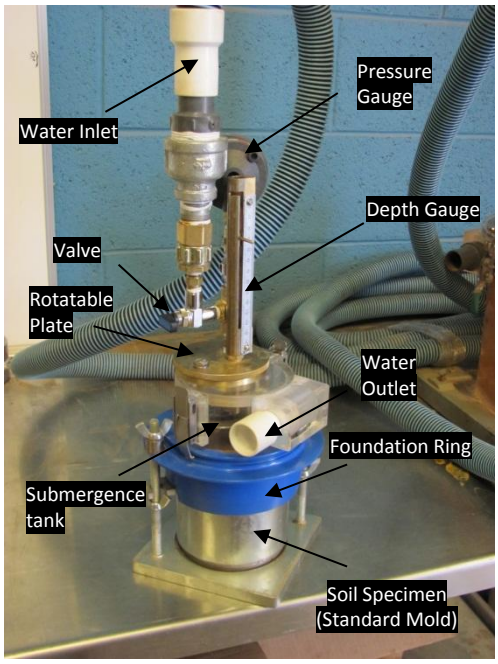

(c) Rotatable Plate of the "Mini" JET Device

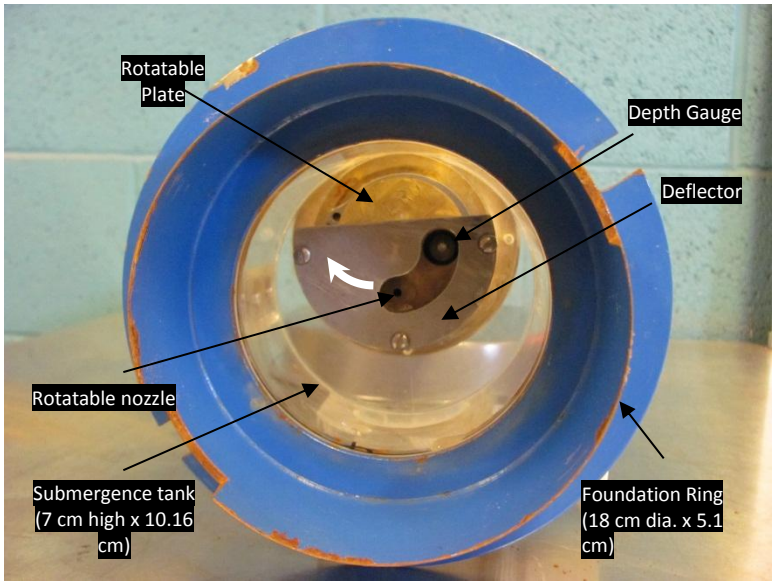

Figure 2.1. Laboratory JET devices.

The jet submergence tank was 305 mm in height and 305 mm in diameter with a 6.4 mm wall thickness. The submergence tank opened from the top with the jet tube and attached lid (Hanson and Hunt, 2007).

2.3.1.2 “Mini” JET device

The “mini” JET apparatus (Figure 2.1b) consists of the following parts: pressure gauge, outlet and inlet water, depth gauge, rotatable plate (depth gauge and nozzle), submergence tank, foundation ring, valve, and hoses. The same adjustable head tank, as was used in the original JET device, was used for the “mini” JET to provide the desired water head. The scour readings were taken using the depth gauge, where the depth gauge of the “mini” JET was different from the point gauge of the original JET, but both have the same function of reading the scour depth. The rotatable plate had a 3.18 mm diameter nozzle (Figure 2.1c). This rotatable plate was used to prevent the water from impinging upon the soil sample at the beginning of testing and during scour depth readings at different times during the test runs. The submergence tank was 70 mm in height and 101.6 mm in diameter with a 6.4 mm wall thickness. The submergence tank did not open from the top, and the rotatable plate and depth gauge were attached to the top of the tank. The foundation ring was 180 mm in diameter and was pushed into the soil 51 mm when used in the field.

2.3.2. Analysis Method

The analytical methods for the original JET presented by Hanson and Cook (1997) were based on diffusion principles developed by Stein and Nett (1997). They assumed that the rate of variation in the depth of scour, dJ/dt, was the erosion rate as a function of the maximum stress at the boundary, which was determined by the diameter of the jet nozzle and the distance from jet origin to the initial channel bed (Figure 2.2). Therefore, the erosion rate equation for jet scour is written as (Hanson and Cook, 1997):

$$\frac{dJ}{dt} = k_d\left[\frac{\tau_o J_p{}^2}{J^2} - \tau_c\right], \qquad \text{for } J >= J_p \tag{2.2}$$

where J is the scour depth (cm) and J_p is the potential core length from jet origin (cm). Accordingly, the critical shear stress was assumed to occur when the rate of scour was equal to zero at the equilibrium depth, J_e (Hanson and Cook, 1997; Hanson et al., 2002a):

$$\tau_c = \tau_o\left(\frac{J_p}{J_e}\right)^2 \tag{2.3}$$

where $\tau_o = C_f \rho_w U_o^2$ is the maximum shear stress due to the jet velocity at the nozzle (Pa); C_f = 0.00416 is the coefficient of friction; ρ_w is water density (kg/m^3); $U_o = C\sqrt{2gh}$ is the velocity of jet at the orifice (cm/s); C is discharge coefficient; h is the pressure head (cm); $J_p = C_d\, d_o$; d_o is the nozzle diameter (cm); and C_d = 6.3 is the diffusion constant. Equations (2.2) and (2.3) can be incorporated in a dimensionless form as the following equation (Hanson and Cook, 1997; Hanson et al., 2002a):

$$\frac{dJ^*}{dT^*} = \frac{\left(1 - J^{*2}\right)}{J^{*2}} \tag{2.4}$$

where $J^* = J/J_e$; and $J_p{}^* = J_p/J_e$. Stein and Nett (1997) presented the reference time, T_r, as the following:

$$T_r = \frac{J_e}{k_d \tau_c} \tag{2.5}$$

and the dimensional time (T^*) is given as:

$$T^* = t / T_r \tag{2.6}$$

where t is the time of a data reading or scour depth measurement.

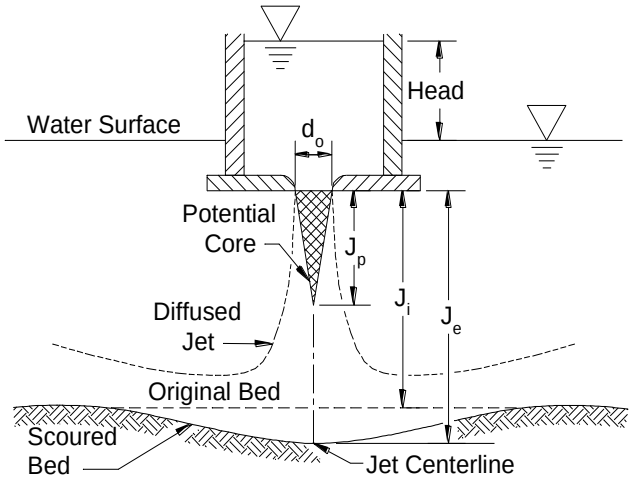

Figure 2.2. Schematic of JET device with factor definitions (Hanson and Cook, 2004).

Equation (2.4) refers to the change in scour depth with time, for time T^*. Integration of equation (2.4) gives the following equation (Hanson and Cook, 1997; Hanson et. al., 2002a):

$$T^* - T_p^* = -J^* + 0.5\ln\left(\frac{1+J^*}{1-J^*}\right) + J_p^* - 0.5\ln\left(\frac{1+J_p^*}{1-J_p^*}\right) \tag{2.7}$$

An Excel spreadsheet and equations (2.3) through (2.7) were used to determine τ_c and k_d. The critical stress, τ_c, was determined from equation (2.3) based on the equilibrium scour depth, J_e. Blaisdell et al. (1981) found that it is difficult to determine the equilibrium scour depth due to very large time to reach J_e. Therefore, the spreadsheet calculated the equilibrium scour depth using the scour depth data versus time and a hyperbolic function for determining the equilibrium scour depth developed by Blaisdell et al. (1981). The general form of this equation is:

$$(f - f_o)^2 - x^2 = A_1^2 \tag{2.8}$$

where A_1 is the value for the semi-transfer and semi-conjugate of the hyperbola; $f = \log(J/d_o) - x$, $x = \log[(U_o\, t)/d_o]$; and $f_o = \log(J_e/d_o)$. From fitting the scour depth data based on plotting f versus x, the coefficients A_1 and f_o can be determined using Microsoft Excel Solver. Then, J_e can be determined ($J_e = d_o\, 10^{fo}$). The spreadsheet was also used to calculate k_d by fitting the curve of

measured data based on equation (2.7). The k_d depends on the measured scour depth, time, pre-estimated τ_c, and the dimensional time function (Hanson et al., 2002b).

The same analytical method used for the original JET device was used for analysis of the "mini" JET apparatus. The only modification was the value of discharge coefficient (*C*). Experiments in this study suggested *C* values for the "mini" JET of 0.70 to 0.75 while the *C* value for original JET was 0.95 to 1.00. The *C* value was the slope of the plotted measured discharge data versus $A\sqrt{2gh}$ based on the following discharge equation for each applied water head, *h*:

$$Q = CA\sqrt{2gh} \tag{2.9}$$

where Q is the measured discharge (measured volume of water to the recorded time), and *A* ($= \frac{\pi}{4} d_o^{\,2}$) is the nozzle area for JET devices.

2.3.3. Soil Characteristics

Two soils were utilized in the laboratory experiments for this study: a silty sand soil and clayey sand soil. The silty sand soil was acquired from streambanks of Cow Creek in Stillwater, Oklahoma. The clayey sand soil was acquired from the USDA Hydraulic Engineering Research Unit in Stillwater, Oklahoma. These soils were tested and analyzed according to ASTM Standards (2006). Sieve analysis and hydrometer tests were conducted according to ASTM Standard D422. Liquid limit and plasticity limit tests were performed according to ASTM Standard D4318. These soils were classified according to the Unified Soil Classification System (USCS) as given in Table (2.1).

Table 2.1. Properties of the two soils for testing the two JET devices.

Soil Location	Soil Texture			Plasticity Index (%)	Standard Compaction		Soil Classification USCS
	Sand (%)	Silt (%)	Clay (%)		Maximum Density (Mg/m^3)	Optimum Water Content (%)	
USDA Hydraulic lab	57	18	25	4	2.00	10.8	SC – Clayey Sand
Streambank of Cow Creek	72	13	15	Non-Plastic	1.83	12.9	SM – Silty Sand

2.3.4. Experimental Procedures

Soil samples were prepared for testing with the original and "mini" JET devices at the same time and in the same manner. The soils were air dried and then passed through the U.S. Sieve No. 4 (4.75 mm). To achieve the desired water content, the soils were mixed with different quantities of water and left for 24 hr in a closed bucket to allow for moisture equilibrium. Then, soil moisture content (ω) of the samples was determined. Soils were compacted at three water contents: dry side of optimum water content, optimum water content, and wet side of optimum water content. The samples were compacted in three different lifts in a standard mold using a manual rammer according to ASTM Standard D698A. The standard mold was 944 cm^3 (101.6 mm in diameter and 116.4 mm in height). The manual rammer was 30.5 cm in height, 50.8 mm in diameter, and 2.49 kg in weight. Soils were compacted with a 600 kN-m/m^3 (25 blows per layer) standard compaction effort. Following the compaction procedure, the top of soil specimen was trimmed and dry density (ρ_d) was determined for each soil sample:

$$\rho_d = \frac{w_s}{V(1+\omega)} \tag{2.10}$$

where w_s was the net weight of soil sample and V was the volume of standard mold. Finally, the soil specimen was placed in the center of the submergence tank directly below the jet nozzle

(Figures 2.1a and 2.1b). The adjustable head tank was then set at the desired constant head (109 cm for all experiments) and hoses (including water source) were connected to the JET devices. The soil samples were tested immediately after they were prepared. Tests were repeated three times for each water content (i.e. nine tests for each soil per device).

For the original JET device, steps for running the jet and collecting data followed Hanson and Hunt (2007). For the "mini" JET device, the following steps were used for running the jet and collecting data (Figure 2.1b). Before turning on the water, the depth gauge was used to determine the height of the jet nozzle by taking the depth gauge readings at the nozzle and the soil specimen surface at time zero. The jet nozzle and depth gauge were part of a rotatable plate. The nozzle was rotated away from impinging on the soil specimen while depth gauge readings were taken (Figure 2.1c). Following depth gauge readings, the jet valve was closed and the water source was opened to fill the head tank, and all air was released from the adjustable head tank. Then, the jet valve was opened to start filling the submergence tank. After the submergence tank was filled with water, an initial reading of water head was acquired from the top of the adjustable head tank to the water surface at the submergence tank. This reading was held constant during the test. The nozzle was then rotated to impinge directly on the soil specimen surface to start the test and the time was recorded. The readings of the scour bed were taken using the depth gauge at different time intervals. Usually, the first reading was acquired after 30 s while subsequent readings were acquired each 5 to 10 minutes for the clayey sand soil with a maximum test period of 120 minutes and each 1 to 5 minutes for the silty sand soil with a maximum test period of 60 minutes.

Mann-Whitney rank sum tests (Mann and Whitney, 1947) were performed to determine statistical differences between the measured dry densities (ρ_d), k_d, and τ_c estimated from the original and "mini" JET devices and for both soils. The median values and the difference between the 25th and 75th percentiles were reported for ρ_d to verify the compaction procedure and for k_d, and τ_c from both devices.

2.4. RESULTS AND DISCUSSION

Thirty six tests were performed using the laboratory JET device (the original JET device) and the "mini" JET device to measure τ_c and k_d for both silty sand and clayey sand soils at three water contents. The unit of k_d was reported in cm^3/N s instead of m^3/N s to be consistent with previous research (Simon et al., 2010). The ratio of the nozzle diameter (d_o) to nozzle height (J_i) for the original JET device and "mini" JET were set equivalent in-order to maintain consistent methodology in the test set-up while measuring τ_c and k_d between the devices (where the J_i / d_o ratio was 10.4 and 10.2 for original and "mini" JET devices, respectively). As an example, "mini" and original JET scour depth reading results for the silty sand soil prepared at a compaction water content of 12% and clayey sand soil prepared at compaction water content of 17% are shown in Figures (2.3a) and (2.3b). As expected, the "mini" JET device provided lower scour readings relative to the original JET device due to size differences. Tested samples for both the "mini" and original JET devices were equivalent in terms of packing based on determining the density of each soil sample at the different water contents (Figures 2.4a and 2.4b).

Even though the clayey sand soil was more resistant than the silty sand soil for the two higher water contents tested, the k_d for clayey sand soil approached that of the silty sand soil at lower water content (Figures 2.4c and 2.4d). Both JET devices provided statistically equivalent values of measured k_d for both soils (Table 2.2). The IQR of measured k_d from the original JET was greater than the IQR when using the "mini" JET especially for clayey sand soil due to scouring all the soil sample of the standard mold when tests were performed at lower water contents for the original JET (Table 2.2). The relationship between measured k_d from both devices followed the 1:1 trend line as shown in Figure (2.5) with a slope of 1.12, intercept of -0.18, and R^2 of 0.81. The fact that the measured k_d was the same between the original and "mini" jets in this study contradicts the findings of Simon et al. (2010) when using the JET devices in the field. Soil heterogeneity and differences in soil moisture content may have likely led to

differences in k_d in the Simon et al. (2010) study.

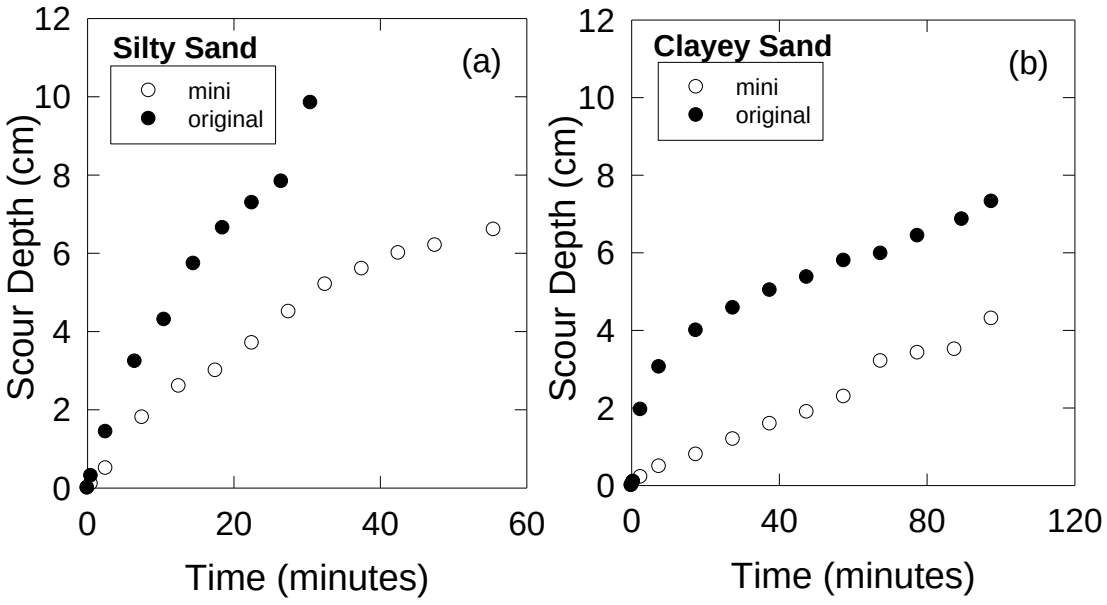

Figure 2.3. Example of Scour depth versus time for original JET versus "mini" JET for a) silty sand tested at a compaction water content of 12% and b) clayey sand tested at a compaction water content of 17%.

Relationships between critical shear stress (τ_c) and water contents (ω) for both JET devices are shown in Figures (2.4e) and (2.4f). Mann-Whitney tests indicated significant differences between the devices for the τ_c (Table 2.2). This was hypothesized to be the result of differences in the scale of jet nozzles (1:2) between the "mini" and original JET devices and the effect of the compaction method on the structure of the soil sample and how it eroded under the impacting jet. The method of compaction involves three layers placed in the compaction mold with 25 blows of the hammer per layer. The compacted sample therefore has a three layered soil structure with a layer interface at approximately 3-4 cm and 6-8 cm. During JET testing this layering becomes apparent in the measured scour versus time as can be observed in Figure (2.3) for the "mini" and "original" JET devices. In Figure (2.3) this is actually more clearly observed

in the "mini" JET scour results with the scour leveling off at 3 cm and then accelerating and then leveling off again at 6 cm. This pattern of observed scour has less impact on the measurement of the detachment coefficient k_d because the method of analysis averages the rate of scour over the entire test, whereas the method of predicting the critical stress is based on the equilibrium depth, an estimate of a single point in time. The relative scale of this inherent soil structure is larger for the "mini" JET than the "original" JET and therefore, it would be expected that the predicted the equilibrium depth J_e to the nozzle height J_i ratio for the "mini" JET would be greater.

Table 2.2. Results from Mann-Whitney Rank Sum tests for differences between the original JET and "mini" JET devices for measuring erodibility, k_d, and critical shear stress, τ_c. Results for dry density (ρ_d) are shown to verify the compaction procedure. All tests were performed with n = 18.

Soil Type	Test	Median Values (IQR[a])		P-value	Significantly Different
		"Mini" JET	Original JET		
Silty Sand	ρ_d, Mg/m^3	1.74 (0.08)	1.73 (0.08)	0.930	No
	k_d, cm^3/N-s	13.4 (13.0)	8.8 (16.1)	0.791	No
	τ_c, Pa – Pre-Adjustment	0.002 (0.004)	0.031 (0.052)	0.003	Yes
	τ_c, Pa – Post-Adjustment	0.025 (0.069)	0.031 (0.052)	0.860	No
Clayey Sand	ρ_d, Mg/m^3	1.89 (0.17)	1.90 (0.17)	0.791	No
	k_d, cm^3/N-s	0.42 (5.6)	0.39 (17.3)	0.659	No
	τ_c, Pa – Pre-Adjustment	0.005 (0.062)	0.687 (1.353)	0.010	Yes
	τ_c, Pa – Post-Adjustment	0.075 (0.992)	0.687 (1.353)	0.791	No

[a] IQR = interquartile range, defined as the difference between the 25th and 75th percentiles.

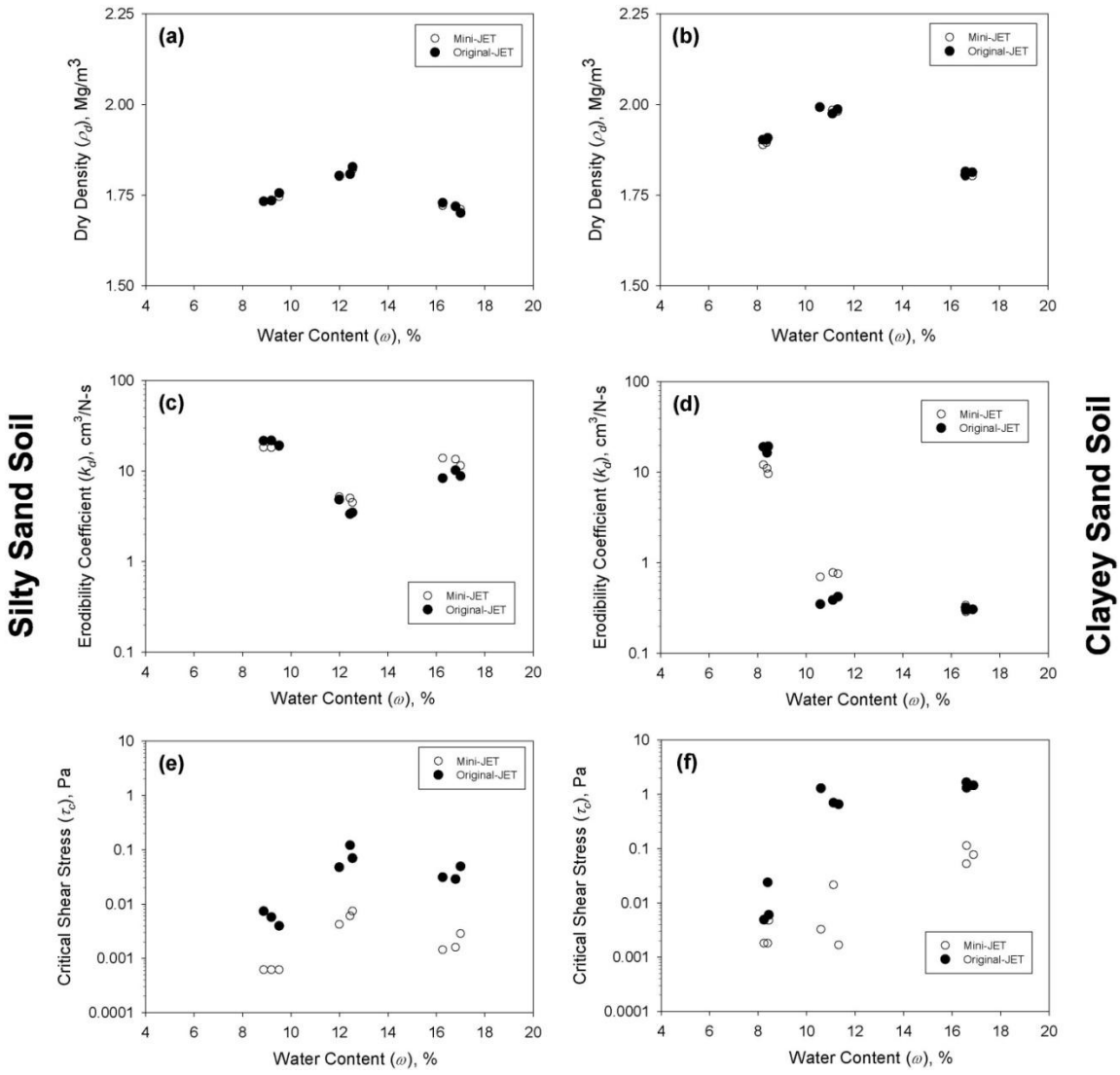

Figure 2.4. Measured τ_c and k_d from the original JET and "mini" JET devices for the silty sand and clayey sand soils for three repeated tests for each water content. Note that (a) and (b) compare dry densities (ρ_d) - water content (ω) relationships between prepared samples.

The initial ratio settings for both the "mini" and original JET devices were set to be equivalent (i.e., the d_o/J_i ratio of the "mini" JET to the ratio of the original JET were equal to unity); therefore, the ratio of the equilibrium depth (J_e) to the nozzle height (J_i) for both devices should be expected to be equivalent at the end of the test if they both estimate equivalent τ_c. However, due to differences in the scales between the devices, the J_e/J_i ratio of the "mini" JET was greater than that of the original JET (i.e., the J_e/J_i ratio of the "mini" JET was not equal to the

J_e/J_i ratio of the original JET) as shown in Figure (2.6). The J_e/J_i ratios from both devices indicated that the "mini" JET produced higher scour ratios compared to the original JET, resulting in lower measured τ_c for the "mini" JET compared to the original JET. Therefore, it is also hypothesized that an additional possible cause for the difference in the critical stress is the differences in the scales of submergence tank (1:3) and nozzle (1:2) between the "mini" and original JET devices.

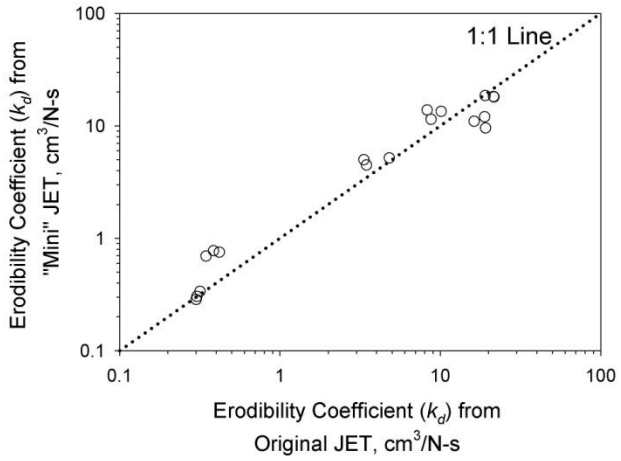

Figure 2.5. Measured k_d from the original JET and "mini" JET devices for the silty sand and clayey sand soils.

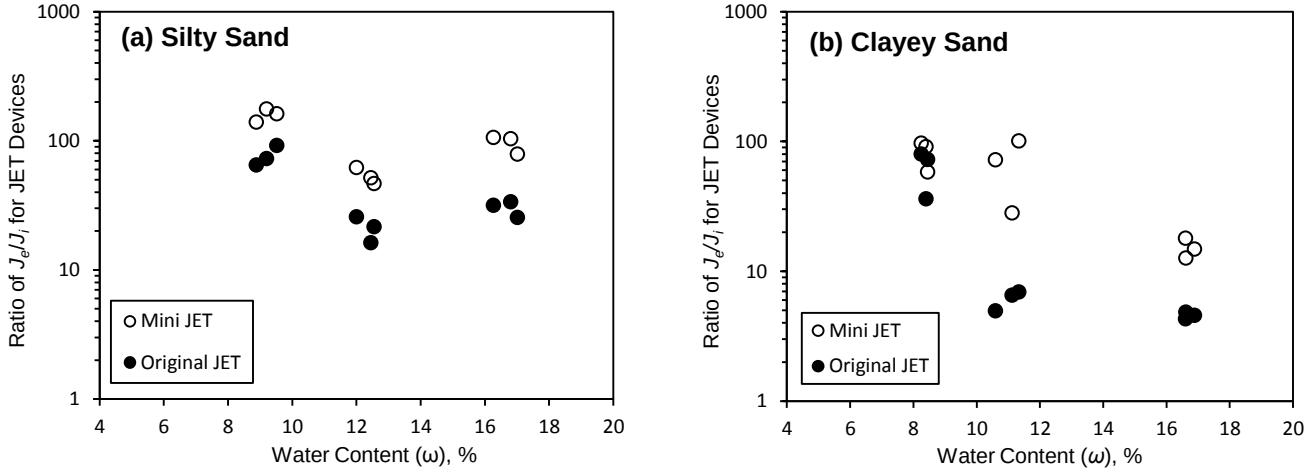

Figure 2.6. The J_e/J_i ratio from the "mini" and original JET devices for silty sand and clayey sand soils.

Based on observed J_e/J_i ratios of both devices (Figure 2.6), it was determined that the following adjustment procedure could be used to adjust the τ_c determined from the "mini" JET to match the original JET value. The adjustment was based on recalculating the τ_c of the "mini" JET by multiplying the J_e of the "mini" JET by a coefficient, C_{je}:

$$C_{je} = \frac{(J_e / J_i)_o}{(J_e / J_i)_m} \tag{2.11a}$$

$$\tau_c = \tau_o \left(\frac{J_p}{C_{je} J_e} \right)^2 \tag{2.11b}$$

where $(J_e / J_i)_o$ corresponds to the values for the original JET, and $(J_e / J_i)_m$ corresponds to values for the "mini" JET. The C_{je} was equal to 0.25 based on the average of observed values in this study (Figure 2.6), and future research should be conducted to validate this coefficient. Using equation (2.11b) to calculate the adjusted τ_c for the "mini" JET device resulted in no statistical significant differences in measured τ_c between the JET devices for both soils (Figures 2.7a, 2.7b, and Table 2.2). The relationship between measured τ_c from the original JET and adjusted τ_c from the "mini" JET device followed the 1:1 trend line as shown in Figure (2.7c) with an R^2 of 0.58.

Figure (2.8) shows a comparison between the "mini" and original JET devices for the τ_c - k_d relationships for data reported by Simon et al. (2010). Parallel relationships between both devices for the τ_c -k_d relationships were observed. Figure (2.9) shows the τ_c -k_d relationships for this study for silty sand and clayey sand soils and a comparison between both devices for data before and after adjusted τ_c. Figure (2.9a) shows parallel τ_c -k_d relationships between both devices as observed by Simon et al. (2010) prior to adjusting τ_c. The gap in the τ_c -k_d relationships between the "mini" and original JET devices in this study (Figure 2.9a) was due to differences in

measured τ_c between both JET devices as explained in Figures (2.4e) and (2.4f). Figure (2.9b) demonstrates the equivalent performance between the "mini" and original JET devices in this study with the adjusted τ_c for the "mini" JET device.

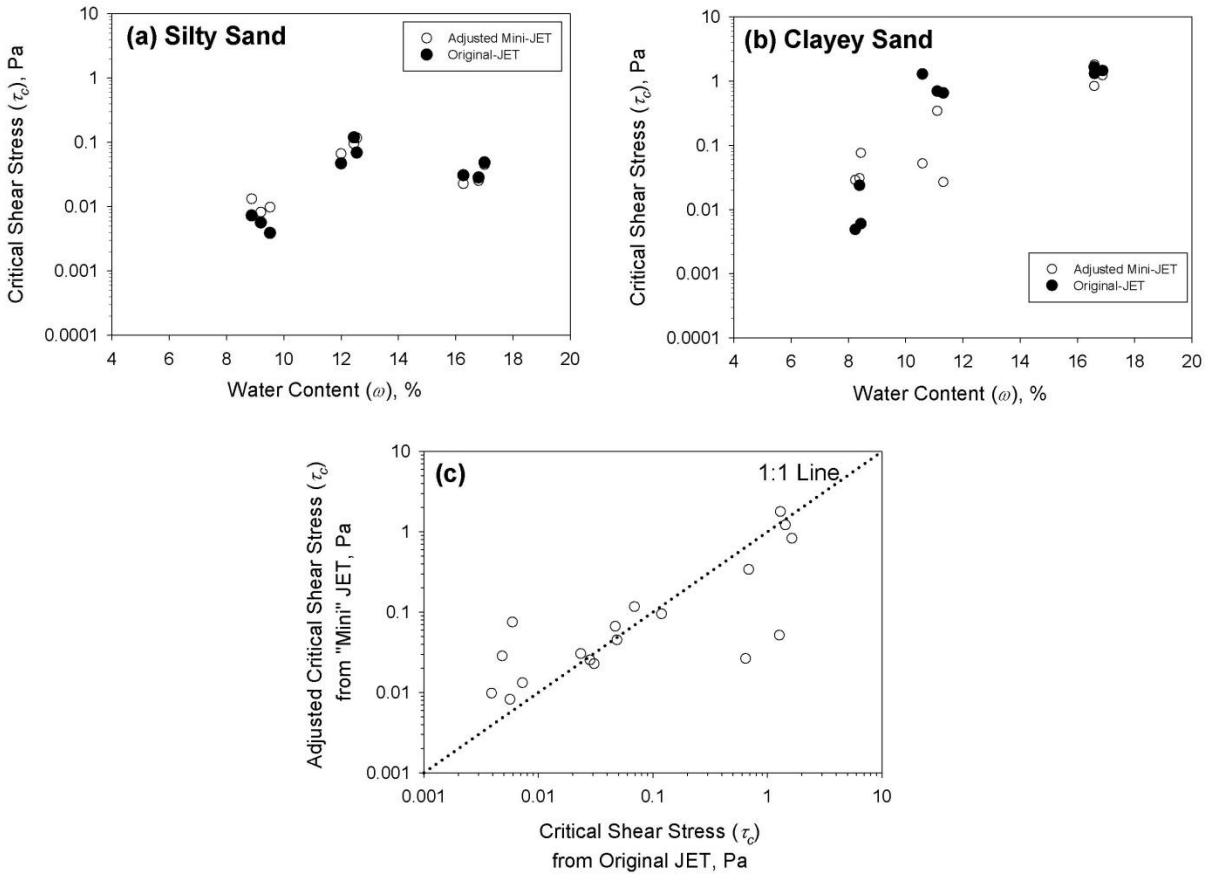

Figure 2.7. Measured τ_c from the original JET and "mini" JET devices after adjustment of the "mini" JET results for: (a) silty sand, (b) clayey sand. (c) Regression between τ_c from the original JET and after adjustment of the "mini" JET.

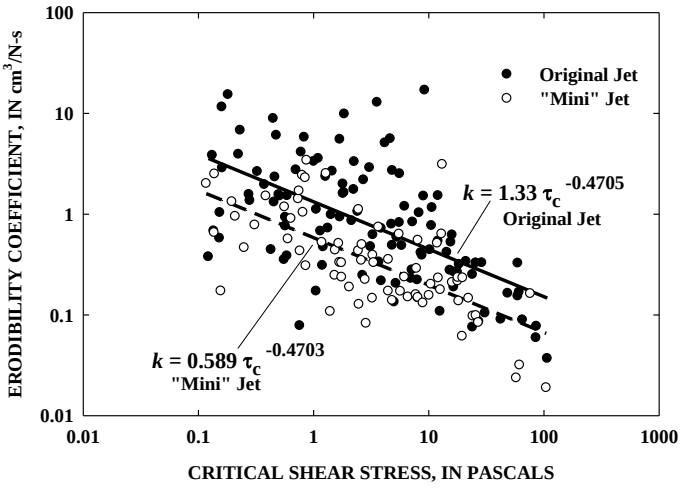

Figure 2.8. Comparison between the original and "mini" JET devices for the τ_c -k_d relationships for Simon et al. (2010) study.

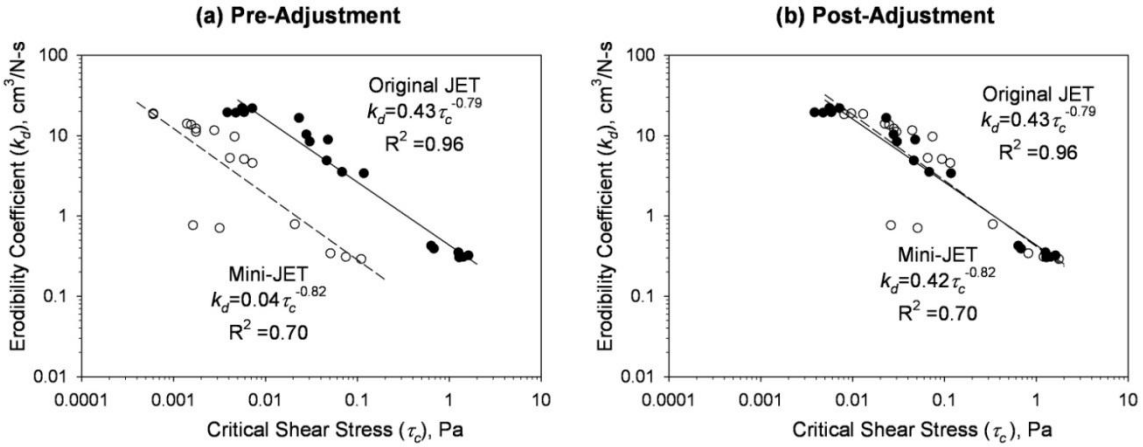

Figure 2.9. Comparison between the original and "mini" JET devices for the τ_c -k_d relationship for the silty sand and clayey sand soils: (a) pre-adjustment and (b) post–adjustment.

2.5. SUMMARY AND CONCLUSIONS

A laboratory JET apparatus (original JET) and a new miniature version of the JET device ("mini" JET) were compared in terms of measuring τ_c and k_d for two soils: silty sand and clayey sand. Thirty six tests were conducted using both JET devices to measure τ_c and k_d for both soils at

different water contents under equivalent standard compaction effort (25 blows/layer). In order to compare the performance and repeatability of both JET devices, tests were performed on paired samples prepared in the same way and tested at the same time using the same scaling ratios of the "mini' JET and original JET orifice diameters and height. Both JET tests measured equivalent k_d with no significant differences based on Mann-Whitney rank sum tests. Variability in the soil texture of the samples and variations in water content caused some variability in measuring τ_c and k_d. Differences were observed in the measured τ_c between both JET devices. This difference could possibly be explained as due to the method of sample preparation (lifts) and methodology used to determine critical shear stress. A secondary reason may be the differences in the scales of submergence tanks and nozzles between the "mini" and original JET devices. An adjustment coefficient was developed based on the equilibrium depth of the "mini" JET tests relative to the original JET results to reduce the differences in measuring τ_c between both devices. In order to compare the results of these two devices, the d_o/J_i ratio should be the same and test samples should be prepared in the same manner to reduce the differences in heterogeneity of the soil samples. Parallel relations of the τ_c -k_d relationships were obtained from both devices as observed in a previous study. The results from this study indicate that the "mini" JET can provide essentially equivalent results to the original JET. The "mini" JET also provides advantages of being smaller, easier and more convenient to use in many settings, and requires a smaller water supply.

2.6. ACKNOLWEDGEMENTS

This research is based upon work supported by the National Science Foundation under Grant No. 0943491. Any opinions, findings, and conclusions or recommendations expressed in this material are those of the authors and do not necessarily reflect the views of the National Science Foundation.

CHAPTER III

DERIVING PARAMETERS OF A FUNDAMENTAL DETACHMENT MODEL FOR COHESIVE SOILS FROM FLUME AND JET EROSION TESTS[2]

3.1. ABSTRACT

The erosion rate of cohesive soils is commonly quantified using the excess shear stress model, dependent on two major soil parameters: the critical shear stress (τ_c) and the erodibility coefficient (k_d). A submerged jet test (JET – Jet Erosion Test) is one method that has been developed for measuring these parameters. The disadvantage of using the excess shear stress model is that τ_c and k_d parameters change according to erosion conditions, such as soil structure, soil orientation, type of clay, presence of roots, and seepage forces. A more mechanistically based detachment model, the "Wilson Model," is proposed in this study for modeling the erosion rate of soils using the hydraulic analysis of a JET. The general framework of the "Wilson Model" is based on two soil parameters (b_0 and b_1). The objectives of this study were to: 1) develop

[2] In review in *Transactions of the ASABE*
Al-Madhhachi, A.T., Hanson, G. J., Fox, G. A., Tyagi, A. K., and Bulut, R. 2012b. Deriving parameters of a fundamental detachment model for Cohesive Soils from flume and Jet Erosion Tests. T. ASABE.

methods of analysis of the JET to determine the b_0 and $b_1$parameters from the "Wilson Model", in a similar fashion to the previous methodology developed for open channel flow; and 2) compare the excess stress model parameter k_d and the "Wilson Model" parameters b_0 and b_1 determined from the flume tests and JETs for two cohesive soils. Flume tests, treated as the standard test method, and original and "mini" JETs tests were conducted on two soils to independently measure the excess shear stress model parameter k_d, and the "Wilson Model" parameters b_0 and b_1. Soil samples of two cohesive soils (silty sand and clayey sand) were packed in a soil box for the flume tests and the JETs at water contents ranging from 8.7% to 18.1%. No statistically significant differences were observed for the excess shear stress model parameter k_d and for the "Wilson Model" parameters b_0 and b_1 when determined from the flume tests and JET devices, except for b_1 with the original JET. The "Wilson Model" is advantageous in being a more mechanistic, fundamentally based erosion equation as compared to the excess shear stress model; the "Wilson Model" can be used in the place of the excess shear stress model with parameters that can be estimated using existing JET techniques.

3.2. INTRODUCTION

Quantifying the erodibility of cohesive soils is an important challenge for many engineers and scientists because erosion and sedimentation are major water resource management issues in the world. One indication of the importance of quantifying the erodibility of soil materials is the number of methods that have recently been developed to measure it in the laboratory and the field (Hanson, 1990a, 1990b; Briaud et al., 2001; Hanson and Cook, 2004; Wan and Fell, 2004; Mazurek, 2010; Marot et al., 2011). Many factors influence the erodibility of cohesive soils, such as soil texture, structure, unit weight, water content, swelling potential, clay mineralogy, and pore water chemistry. Generally the erosion rate of cohesive soils is approximated using an excess shear stress model, based on the average hydraulic boundary shear stress (τ, Pa) and two major

soil parameters: the critical shear stress (τ_c, Pa) and the erodibility coefficient (k_d, $cm^3/N\ s$). The erosion rate is typically expressed as (Partheniades, 1965; Hanson, 1990a, 1990b):

$$\varepsilon_r = k_d(\tau - \tau_c)^a \tag{3.1}$$

where ε_r is the erosion rate (cm/s) and a is an empirical exponent commonly assumed to be unity (Hanson, 1990a, 1990b; Hanson and Cook, 1997).

Numerous studies have derived k_d and τ_c for cohesive soils using different techniques: large flumes (Hanson, 1990a; Hanson and Cook, 2004), small flumes (Briaud et al., 2001), laboratory hole erosion test (Wan and Fell, 2004), and a submerged jet (Hanson and Cook, 2004; Mazurek, 2010; Marot et al., 2011). The submerged jet test (JET - Jet Erosion Test) apparatus is one of the methods developed for measuring these parameters in situ as well as in the laboratory (Hanson, 1990b; Hanson and Cook, 1997; Hanson and Simon, 2001; Hanson et al., 2002a, 2002b; Hanson and Cook, 2004; Hanson and Hunt, 2007). A description of the JET (referred to in this study as the original JET), step by step testing methodology, and development of analytical procedure were presented by numerous studies (Hanson and Cook, 1997; Hanson and Simon, 2001; Hanson et al., 2002a; Hanson and Cook, 2004). Hanson (1990b) performed seven tests on four types of soils using the in-situ JET device. Hanson and Cook (1997) and Hanson et al. (2002a) developed the analytical methods to directly measure k_d and τ_c based on diffusion principles of the submerged jet using an Excel spreadsheet approach. Hanson and Simon (2001) measured the soil erodibility of streambeds in the Midwestern United States using the in-situ original JET apparatus to measure k_d and τ_c and observed an inverse relationship between the two parameters. Additional research (Hanson and Robinson, 1993; Hanson and Hunt, 2007; Regazzoni et al., 2008) has focused on the impact of soil parameters, such as the influence of water content, soil texture, bulk density, and soil compaction, on measuring soil erodibility using the JET apparatus.

The analytical methods for the JET device were developed by Hanson and Cook (1997) based on diffusion principles developed by Stein and Nett (1997). The rate of variation in the depth of scour was assumed to be the erosion rate as a function of the maximum stress at the boundary (Stein and Nett, 1997). The maximum shear stress was based on determining the diameter of the jet nozzle and the distance from the jet origin to the initial channel bed. Accordingly, the critical shear stress was assumed to occur when the rate of scour was equal to zero at the equilibrium depth. Blaisdell et al. (1981) developed a hyperbolic function for predicting the equilibrium depth which was used in the spreadsheet to calculate τ_c. The k_d is then determined depending on the measured scour depth, time, predetermined τ_c, and a dimensionless time function (Hanson et al., 2002b).

Several flume studies have been conducted to measure the erosion of cohesive soils in order to verify the use of the JET (Hanson, 1990a; Hanson and Cook, 1999; Hanson, 2001; Hanson and Cook, 2004). Hanson (1990a) measured soil erodibility in large outdoor channels with soil material placed throughout the entire length of the channel beds. Six channels were constructed (0.91 m wide and 30.5 m long) with different slopes: 0.5, 1.5, and 3%. Hanson (1990b) empirically related JET index values determined from the three soils to the soil erodibility values determined from the flume studies of Hanson (1990a). Hanson and Cook (1999) performed two open channel flow tests in a large outdoor open channel (1.8 m wide and 29 m long with 2.4 m sidewalls) on compacted samples of lean clay and silty clay. The k_d and τ_c determined from the flume tests verified the use of in-situ and laboratory JET experiments. This study as well as other studies (Hanson et al. 2002a, Hanson and Cook, 2004, Hanson and Hunt 2007, and Hanson et al., 2011) have verified the use of the original JET to predict the rates of erosion for headcut migration, impinging jet scour, and embankment breach formation and widening.

In addition to the original JET, a new miniature version of the JET device, which is referred to as the "mini" JET, was recently developed by Hanson (Al-Madhhachi et al., 2012a, Chapter II). The "mini" JET device is smaller and lighter than the original JET device and thus can be more easily handled in the field as well as in laboratory. The "mini" JET device was first used by Simon et al. (2010) in the field, where they performed 279 tests using the "mini" JET to measure k_d and τ_c. The initial method of testing and analysis conducted by Simon et al. (2010) was based on the methods developed for the original JET. They compared the "mini" JET results with the original JET device at 35 sites in the Tualatin River Basin, Oregon. Simon et al. (2010) observed good agreement in derived values of τ_c, but observed differences in k_d and the k_d - τ_c relationships between the two JET devices. Simon et al. (2010) hypothesized that observed differences in results were due to differences in the size of the submergence cans between the original and "mini" JET devices. These tests were conducted in-situ at side by side locations, but results were likely influenced by in-situ heterogeneity and possible differences in methodology and set-up.

Al-Madhhachi et al. (2012a, Chapter II) compared measured excess shear stress model parameters using the two JET devices in a more controlled laboratory setting using two cohesive soils (clayey sand and silty sand). Statistically equivalent k_d values were derived by the two JET devices for both soils based on Mann-Whitney rank sum tests but the τ_c values derived by the "mini" JET were consistently lower. Al-Madhhachi et al. (2012a, Chapter II) hypothesized that the measured differences in τ_c were due to the relative scale of the two submerged jets in comparison to the inherent soil structure created by the compaction method. Adjusting the equilibrium depth of the "mini" JET by a coefficient in the analysis resulted in insignificant differences in the estimated τ_c between the two JET devices. This study concluded that the "mini" JET measurements, based on the excess stress model parameters, provided erosion rate predictions equivalent to the original JET.

In addition to the excess shear stress model, several other models have been proposed to predict the erosion rate of cohesive soils including numerous models based on excess shear stress formulations, some of which include the bulk density of beds (Parchure and Mehta, 1985; Sanford and Maa, 2001), and turbulent burst erosion models (Cleaver and Yates, 1973; Nearing, 1991; Sharif and Atkinson, 2012). Turbulent burst erosion models have been developed for cohesive beds based on the average area of the turbulent burst acting on the bed, the mass of sediment eroded, probability distributions of fluid forces and resistive forces, and a turbulent burst time period. Cleaver and Yates (1973) and Nearing (1991) applied a turbulent burst erosion model to the detachment of aggregates from the surface of a bed. Sharif and Atkinson (2012) developed an aggregate size distribution relationship as function of the bed bulk density and the concept of self-similar growth of aggregates in the turbulent burst erosion model.

Even though the excess shear stress and turbulent burst erosion models provide a method of characterizing the erodibility of soil materials and predicting erosion rates, the disadvantage of these models are the lack of mechanistic predictions of its parameters for specific soil and hydraulic conditions. A more fundamentally based detachment model using the mechanics of particle and/or aggregate motion would be preferred for modeling the range of environmental conditions experienced during fluvial erosion. For example, recent research on seepage processes on hillslopes and streambanks suggest these forces may be important even during fluvial erosion in increasing the erodibility of cohesive soils (Fox and Wilson, 2010; Midgley et al., 2012a). A mechanistic detachment model has the advantage of allowing a more in depth accounting and evaluation of the impact of factors such as turbulence, roughness, seepage forces, material soil orientation (i.e. streambed versus streambank), root effects, negative pore water pressure effects, etc.

Wilson (1993a, 1993b) developed a fundamental mechanistic detachment model to provide a general framework for studying soil and fluid characteristics and their impact on

cohesive soil erodibility. The model was developed based on a simple two-dimensional representation of particles. However, the detachment model is not restricted to a single particle and can be applied for aggregates. The model was evaluated using erosion rate data for cohesive soils. The model was calibrated to the observed data based on two dimensional parameters b_0 and b_1. The model represented the observed data as well as or better than the excess shear stress model. However, the parameters can only be derived from observed erosion data from flumes or open channels which limits its applicability at the time of development.

The objectives of this research were to: 1) develop methods of analysis of the JET to determine the b_0 and b_1 parameters in a fashion similar to the methodology developed by Wilson (1993a, 1993b) for open channel flow; and 2) compare the excess shear stress model parameters k_d and the "Wilson Model" parameters b_0 and b_1 determined from flume and JETs on two cohesive soils. It is also important to note that the author's developments are consistent with Wilson's simple two dimensional representations of particles even though it is not restricted to a single particle and can be applied for aggregates as well.

3.3. GENERAL THEORETICAL FRAMEWORK OF "WILSON MODEL"

The general framework for predicting the erosion rate in the "Wilson Model" is based on dislodging and stabilizing forces and associated moment lengths for particle detachment (Wilson, 1993a). Figure (3.1) is a conceptual sketch of the forces that act to remove a soil particle including the lift force, F_L, drag force, F_d, particle weight, w_s, and contact forces between adjacent particles (F_{c1}, F_{c2},……, F_{cn}). Particle detachment occurs if the driving moment is greater than the resisting moment (Wilson, 1993a). Wilson (1993a) assumed that the moments acting around point *A* and the point of incipient motion is defined as:

$$F_d(l_3) + F_L(l_4) + w_s \sin(\alpha)(l_1) = w_s \cos(\alpha)(l_2) + M_c \qquad (3.2)$$

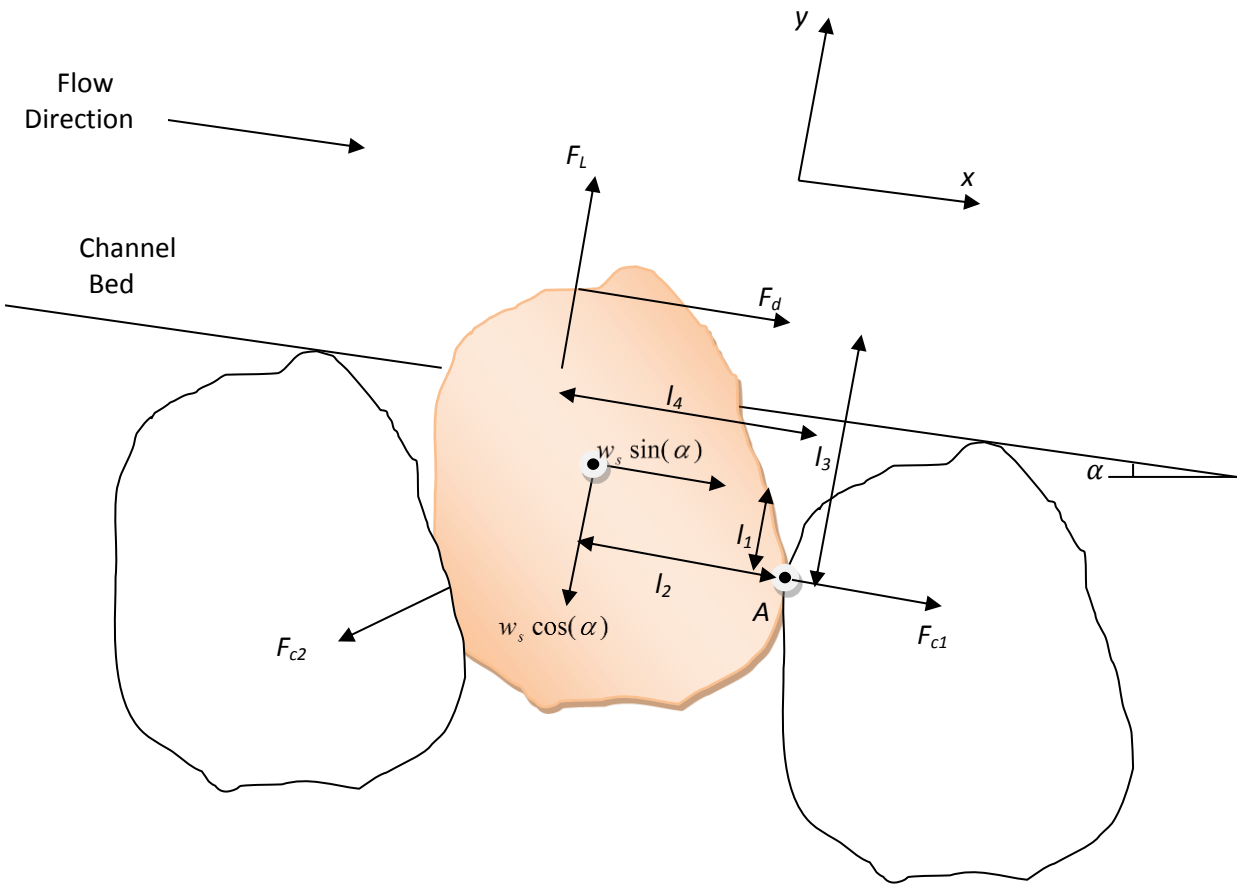

Figure 3.1. Forces and moment lengths acting on a single soil particle in a channel bed (variables in the figure are defined in the text).

where $w_s = g(\rho_s - \rho_w)k_v d^3$ is the submerged particle weight; ρ_s is a particle density; ρ_w is the water density, d is an equivalent particle diameter; $k_v (= \frac{\pi}{6})$ is the volume constant of a sphere particle; $M_c = \sum_{i=1}^{n_c} \sigma_{ci} a_i \bar{l}_i$ is the sum of moments of cohesive and frictional forces; n_c is the number of contact areas; σ_{ci} is a particle to particle stress; a_i is the contact area; $\bar{l}_i$ is the moment length for each contact force; l_1, l_2, l_3, and l_4 are lengths of moments for forces; and α is

the channel angle slope. By assuming that the drag force and lift force are proportional (i.e., $\frac{K_L}{K_f} = \frac{F_L}{F_d}$) (Chepil, 1959; Wilson, 1993a), equation (3.2) can be rewritten as:

$$F_d = w_s \left[\frac{\cos(\alpha)(l_2) - \sin(\alpha)(l_1)}{l_3 + l_4 \frac{K_L}{K_f}} \right] + \left[\frac{M_c}{l_3 + l_4 \frac{K_L}{K_f}} \right] \tag{3.3}$$

The above equation can be rearranged by introducing K_{ls} and f_c terms:

$$F_d = w_s (K_{ls} + f_c) \tag{3.4a}$$

$$K_{ls} = \frac{\cos(\alpha)(l_2 - l_1 S)}{l_3 + l_4 \frac{K_L}{K_f}} \tag{3.4b}$$

$$f_c = \frac{M_c}{w_s (l_3 + l_4 \frac{K_L}{K_f})} \tag{3.4c}$$

where K_{ls} is the dimensionless parameter that depends on particle size, its orientation within the bed, and slope; f_c is the dimensionless parameter based on cohesion; K_L is the ratio of drag and lift coefficients along with the ratio of velocities equal to 1 (Wilson 1993a, 1993b); K_f is the ratio of projected area drag and lift forces; $k_r (= \frac{k_v}{k_a} = \frac{2}{3})$ is the geometry ratio for a spherical particle; $k_a (= \frac{\pi}{4})$ is the area constant of a spherical particle; and $S (= \tan\alpha)$ is the channel slope.

The particle is detached if the flow characteristic on the left side (F_d) of equation (3.4a) is greater than the right side: $w_s (K_{ls} + f_c)$, which is primarily a function of particle and bed characteristics (Wilson, 1993a). Wilson (1993b) suggested that the values of moment lengths for

equal radii are: l_1 = 0.86 d/2, $l_2 = l_4$ = 0.5 d/2, and l_3 = 1.18 d/2. These moment lengths were computed based on combinations of particle sizes and gaps developed by Wilson (1993b). Similarly, based on a combination of particle sizes and gaps, Wilson (1993b) suggested that K_f ranges between 0 to 1 with a value equal to 0.92 for equal radii.

3.3.1. Flow Characteristics

The flow in an open channel is always turbulent and the drag force rapidly changes with time and space. Therefore, the mean value is important in characterizing the turbulent flow properties (Wilson, 1993a). Einstein and El-Samni (1949) presented the time averaged forces at the channel bed using the time averaged velocity. The time averaged drag force ($\overline{F}_d$) is expressed as:

$$\overline{F}_d = C_D K_f k_a d^2 \frac{\rho_w U_d^{\,2}}{2} \tag{3.5}$$

where C_D is the drag coefficient and U_d is the time averaged velocity defined by Wilson (1993a) as:

$$U_d = \frac{u_*}{k}\ln(\phi) + B \tag{3.6a}$$

where k is the von Karmon constant equal to 0.4 (Schlichting, 1979); $\phi = \frac{z_d}{k_s}$ is a fraction assumed to be unity by Yang (1973), 0.35 by Einstein and El-Samni (1949), and 0.6 by Wilson (1993b); z_d is a height that the drag velocity is acting upon and it is equal to ($l_3 + y_p$) according to Wilson (1993b); y_p (= $k_s - d/2 - l_1$) is a pivot point; k_s ($= d/2\sqrt{3}$) is a roughness height; B is a dimensionless term that depends on the laminar sublayer thickness and roughness height defined

by shear Reynolds number, where B ranges from 6.5 to 9.9 dependent on shear Reynolds number (Schlichting, 1979); and u_* is shear velocity expressed as:

$$u_* = \sqrt{\frac{\tau}{\rho_w}} \tag{3.6b}$$

Substituting equations (3.6a) and (3.6b) into equation (3.5) yields:

$$\overline{F}_d = K_o k_a d^2 \tau \tag{3.7a}$$

$$K_o = \frac{[C_D K_f (\frac{1}{k}\ln(\phi) + B)^2]}{2} \tag{3.7b}$$

where K_o is known as a velocity flow parameter in this study.

3.3.2. Incipient Motion

Wilson (1993a) suggested that the incipient motion could be estimated using the time averaged velocity; then, critical shear stress, τ_c, can be calculated. If the drag force from equation (3.4a) is equal to the time averaged drag force from equation (3.7a), then the critical shear stress to initiate motion (i.e. $\tau_c = \tau$) is determined from (Wilson, 1993a):

$$w_s(K_{ls} + f_c) = K_o k_a d^2 \tau_c \tag{3.8a}$$

$$\tau_c = \frac{k_r}{K_o} g(\rho_s - \rho_w) d(K_{ls} + f_c) \tag{3.8b}$$

$$\tau_c^* = \frac{\tau_c}{g(\rho_s - \rho_w)d} = \frac{k_r}{K_o}(K_{ls} + f_c) \tag{3.8c}$$

where τ_c^* is known as the critical Shields parameter. The right side of equations (3.8b) and (3.8c) were related to the soil and bed characteristics (Wilson, 1993a). Wilson (1993b) evaluated the

general framework without calibration by predicting the incipient motion of non-cohesive particles (i.e. f_c = 0) and compared them with those obtained from Simons and Senturk (1977). Wilson (1993b) reported that the average predicted detachment rate was 18-22% smaller when using the "Wilson Model" compared to the excess shear stress model.

3.3.3. Detachment Rate Model

Particle detachment occurs when the drag force in equation (3.4a) is greater than the weight and cohesive forces. Wilson (1993a) developed a similar probability framework for turbulent forces developed by Einstein (1950) and Partheniades (1965). The probability of the drag force (equation 3.4a) is defined as (Wilson, 1993a):

$$P = 1 - \int_{-\infty}^{w_s(K_s + f_c)} f(F_d) d(F_d) \tag{3.9}$$

where P is the exceedance probability of drag force and $f(F_d)$ is a probability density function.

To determine the detachment rate, assume that P is the fraction of the total bed area at a given time, then the number of particles of diameter d for potential detachment per unit bed area (n_{di}) is expressed as (Wilson, 1993a):

$$n_{di} = \frac{\Delta FF_i P}{k_a d^2} \tag{3.10}$$

where ΔFF_i is the fraction finer value for bed materials and $k_a d^2$ is the projected horizontal area of a single particle. The rate of particle detachment, which is the number of detached particles divided by the time required for those particles to leave other particles, is expressed as (Wilson, 1993a):

$$n_{ri} = \frac{\Delta FF_i P}{k_a d^2 (K_e t_e)} \tag{3.11}$$

where n_{ri} is the particle detachment rate; t_e is the exchange time of a single particle; and K_e is the exposure of lower particle parameter (i.e., additional time to remove surrounding particles). Therefore, the erosion or detachment rate in units of mass per area per time is determined by multiplying equation (3.11) by the density and volume of each particle and can be expressed as (Wilson, 1993a):

$$\varepsilon_{ri} = n_{ri}\rho_s k_v d^3 = \Delta F F_i P \rho_s k_r \left(\frac{d}{K_e t_e}\right) \tag{3.12}$$

The exceedance probability, P, and the exchange time, t_e, can be estimated to determine the erosion or detachment rate. Wilson (1993a) developed an equation for particle exchange time, t_e, expressed as:

$$t_e = d\sqrt{\frac{k_{dd}}{gd(K_n\tau^* - \mu_f)}} \qquad \text{if } K_n\tau^* > \mu_f \tag{3.13a}$$

$$\tau^* = \frac{\tau}{g(\rho_s - \rho_w)d} \tag{3.13b}$$

$$K_n = K_t\ K_o / k_r \tag{3.13c}$$

where τ^* is the Shields parameter; k_{dd} is the detachment distance parameter equal to 2 according to Einstein (1950); K_n is a combination of particle and fluid factors; K_t is a factor of cumulating of instantaneous fluid forces equal to 2.5 (Chepil, 1959); and μ_f is a coefficient of friction.

Wilson (1993a) used three probability distributions for equation (3.9) to calculate the exceedance probability, P: Extreme Value Type I, normal, and log-normal distributions. Wilson (1993a) recommended the Extreme Value Type I as the best to represent the turbulent detachment forces because it simplified the detachment model calculations, predicted similar results to the log-normal distribution, and obtained low probabilities for negative drag forces. Therefore, the

Extreme Value Type I distribution was also used in this study to represent the exceedance probability of drag force. The Extreme Value Type I distribution is expressed as (Wilson, 1993a):

$$P = 1 - \exp[-\exp(-\mu_e)] \tag{3.14a}$$

$$\mu_e = (\frac{\pi}{e_v\sqrt{6}})[\frac{k_r(K_{ls} + f_c)}{K_o\tau^*} - (1 - \frac{1.365e_v}{\pi})] \tag{3.14b}$$

where μ_e is the upper limit of integration for Extreme Value Type I distribution and e_v is the coefficient of variation equal to 0.35 according to Einstein and El-Samni (1949). By combining equations (3.12), (3.13a), and (3.14a), the erosion or detachment rate (ε_{ri}, mass/area/time) based on turbulent probability is expressed as (Wilson, 1993a):

$$\varepsilon_{ri} = \frac{\Delta FF_i}{K_e}\rho_s k_r\sqrt{\frac{gd(K_n\tau^* - \mu_f)}{k_{dd}}}\{1 - \exp[-\exp(-\mu_e)]\} \quad \text{if } K_n\tau^* > \mu_f \tag{3.15}$$

Wilson (1993a, 1993b) used a calibration procedure to obtain some parameters included in the cohesive parameter, f_c, and the exposure parameter, K_e, because there was little information available on these parameters. Due to difficulty in determining the interaction between bed particle sizes when the total erosion or detachment rate was determined from equation (3.15), Wilson (1993a, 1993b) developed a single approach to determine the total detachment rate by incorporating the effect of particle sizes indirectly in the calibration procedures. This approach was based on a two parameter model by assuming that μ_f was small relative to the value of $K_n\tau^*$ and e_v was 0.36. The results of this approach corresponded to those obtained from Einstein and El-Samni (1949). Therefore, the total erosion or detachment rate, ε_r, is expressed using dimensional parameters b_0 and b_1 (Wilson,1993a, 1993b):

$$\varepsilon_r = b_0 \sqrt{\tau}\left[1 - \exp\{-\exp(3 - \frac{b_1}{\tau})\}\right] \tag{3.16a}$$

$$b_0 = \rho_s \frac{k_r}{K_e}\sqrt{\frac{K_n}{k_{dd}(\rho_s - \rho_w)}} \tag{3.16b}$$

$$b_1 = (\frac{\pi}{e_v\sqrt{6}})\frac{k_r(K_{ls} + f_c)}{K_o} g(\rho_s - \rho_w)d \tag{3.16c}$$

where b_0 has dimensions of $(M/L^3)^{0.5}$ and b_1 has dimensions of F/L^2. In this study, equations (3.16a)-(3.16c) are referred to as the "Wilson Model". The parameters b_0 and b_1 can be derived using curve fitting techniques and iteratively minimizing the error of these functions relative to measured erosion data.

3.4. DEFINING THE FLOW CHARACTERISTICS IN THE "WILSON MODEL" FOR THE JET DEVICE

The submerged jet boundary shear stress and velocity distribution profile are different than that used in the derivation of the "Wilson Model" (i.e., different velocity flow parameter, K_o) for the open channel flow environment. Hanson and Cook (2004) presented the average maximum shear stress along the boundary, τ_j, in the jet impingement zone as the following (Figure 3.2):

$$\tau_j = \tau_o\left(\frac{J_p}{J}\right)^2 \tag{3.17}$$

where $\tau_o = C_f\ \rho_w U_o^2$ is the maximum shear stress due to the jet velocity at the nozzle (Pa); C_f = 0.00416 is the coefficient of friction; $U_o = C\sqrt{2gh}$ is the velocity of jet at the orifice (cm/sec); C

is discharge coefficient; h is the pressure head (cm); $J_p = C_d\, d_o$; d_o is the nozzle diameter (cm); C_d = 6.3 is the diffusion constant; J_i is the jet nozzle height, and J is the scour depth from jet nozzle.

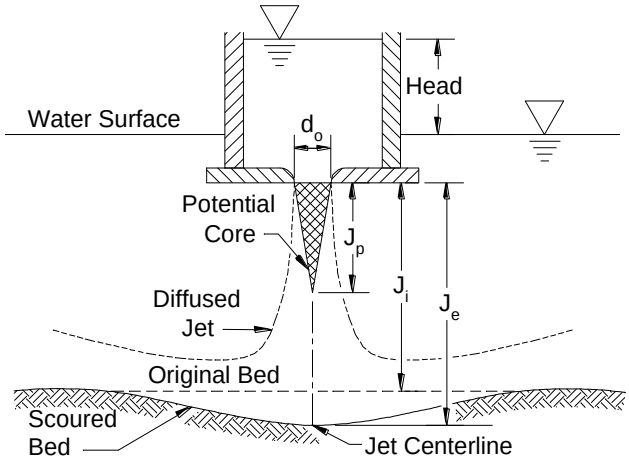

Figure 3.2. **Schematic of JET device with factor definitions (Hanson and Cook, 2004) (variables in the figure are defined in the text).**

Poreh and Cermak (1959) developed an equation for defining the velocity profile for an unconfined radial jet outside the boundary layer:

$$V_r = V_{RB} \exp[-100(\frac{z}{r})^2] \qquad \text{for } (z > \delta) \tag{3.18}$$

where V_r is the velocity profile along jet radius r; V_{RB} is the boundary reference velocity; z is a height that the drag velocity is acting upon (equivalent to z_d); and δ is boundary sublayer.

Poreh and Cermak (1959) presented the boundary reference velocity, V_{RB}, in three different zones: the zone of the stagnation point ($\frac{r}{J_i} < 0.05$), the zone of the diffusion effect ($0.05 < \frac{r}{J_i} < 0.3$), and the zone of established radial flow ($\frac{r}{J_i} > 0.3$). Of interest for this study

is defining the profile of the maximum V_{RB} for the submerged jet when $\frac{r}{J_i}$ is equivalent to a value ranges between 0.10 to 0.15. Rajaratnam (1976) suggested that $\frac{r}{J_i}$ is equal to 0.14 while Weidner et al. (2012) suggested that $\frac{r}{J_i}$ is equal to 0.12. This study assumed $\frac{r}{J_i}$ is equal to 0.13. Accordingly, the V_{RB} at $\frac{r}{J_i}$ equivalent to ~ 0.13 reaches a maximum and can be defined as:

$$V_{RB} = 4.8\sqrt{\frac{K}{J_i^{\,2}}} \qquad \text{for } (\frac{r}{J_i} \text{ equivalent to } \sim 0.13) \tag{3.19}$$

where $K = 0.153\pi d_0^{\,2} U_0^{\,2}$ is a kinematic moment flux (Poreh et al., 1967). By substituting equation (3.19) into equation (3.18), the velocity profile for the submerged jet at the point of interest is expressed as:

$$V_r = 4.8\sqrt{\frac{K}{J_i^{\,2}}}\exp[-100(\frac{z_d}{r})^2] \tag{3.20}$$

By substituting the velocity profile of the submerged jet, i.e., equation (3.20) for U_d in equation (3.5), the time averaged drag force for the submerged jet can be expressed as:

$$\overline{F}_d = C_D K_f k_a d^2 \frac{\rho_w\left(4.8\sqrt{\frac{K}{J_i^{\,2}}}\exp[-100(\frac{z_d}{r})^2]\right)^2}{2} \tag{3.21}$$

where all terms were previously defined. By substituting for K and τ_j, equation (3.21) can be rearranged as following:

$$\overline{F}_d = K_{oj} k_a d^2 \tau_j \tag{3.22a}$$

$$K_{oj} = \frac{11.52 C_D K_f \rho_w K \exp[-200(\frac{z_d}{r})^2]}{J_i^{\,2} \tau_i} = \frac{5.537 C_D K_f \exp[-200(\frac{z_d}{r})^2]}{C_f c_d^{\,2}} \tag{3.22b}$$

where K_{oj} is known as a jet velocity flow parameter in this study. Following the same procedure as above in developing the "Wilson Model" and incorporating equations (3.17) and (3.22), the detachment rate model for JET data can be expressed as:

$$\varepsilon_r = b_{0j} \sqrt{\tau_j} \left[1 - \exp\{-\exp(3 - \frac{b_{1j}}{\tau_j})\} \right] \tag{3.23a}$$

$$b_{0j} = \rho_s \frac{k_r}{K_e} \sqrt{\frac{K_{nj}}{k_{dd}(\rho_s - \rho_w)}} \tag{3.23b}$$

$$b_{1j} = (\frac{\pi}{e_v \sqrt{6}}) \frac{k_r (K_{ls} + f_c)}{K_{oj}} g(\rho_s - \rho_w) d \tag{3.23c}$$

where $K_{nj} = K_t \; K_{oj} / k_r$ is a combination of particle and fluid factors for the JET, b_{0j} has dimensions of $(M/L^3)^{0.5}$, and b_{1j} has dimensions of F/L^2. Similarly, by using curve fitting techniques and solver routines, the parameters b_{0j} and b_{1j} can be derived from observed erosion data of JET.

As a side note, the b_0 and b_1 parameters of the "Wilson Model" for either the open channel development or the submerged jet development can be re-arranged to predict the critical shear stress as defined in equation (3.8b). The observed b_1 and b_{1j} can be used to find the parameter f_c. Accordingly, equation (3.16c) can be rewritten for the flume data as:

$$f_c = \frac{b_1 \; K_o e_v \sqrt{6}}{\pi \; k_r g(\rho_s - \rho_w) d} - K_{ls} \tag{3.24a}$$

and equation (3.23c) can be rewritten for the JET device data as:

$$f_c = \frac{b_{1j}\ K_{oj} e_v \sqrt{6}}{\pi\ k_r g(\rho_s - \rho_w) d} - K_{ls} \tag{3.24b}$$

The parameters in the above equations can be calculated or estimated from test results as the following: the e_v was assumed 0.35 as proposed by Wilson (1993b); the parameter k_r (= 2/3); the flow velocity parameter, K_o, depended on K_f (= 0.92), ϕ (=0.6), k (=0.4), B (ranged from 6.5 to 9.5), and C_D (which was equal to 0.2 for non-cohesive soil according to Einstein and El-Samni,1949); d was equal to d_{50} for silty sand and clayey sand soils; the parameter K_{ls} depended on S (=energy slope), K_L (=1), and l_1, l_2, l_3, and l_4 were previously defined; and the flow jet velocity parameter, K_{oj}, depended on z_d (= $l_3 + y_p$), y_p ($= d/2\sqrt{3} - d/2 - l_1$), C_f (=0.00416), r was equal to $0.13J_i$, and J_i was the initial nozzle height for the JET devices. By substituting equations (3.24a) and (3.24b) into equation (3.8b), the critical shear stress from the "Wilson Model" for the flume data can be estimated by:

$$\tau_c = \frac{b_1\ e_v \sqrt{6}}{\pi} \tag{3.25a}$$

and for the JET device data can be estimated by:

$$\tau_c = \frac{b_{1j} e_v \sqrt{6}}{\pi} \tag{3.25b}$$

3.5. MATERIALS AND METHODS

3.5.1. Flume Structure

Open channel erosion tests were conducted in a flume at the USDA Hydraulic Engineering Research Unit in Stillwater, Oklahoma. The flume was constructed inside a pre-

existing basin 12.2 m long and 3 m wide with 0.75 m side walls. The flume consisted of the following parts: water delivery pipe, upstream water reservoir, flume, soil box, and tailgate (Figures 3.3 and 3.4). The water pipe was 305 mm in diameter and it was attached to the water reservoir to provide the required discharge (maximum discharge was 0.17 m^3/s) from Lake Carl Blackwell. The upstream water reservoir was 1.2 m long, 1.2 m wide, and 1.4 m deep, and served the function of providing a smooth entrance flow condition to the flume. The flume was 4.9 m long and 0.6 m wide with 0.6 m wall sides. A soil box (1 m long, 61 cm wide, and 25 cm deep) was placed in the middle of the flume (Figure 3.4a). Soil was packed at different water contents (8.7% to 18.1%) at uniform bulk density in the soil box prior to testing. A tailgate was placed at the end of the flume with a fixed height of 0.14 m for all tests to provide desired flow conditions during testing. The effective shear stress was varied (ranging from 0.1 to 9.3 Pa) by changing the discharge into the flume (maximum discharge was 0.17 m^3/s). A mechanical jack was attached beneath the flume to provide the desired channel slope (1% to 3%). The design slope for testing was fixed at 1.5% for all tests to provide the desired flow condition.

3.5.2. In-Situ Original and "Mini" JET Devices

Original JET and "mini" JET devices were set-up and used for testing soils in-situ on the soil bed in the flume (Figure 3.4). The original JET device was the same as that used by Hanson and Hunt (2007). This apparatus consisted of the following parts: jet tube, adjustable head tank, point gage, nozzle, deflection plate (deflector), jet submergence tank, lid, and hoses as shown in Figure (3.4b). The jet tube had a 50 mm inner diameter with 6.4 mm wall thickness and an 89 mm diameter orifice plate with a nozzle at the center of this plate. The nozzle was 6.4 mm in diameter. The adjustable head tank was 910 mm in height with a 50 mm inner diameter and was utilized to provide a desired water head upstream of the nozzle. Scour readings were taken using the point gage, which was passed through the jet nozzle and extended to the soil surface. The point gage diameter was equivalent to the jet nozzle diameter; therefore, the water jet was shut off

during scour readings. The deflection plate (deflector) was used to prevent the water jet from impinging on the soil sample at the beginning of the test and prior to taking a scour reading. During the first filling of the jet tube, the air relief valve was used to remove air from the jet tube. The jet submergence tank was 305 mm in height and 305 mm in diameter with a 6.4 mm wall thickness. The submergence tank opened from the top with the jet tube and attached lid (Hanson and Hunt, 2007).

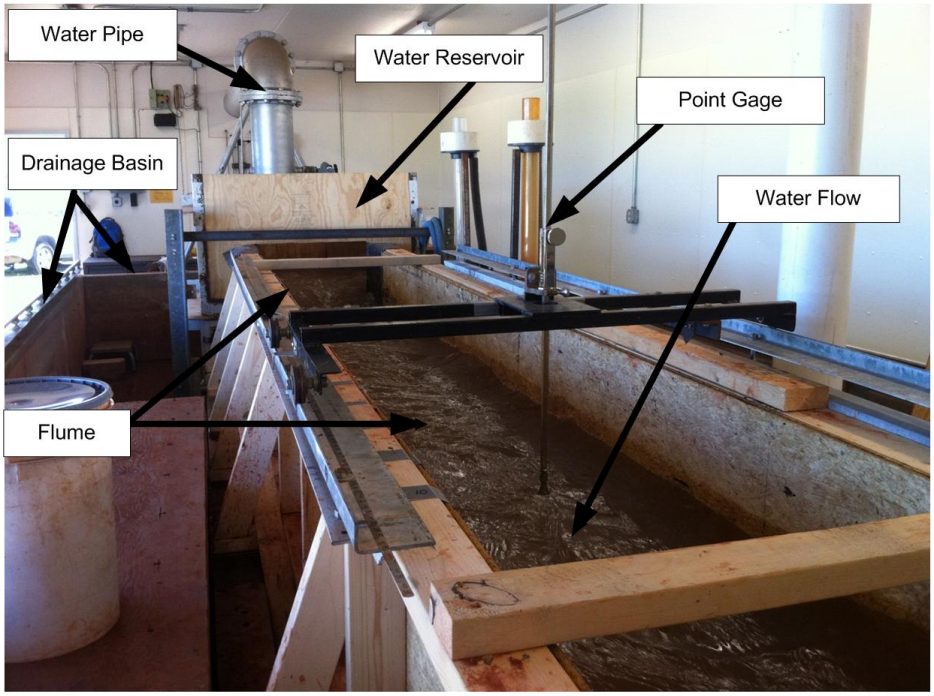

Figure 3.3. An indoor flume.

The "mini" JET apparatus (Figure 3.4c) consisted of the following parts: pressure gauge, outlet and inlet water, depth gauge, rotatable plate, submergence tank, foundation ring, valve, and hoses. The adjustable head tank was used to provide the desired water head. The scour readings were taken using the depth gauge, where the depth gauge of the "mini" JET was different from the point gauge of the original JET, but both have the same function of reading the scour depth. The rotatable plate had a 3.18 mm diameter nozzle. This rotatable plate was used to prevent the water from impinging upon the soil sample at the beginning of testing and during scour depth

readings at different times during the test runs. The submergence tank was 70 mm in height and 101.6 mm in diameter with a 6.4 mm wall thickness. The submergence tank did not open from the top, and the rotatable plate and depth gauge were attached to the top of the tank. The foundation ring was 180 mm in diameter and was pushed into the soil 51 mm when used in the flume.

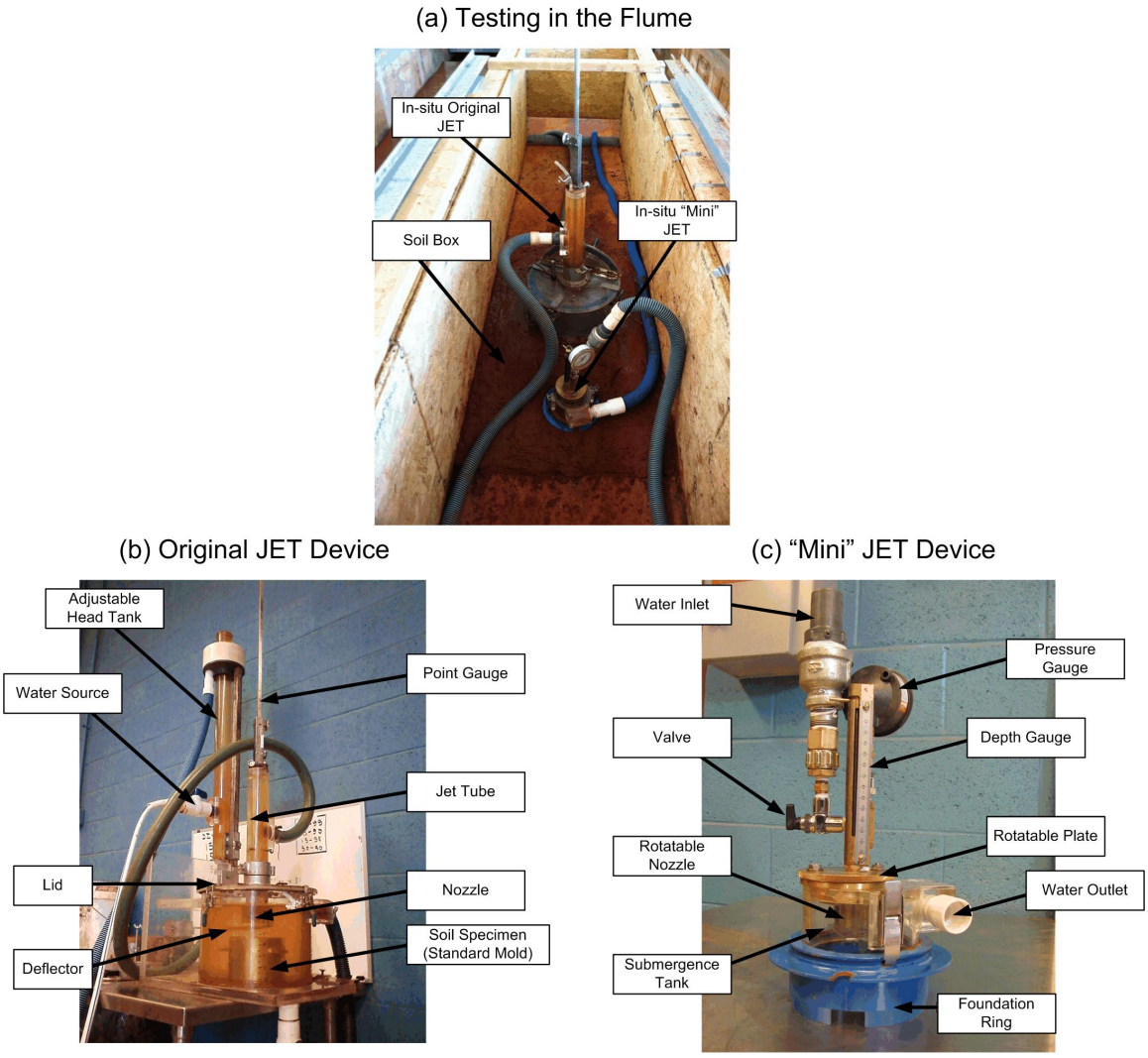

Figure 3.4. In-situ original and "mini" JET devices.

3.5.3. Flow Characteristics for the Flume

For the open channel tests conducted in the flume, the erosion data were used to determine parameters for the excess shear stress model and the "Wilson Model". The effective

stress, τ_e, was defined by accounting for the channel roughness using the Meyer-Peter and Muller formula for stress partitioning in the same manner as defined by Hanson (1990a):

$$\tau_e = \gamma_w DS(\frac{n}{M_n})^b \tag{3.26}$$

where D is the water depth, n is the Manning's roughness coefficient for the soil grain roughness and assumed to be 0.0156 (Temple et al., 1987; Hanson, 1989), M_n is the Manning's roughness for overall roughness, and b is a variable ranging from 4/3 to 2. A b value of 2 was used for bare channels similar to Temple (1980) and Hanson (1989). The value of M_n was calculated using Manning's formula and the measured discharge and slope for each flume run. The effective shear stress (τ_e) was used instead of the average shear stress (τ) in the "Wilson Model" when applied to the flume test data.

The excess shear stress model parameters (k_d and τ_c) were evaluated in a similar fashion to the procedure used by Hanson (1990a) by assuming that the critical stress was approximately zero. This assumption was verified for these soils from previous JETs (Al-Madhhachi et al., 2012a). Therefore, the erosion rate can be simplified to:

$$\varepsilon_r = k_d \tau_e \tag{3.27a}$$

By substituting equation (3.26) into equation (3.27a) yields:

$$\varepsilon_r = k_d \gamma_w DS(\frac{n}{M_n})^2 \tag{3.27b}$$

and integrating equation (3.27b) for the specified time intervals during testing yields:

$$d_{t_0} - d_{t_1} = k_d \int_{t_0}^{t_1} \gamma_w DS(\frac{n}{M_n})^2 dt \tag{3.28a}$$

The integral form of equation (3.28a) was chosen for data analysis to reduce the sensitivity of short term fluctuations (Hanson, 1990a). The integral form provides the average scour versus average shear stress. For *N* shear stresses, equation (3.28a) represented the series of readings (average effective shear stress versus time) expressed as (Hanson, 1990a):

$$d_{t_0} - d_{t_1} = k_d \sum_{i=1}^{N} \tau_{ei} \Delta t_i \qquad (3.28b)$$

where d_{t_0} is the soil surface elevation at starting time (t = 0) and d_{t_1} is the soil surface elevation at time t_1. The k_d is the slope of cumulated scour depth versus the effective shear stress times the time interval Δt.

3.5.4. Flow Characteristics for the "Mini" JET

The analytical method used in this study was the same for both the "mini" and original JET devices. The only modification was the value of the discharge coefficient (*C*). Al-Madhhachi et al. (2012a, Chapter II) suggested that *C* values for the "mini" JET were 0.70 to 0.75 while the *C* value for original JET was 0.95 to 1.00. The *C* value was the slope of the measured discharge rate versus $A\sqrt{2gh}$ (where *A* is the nozzle area for JET devices) for each applied water head, *h*.

3.5.5. Soil Characteristics and Experimental Procedure

The two soils utilized in the flume and in-situ JET experiments were a silty sand soil and clayey sand soil (Table 3.1). These soils have been tested and analyzed according to ASTM Standards (2006). Sieve analysis and hydrometer tests were conducted according to ASTM Standard D422. Liquid limit and plastic limit tests were performed according to ASTM Standard D4318.

The method of sample preparation for the flume and the JET devices were the same but tests were conducted at different times. The soils were air dried and crushed into small pieces. In order to achieve the desired water content for compaction, the soils were mixed with a pre-defined quantity of water and left for 24 hr to allow for moisture equilibrium. The soils were packed at the dry side of optimum water content (10% to 12% for silty sand and 9% for clayey sand), at optimum water content (14 % to 15% for silty sand and 11 % for clayey sand), and on the wet side of optimum water content (18 % for silty sand and 15% to 17 % for clayey sand). Then, the soil was compacted in the flume soil box in five equal lifts to a pre-defined volume using a hand packer (25 cm by 25 cm base plate). Soil samples were prepared and tested immediately after placement. Tests were repeated twice for each test method.

Table 3.1. Properties of the two soils for testing the two JET devices (Al-Madhhachi et al., 2012a).

Soil Location	Soil Texture			Plasticity Index (%)	Standard Compaction		Soil Classification USCS
	Sand (%)	Silt (%)	Clay (%)		Maximum Density (Mg/m^3)	Optimum Water Content (%)	
USDA Hydraulic lab	57	18	25	4	2.00	10.8	SC – Clayey Sand
Streambank of Cow Creek	72	13	15	Non-Plastic	1.83	12.9	SM – Silty Sand

Steps for running the JET devices and collecting data followed the procedure described by Al-Madhhachi et al. (2012a, Chapter II). For flume tests, the following steps were used for running the flume and collecting data (Figure 3.3). Before turning flow into the flume, point gage readings were taken to determine the channel bed level and the initial soil surface at time zero for each station. The flume was usually divided into 10 stations with an interval of 30 cm upstream and downstream of the test section and intervals of 15 cm in the test area of the channel bed. Following point gage readings, the water source was opened to fill the water reservoir and the time of testing was started when the water reached the soil surface in the test section of the flume.

The readings of the scour bed and water depth were taken using the point gage at different time intervals. Usually, the readings were acquired each 5 to 10 minutes with a maximum test period of 120 minutes.

3.5.6. Comparing the "Wilson Model" versus Excess Shear Stress Model

Data from the flume and JET devices (original and "mini" JET devices) were used to determine the excess shear stress model parameter (k_d). The excess shear stress model parameter τ_c was assumed equal to zero for flume analysis and was found to be small (< 0.1 Pa) for the JET devices. The flume and JET devices were also used to determine the "Wilson Model" parameters (b_o and b_1) for both silty sand and clayey sand soils placed at different water contents. The k_d was determined from the observed flume data and from the observed JET data based on the analytic methods developed by Hanson (1990a) and Hanson and Cook (1997), respectively. The "Wilson Model" parameters (b_o and b_1) were derived from observed JET and flume data using an iterative solution of the parameters using a statistical method to minimize the error between the measured data and the functional solutions of the equations (equation 3.16a for flume data and equation 3.23a for JET data) using the solver routine in Microsoft Excel which utilized the generalized reduced gradient method. Constraints were used within the Excel solver routine to limit potential solutions of the "Wilson Model" parameters (b_o and b_1) as recommended by Wilson (1993b). The maximum allowable change for the parameters (b_o and b_1) was between 50% to 60% of their initial estimated values as recommended by Wilson (1993b).

In order to compare the excess shear stress model and the "Wilson Model", the normalized objective function (*NOF*) (Pennell et al., 1990; Hession et al., 1994) was calculated to quantify the acceptability of the models to fit the observed data. The *NOF* is the ratio of the standard deviation (*STDD*) of differences between observed and predicted data to the overall mean (X_a) of the observed data:

$$NOF = \frac{STDD}{X_a} = \frac{\sqrt{\frac{\sum_{i=1}^{N}(x_i - y_i)^2}{N}}}{X_a} \tag{3.29}$$

where x_i and y_i are the observed and predicted data, respectively, and N is the number of observations. In general, 1%, 10%, and 50% deviations from the observed values result in *NOF* values of 0.01, 0.1, and 0.5, respectively (Fox et al., 2006b). Also, statistical tests were performed to determine the occurrence of statistically significant differences between the dry density of the samples tested, differences between the determined excess shear stress model parameter (k_d), and differences between the determined detachment rate model parameters (b_o and b_1) when using data from the flume and the JET devices. The Shapiro-Wilk normality test was used to determine the appropriate statistical test when comparing data from the three groups: flume, original JET, and "mini" JET. One-way ANOVA was conducted when the Shapiro-Wilk test indicating normality; ANOVA based on ranks was conducted when the Shapiro-Wilk test failed. All statistical tests were performed in SigmaStat (SigmaPlot v11, Systat Software, San Jose, CA).

3.6. RESULTS AND DISCUSSION

The excess stress model parameter k_d and the "Wilson Model" parameters b_0 and b_1 were determined for both the flume and JET devices for tests on a series of soil samples compacted on the dry side of optimum water content, at optimum water content, and on the wet side of optimum water content. Tested samples for the flume and JET devices were statistically equivalent in terms of packing based on determining the dry density of each soil sample at different gravimetric water contents (Figure 3.5 and Table 3.2). As was stated previously, the critical shear stress values were assumed to be zero for the flume analysis which is similar to the assumption by Hanson (1990a). Values of τ_c from previous JET research on these soils confirmed this

assumption as most were less than 0.1 Pa (Al-Madhhachi et al., 2012a). Therefore, Table (3.2) and the discussion of results do not include the statistical tests of τ_c.

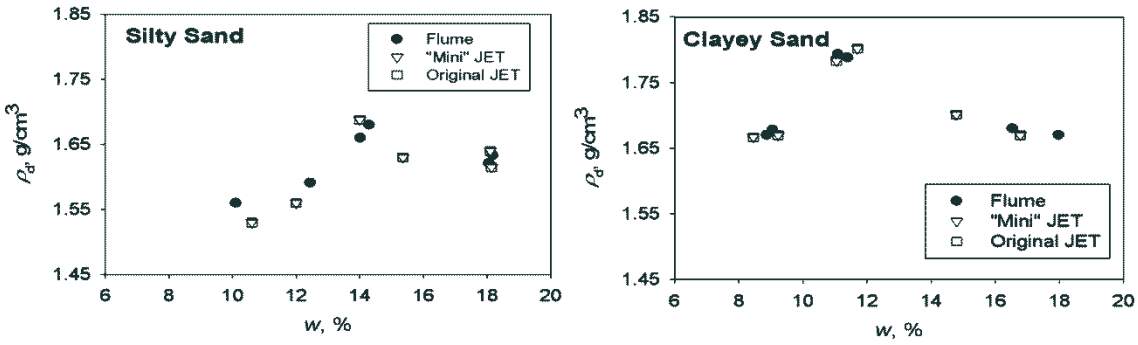

Figure 3.5. The compacted dry densities (ρ_d) and gravimetric water contents (W) relationship between prepared samples for the flume and JET devices prepared channel beds.

Table 3.2. Results from statistical one way ANOVA (used when the Shapiro-Wilk normality test passed) and ANOVA on rank tests (used when the Shapiro-Wilk normality test failed) for differences between the predicted detachment rate model parameters with the "mini" JET, original JET, and flume. All tests were performed based on six observations for the flume and both JET devices (18 total samples across all measurement procedures).

Soil Type	Parameter	Shapiro-Wilk Normality Test	Flume[a] Mean (St. Dev.) or Median (25^{th}-75^{th} Percentiles)	Original JET[a] Mean (St. Dev.) or Median (25^{th}-75^{th} Percentiles)	"Mini" JET[a] Mean (St. Dev.) or Median (25^{th}-75^{th} Percentiles)	P-value
Silty Sand	ρ_d, g/cm^3	Passed, P = 0.31	1.62 (0.04)	1.61 (0.06)	1.61 (0.06)	0.88
	k_d, cm^3/N-s	Failed, P < 0.05	3.11 (6.72)	1.58 (8.18)	3.76 (12.45)	0.47
	b_0, g/m-s-N$^{0.5}$	Failed, P < 0.05	11.42 (16.01)	14.90 (30.97)	14.76 (45.81)	0.59
	b_1, Pa	Passed, P = 0.26	4.47 (1.69)	24.49 (11.33)	8.78 (4.93)	<0.01[b]
Clayey Sand	ρ_d, Mg/m^3	Failed, P < 0.05	1.68 (0.12)	1.69 (0.12)	1.69 (0.12)	0.93
	k_d, cm^3/N-s	Failed, P < 0.05	3.14 (8.87)	1.90 (14.15)	2.79 (17.40)	0.83
	b_0, g/m-s-N$^{0.5}$	Failed, P < 0.05	11.35 (24.05)	14.14 (101.35)	9.48 (134.81)	0.70
	b_1, Pa	Passed, P = 0.05	6.37 (3.37)	21.35 (10.79)	9.28 (5.47)	<0.01[b]

[a] If the Shapiro-Wilk normality test passed, values reported for the flume and JETs are means with standard deviations reported in parentheses. Otherwise, medians are reported along with the difference between the 25^{th} and 75^{th} percentiles.

[b] P-value < 0.05 indicted a statistically significant difference. For both cases the significant difference was when comparing the original JET estimates to the flume and/or "mini" JET.

It can be observed from Figure (3.6) that similar k_d values were derived with the flume and JET devices. The flume and both JET devices results were consistent for all water contents for both soils with the exception of the driest samples. Possible explanations of the observed difference in the results is due to differences in the variability in soil sample texture from test to test, soil compaction, water content levels between prepared soil samples, and the applied shear

stress of the flume. However, the results from the flume tests provided statistically equivalent values of derived k_d to the original and "mini" JET devices at different water contents for both soils (Figure 3.6 and Table 3.2).

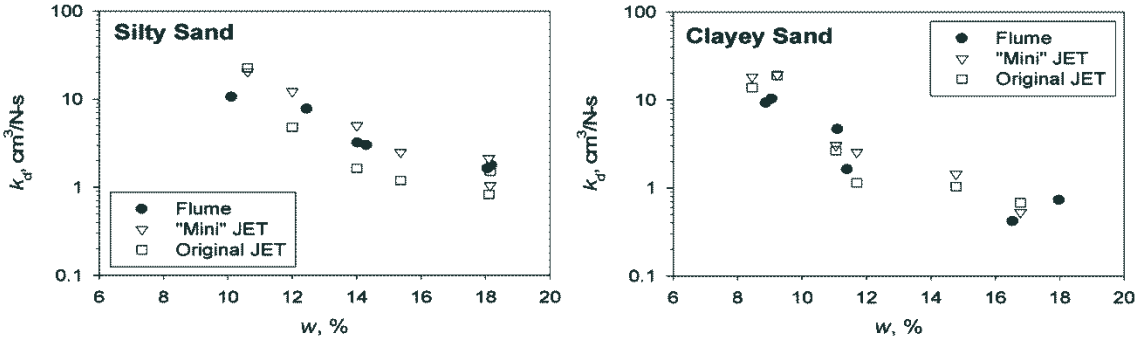

Figure 3.6. Derived k_d values from the flume and the original and "mini" JET devices for the silty sand and clayey sand soils at different water contents.

A comparison of the "Wilson Model" parameters (b_o and b_1) between the flume and JET devices at different water contents for both soils are shown in Figure (3.7). Even though there are factors (i.e., K_o and K_{oj}) in parameters b_o and b_1 that depend on hydraulic conditions, both "Wilson Model" parameters are primarily soil material parameters that depend on properties of the soil particle or aggregate such as its orientation and the soil cohesion. It can be observed from equations (3.16b) and (3.23b) that the "Wilson Model" parameter b_o in particular depends on soil properties such as particle shape and orientation (which influences k_r) and soil cohesion (which influences K_e), which are functions of the water content at which the soil was packed. The b_o decreased as the water content increased due to an increase in the parameter K_e and a decrease in the parameter k_r (Figure 3.7). This pattern matched the commonly observed behavior of eroded materials when the water content of the packed sample increases. Similar observations are reported for k_d. Therefore, b_o has a similar relationship to but different magnitude than k_d relative to the water content of the packed sample (Figures 3.6 and 3.7). No statistically significant differences were observed in b_o from the flume and JETs as shown in Table (3.2).

The "Wilson Model" parameter (b_1) also depends primarily on soil properties such as the soil particle shape and orientation (which influences k_r), soil particle diameter (d), and soil cohesion (f_c) as shown in equations (3.16c) and (3.23c). There was a slight increase in b_1 as the water content increased due to increasing f_c during packing, more so for the clayey sand than the silty sand (Figure 3.7). Some of the scatter observed in the estimated "Wilson Model" parameters, especially b_1, was due to the compaction method which created inherent soil layering within the soil box. The effect of this layering is visible in the observed scour depth versus time data for both the flume and JETs (Figure 3.8). The solver solution was much more sensitive to values of b_0 than b_1; a much smaller range was observed in the calibrated b_1 than b_0. No statistically significant differences were observed in b_1 except when estimated from the original JET device (Table 3.2).

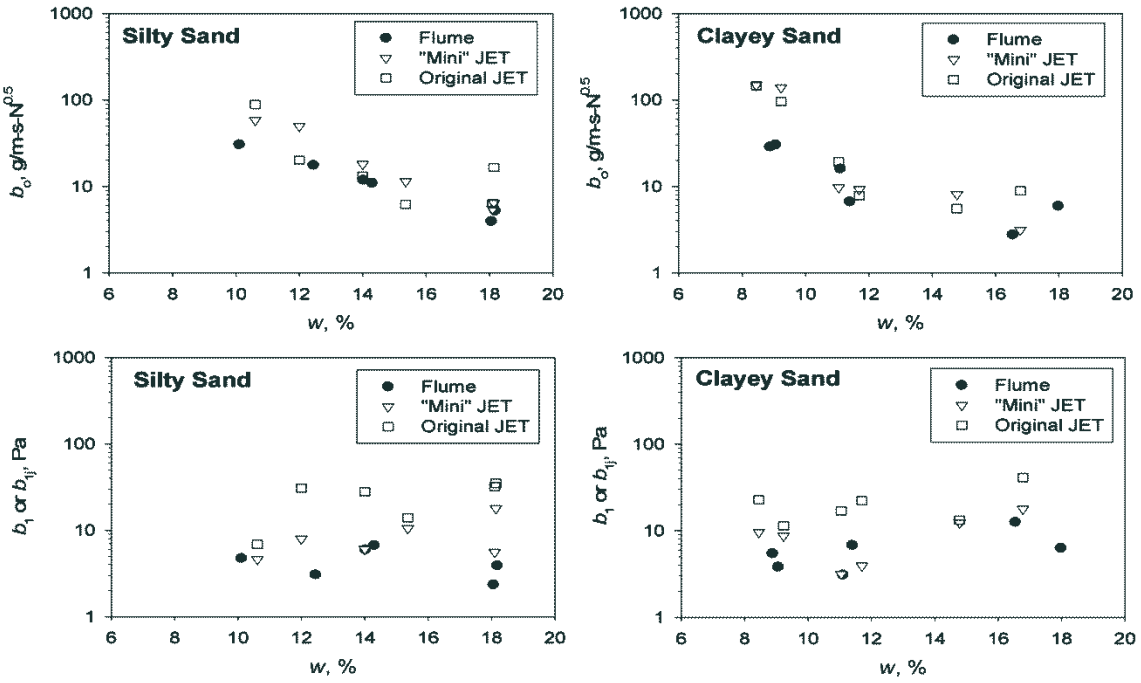

Figure 3.7. Derived b_0 and b_1 from the flume tests and original and "mini" JET devices for the silty sand and clayey sand soils.

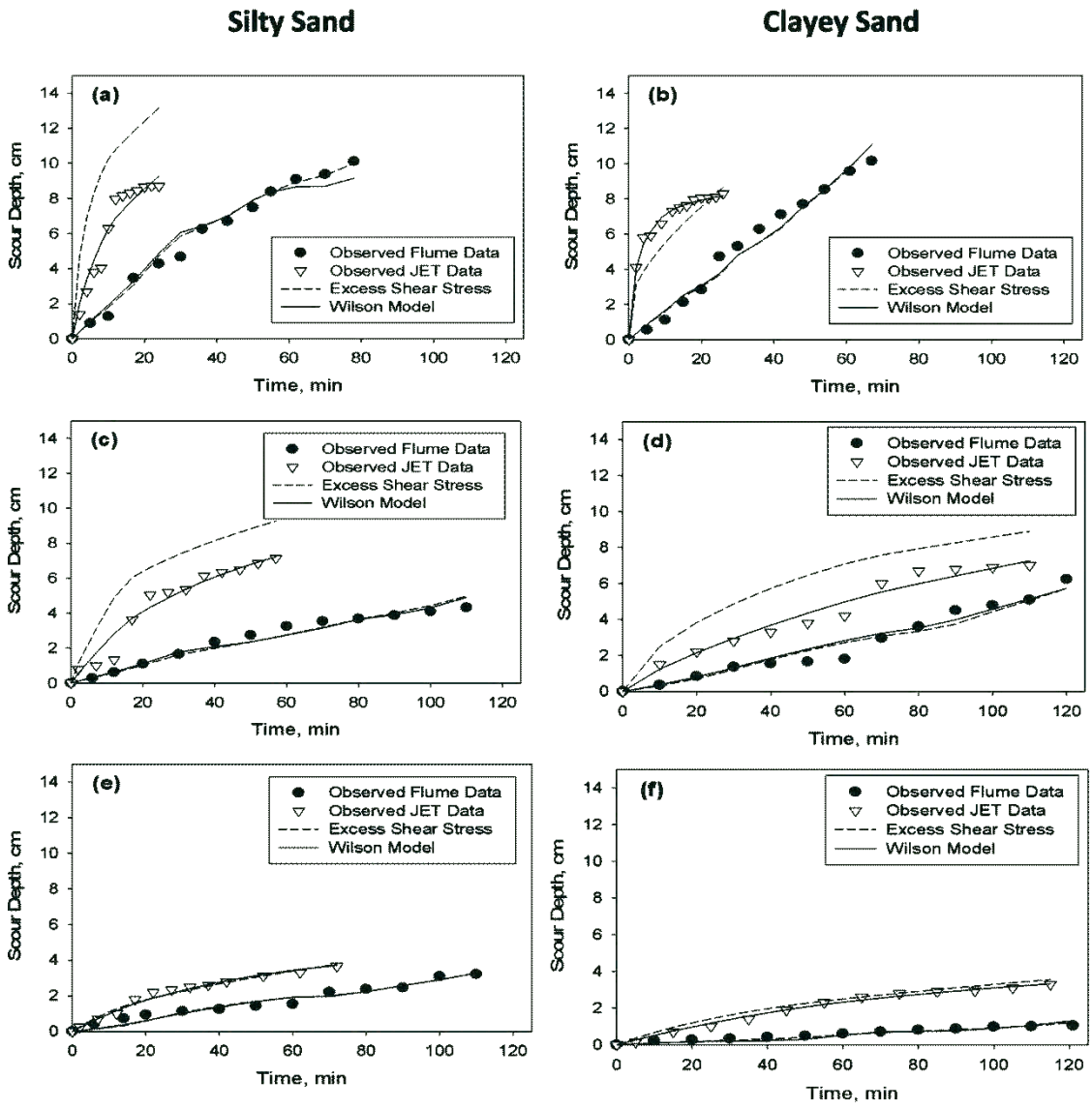

Figure 3.8. Predicting the observed scour depth versus time using the Wilson Model and excess shear stress model from the flume and "mini" JET device for silty sand and clayey sand soils at different water contents: (a) and (b) on the dry side of optimum water content, (c) and (d) at optimum water content, and (e) and (f) on the wet side of the optimum water content.

Comparisons of the actual tests measurements and the predicted scour depths by the excess shear stress model (derived parameter k_d) and "Wilson Model" (derived b_0 and b_1) are shown in Figure (3.8) for the flume tests and "mini" JETs as examples. Based on the *NOF*, the "Wilson Model" predicted the observed data from the flume as well as the excess shear stress model and predicted the observed data from the original and "mini" JET devices better than the

excess shear stress model (Table 3.3). Based on average and maximum *NOF*, the excess shear stress model predicted the observed data from the flume better than data from the original and "mini" JET devices. The performance of the "Wilson Model" was more consistent across the different testing techniques.

Table 3.3. Comparison of the normalized objective function (*NOF*) between the observed scour depth data and either the excess shear stress model or the Wilson Model from the flume tests, original JET device, and "mini" JET device for both soils. All tests were performed with a total number of samples, n = 12 for each device and flume tests.

Models	Flume Tests			"Mini" JET Device			Original JET Device		
	Minimum	Maximum	Average	Minimum	Maximum	Average	Minimum	Maximum	Average
Excess Shear Stress	0.08	0.21	0.14	0.07	0.71	0.31	0.07	0.88	0.36
Wilson Model	0.07	0.23	0.14	0.03	0.13	0.09	0.06	0.31	0.17

3.7. SUMMARY AND CONCLUSIONS

In this study, a mechanistic erosion model (Wilson Model) was described along with the definition of the velocity distributions and methods of analysis for the material parameters b_0 and b_1 for flume and JET data. This model has advantages over the commonly used excess shear stress model because it provides a basis for expanding analysis and in depth accounting of the impact of turbulence, roughness, seepage forces, material soil orientation (i.e. streambed versus streambank), root effects, negative pore water pressure effects, etc. The detachment model, which is referred to as the "Wilson Model", was based on the general framework developed by Wilson (1993a, 1993b) with dimensional soil parameters b_0 and b_1.

Flume test and original and a new miniature version ("mini" JET) of JET devices were used to independently derive the b_0 and b_1 as well as k_d for two cohesive soils: a silty sand and a clayey sand. The flume tests were used as the standard for measurement of the erosion parameters. The advantage of the new "mini" JET is that it is smaller, easier to transport and carry, and requires less water. The "Wilson Model" predicted the observed data for both soils for

flume and the JET data as well as or better than the excess shear stress model. The flume and both JET test devices provided statistically equivalent derived values of b_0 as well as to the excess shear stress model parameter k_d for both soils. The "Wilson Model" parameter b_o has similar relationship but different magnitude as the excess shear stress model parameter k_d relative to the gravimetric water content of the packed sample. The results from this study indicated that the original and "mini' JET can provide equivalent results to flume experiments for deriving the "Wilson Model" parameters. The "Wilson Model" is advantageous in being a more mechanistic, fundamentally based erosion equation as compared to the excess shear stress model; the "Wilson Model" can be used to predict and account for a range of environmental and fluvial conditions experienced (such as seepage forces) using JET techniques.

3.8. ACKNOWLEDGEMENTS

This research is based upon work supported by the National Science Foundation under Grant No. 0943491. Any opinions, findings, and conclusions or recommendations expressed in this material are those of the authors and do not necessarily reflect the views of the National Science Foundation. The authors acknowledge David Criswell and Mohammad Rahi, Oklahoma State University, for assisting with the flume experiments.

CHAPTER IV

MECHANISTIC DETACHMENT RATE MODEL TO PREDICT SOIL ERODIBILITY DUE TO FLUVIAL AND SEEPAGE FORCES: I. MODEL DEVELOPMENT[3]

4.1. ABSTRACT

This is the first of two Chapters that develop and evaluate a mechanistic detachment model to predict soil erodibility due to fluvial and seepage forces. Usually the erosion rate of cohesive soils due to fluvial forces is computed using an excess shear stress model, dependent on two major soil parameters: the critical shear stress (τ_c) and the erodibility coefficient (k_d). A submerged jet test apparatus (JET – Jet Erosion Test) is one method for measuring these parameters. However, no mechanistic approaches are available for incorporating seepage forces into the excess shear stress model parameters. The objectives of this study were 1) to incorporate seepage forces into a mechanistic fundamental detachment rate model to improve predictions of the erosion rate of cohesive soils, and 2) to investigate and predict the influence of seepage gradient forces on the model parameters using JET methods. The new detachment model, which

[3] Submitted to *ASCE, Journal of Hydraulic Engineering*
Al-Madhhachi, A. T., Fox, G. A., Hanson, G. J., Tyagi, A. K., and Bulut, R. 2013a. Mechanistic Detachment Rate Model to Predict Soil Erodibility due to Fluvial and Seepage Forces: I. Model Development. J. Hydraulic Eng., ASCE.

is referred to as the "Modified Wilson Model", was based on two modified dimensional soil parameters (b_0 and b_1) that included seepage forces due to localized groundwater flow. An example is presented to determine the soil erodibility for cases with and without seepage. The influence of seepage forces can be predicted by incorporating the known seepage gradients into the "Modified Wilson Model" parameters (b_0 and b_1) from performed flume and/or JETs without seepage. The more fundamental detachment model can be used in place of the excess shear stress model with parameters that can be derived from flume tests and/or JETs.

4.2. INTRODUCTION

Numerous factors affect the erodibility of cohesive soils such as soil characteristics, soil moisture content, and the physical/chemical properties of the eroding fluid. Typically the erosion rate of cohesive soils due to fluvial forces is approximated using an excess shear stress model, dependent on the hydraulic boundary average shear stress (τ , Pa) and two parameters: the critical shear stress (τ_c, Pa) and the erodibility coefficient (k_d, cm^3/N s). The erosion rate is typically expressed as (Partheniades, 1965; Hanson, 1990a, 1990b; Al-Madhhachi et al., 2012a, 2012b):

$$\varepsilon_r = k_d \left(\tau - \tau_c\right)^a \tag{4.1}$$

where ε_r is the erosion rate (cm/s) and a is an empirical exponent usually assumed to be unity (Hanson, 1990a, 1990b; Hanson and Cook, 1997).

Numerous studies have measured k_d and τ_c for cohesive soils using several techniques. A submerged jet test (JET - Jet Erosion Test) apparatus is one of the methods that has been developed for measuring these parameters in situ as well as in the laboratory (Hanson, 1990a, 1990b; Hanson and Cook, 1997; Hanson and Simon, 2001; Hanson and Hunt, 2007). A new miniature version of the JET device, which is referred to as the "mini" JET, was recently

developed (Al-Madhhachi et al., 2012a). The "mini" JET device is smaller, lighter, and requires less water compared to the original JET device and can be more easily handled in the field as well as in laboratory. The "mini" JET provides results which are essentially equivalent to the original JET (Simon et al., 2010; Al-Madhhachi et al., 2012a).

When quantifying fluvial erosion rates, the interaction between the fluvial forces and adjacent near-surface groundwater forces are generally neglected (Fox and Wilson, 2010). Recent studies have demonstrated the importance of ground water seepage on erosion and bank or hillslope failure (Fox et al., 2007; Wilson et al., 2007; Fox and Wilson, 2010). Several studies have investigated erosion specifically due to seepage, including the development of empirical sediment transport models for this process (Lobkovsky et al., 2004; Fox et al., 2006; Fox et al., 2007; Wilson et al., 2007; Chu-Agor et al., 2008; Chu-Agor et al., 2009). Lobkovsky et al. (2004) presented a quantitative analysis of three modes of sediment mobilization: surface erosion, fluidization, and slumping in a non-cohesive soil. They studied the onset of erosion with shear stresses created by surface and subsurface flow. They derived a critical slope equation with the rationale that slopes greater than the critical were unstable to erosion with seepage.

Fox et al. (2006) developed an empirical sediment transport model for seepage erosion of non-cohesive streambank materials. They performed two-dimensional soil lysimeter experiments with three different soil layers to simulate seepage erosion occurring at Little Topashaw Creek, Northern Mississippi. Their model depended on a dimensionless sediment discharge and dimensional seepage flow shear stress. Fox et al. (2007) reported relationships between erosion rate and seepage discharge mimicking excess stress formulations from field measurements of seepage erosion at Goodwin Creek. Chu-Agor et al. (2008) investigated the underlying mechanisms of hillslope instability by seepage in three-dimensional laboratory soil blocks. Chu-Agor et al. (2009) developed a methodology for simulating seepage erosion undercutting in streambanks through an empirical sediment transport function based on an excess gradient for

cohesive soils. The intricate linkage between seepage and fluvial forces has recently been emphasized in field seepage experiments (Midgley et al., 2012a).

When considering multiple forces, the disadvantage of using an excess shear stress model is the lack of mechanistic predictions of its parameters for specific soil and hydraulic conditions. A more fundamentally-based, mechanistic detachment model is preferred for modeling the range of environmental conditions experienced during fluvial erosion. For example, recent research on seepage processes on hillslopes and streambanks suggests these processes may be important during fluvial erosion in increasing the erodibility of cohesive soils (Fox and Wilson, 2010). A mechanistic detachment model provides the means for incorporating seepage forces directly.

Wilson (1993a, 1993b) developed a mechanistic detachment model to provide a general framework for studying soil and fluid characteristics and their impact on cohesive soil erodibility. The model was developed based on a simple two-dimensional representation of particles. However, the detachment model is not restricted to a single particle and can be applied for aggregates. The model was evaluated using erosion rate data for cohesive soils. The model was calibrated to the observed data based on two dimensional parameters b_0 and b_1. The model represented the observed data as well as or better than the excess shear stress model. However, the parameters could only be derived from observed erosion data from flumes or open channels, which limited its applicability at the time of development.

Recently Al-Madhhachi et al. (2012b, Chapter III) incorporated the hydraulic analysis methods of JET devices into the fundamental detachment model ("Wilson Model") to predict the erodibility of cohesive soils. They used both the original and "mini" JET devices and verified the results with flume tests. The "Wilson Model" predicted the observed data for flume and JET devices as well as or better than the excess shear stress model. The flume and "mini" JET device provided statistically equivalent derived values of b_0 and b_1 as well as the excess shear stress

model parameter k_d. Therefore, a more fundamentally-based detachment model can be used in the place of the excess shear stress model with parameters that can be estimated using existing JET techniques.

The next step is to utilize the "Wilson Model" to analyze the influence of seepage forces on the erodibility of cohesive soils. The objectives of this research were to (1) incorporate seepage forces into the fundamental detachment model with the new model referred to as the "Modified Wilson Model" and (2) to investigate and predict the influence of seepage gradient forces on the model parameters using JET methods.

4.3. GENERAL THEORETICAL FRAMEWORK INCLUDING SEEPAGE

The general framework for predicting erosion rate was based on the dislodging and stabilizing forces and their associated moment lengths for particle detachment (Wilson, 1993a). Figure (4.1) is a conceptual sketch of the forces that act to remove a soil particle including the lift force, F_L, drag force, F_d, particle weight, w_s, contact forces between particles (F_{c1}, F_{c2},……, F_{cn}), and the addition seepage force, F_s. Particle detachment occurs if the driving moment is greater than the resisting moment (Wilson, 1993a). Wilson (1993a) assumed that these moments acted around point *A*. The point of incipient motion with the addition of seepage force can be defined as:

$$F_d(l_3) + F_L(l_4) + w_s \sin(\alpha)(l_1) + F_s \cos\alpha(l_2) = w_s \cos(\alpha)(l_2) + F_s \sin\alpha(l_2) + M_c \qquad (4.2)$$

where $w_s = g(\rho_s - \rho_w)k_v d^3$ is the submerged particle weight; ρ_s is a particle density (a typical value of 2.65 Mg/m^3 has been suggested by Freeze and Cherry (1979) to characterize the soil particle density of a general mineral soil); ρ_w is the water density; *d* is an equivalent particle diameter; $k_v(=\frac{\pi}{6})$ is the volume constant of a spherical particle; $F_s = iVg\rho_w = \frac{H}{L}k_v d^3 g\rho_w$ is

the seepage force on a single particle; i is the hydraulic gradient; V is the volume of a single soil particle; H is a seepage head; L is the soil length over which the gradient is calculated; $M_c = \sum_{i=1}^{n_c} \sigma_{ci} a_i \bar{l}_i$ is the sum of moments of cohesive and frictional forces (Wilson, 1993a); n_c is the number of contact areas; σ_{ci} is a particle to particle stress; a_i is the contact area; $\bar{l}_i$ is the moment length for each contact force; l_1, l_2, l_3, l_4, and l_5 are lengths of moments for the forces; and α is the channel angle slope.

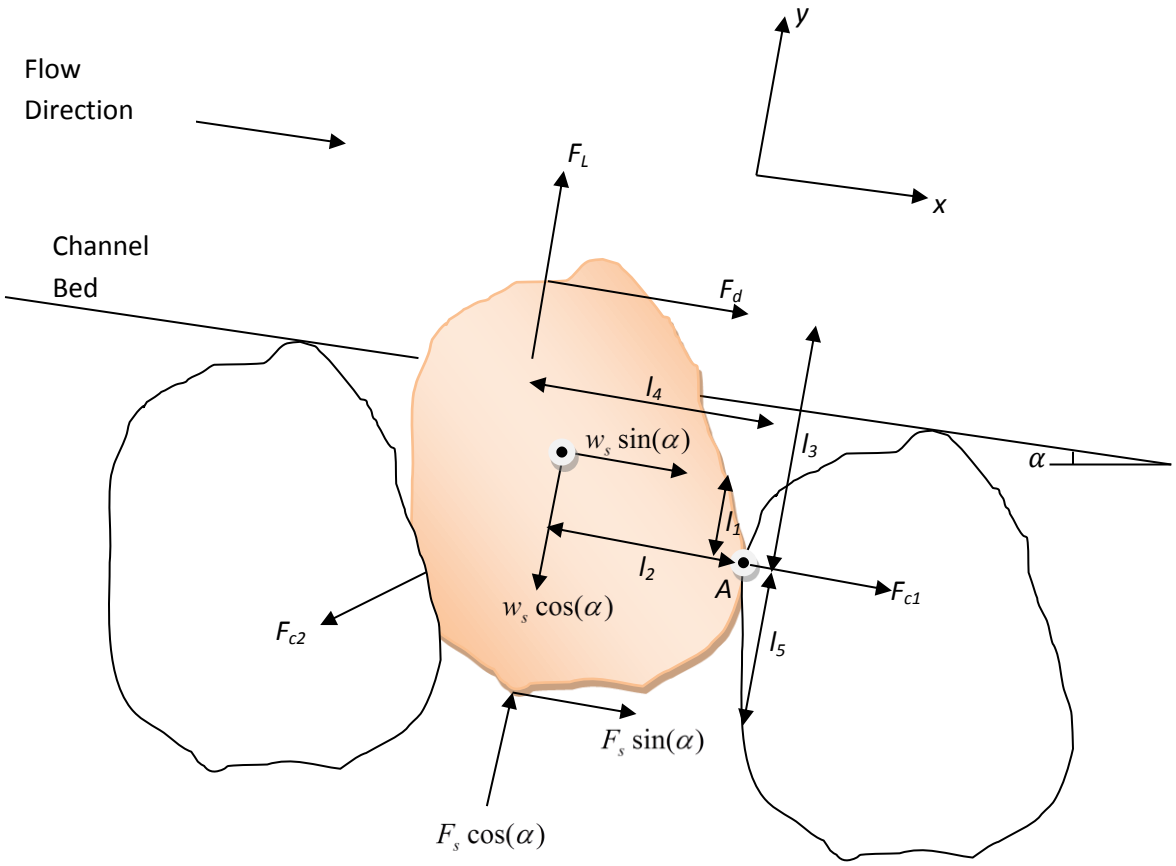

Figure 4.1. Forces and moment lengths acting on a single soil particle in a channel bed in the presence of a seepage force (where F_L is the lift force; F_d drag force; w_s is the submerge particle weight; F_{c1}, F_{c2},……, F_{cn} are contact forces between particles; F_s is the seepage force; l_1, l_2, l_3, l_4 and l_5 are lengths of moments for the forces; and α is the channel angle slope).

By assuming that the drag force and lift force are proportional (i.e., $K_L/K_f = F_L/F_d$) (Chepil, 1959; Wilson, 1993a) and incorporating the seepage force formula, equation (4.2) can be rewritten as:

$$F_d = w_s\left[\frac{\cos(\alpha)(l_2)-\sin(\alpha)(l_1)}{l_3 + l_4\frac{K_L}{K_f}}\right] - \frac{H}{L}k_v d^3 g\rho_w\left[\frac{\cos(\alpha)(l_2)-\sin(\alpha)(l_5)}{l_3 + l_4\frac{K_L}{K_f}}\right] + \left[\frac{M_c}{l_3 + l_4\frac{K_L}{K_f}}\right] \quad (4.3)$$

The above equation can be rearranged by introducing K_{ls}, K_s, and f_c terms:

$$F_d = w_s(K_{ls} - K_s + f_c) \quad (4.4a)$$

$$K_{ls} = \frac{\cos(\alpha)(l_2 - l_1 S)}{l_3 + l_4\frac{K_L}{K_f}} \quad (4.4b)$$

$$K_s = \frac{H\rho_w}{L(\rho_s - \rho_w)}\frac{\cos(\alpha)(l_2 - l_5 S)}{l_3 + l_4\frac{K_L}{K_f}} \quad (4.4c)$$

$$f_c = \frac{M_c}{w_s(l_3 + l_4\frac{K_L}{K_f})} \quad (4.4d)$$

where K_{ls} is a dimensionless parameter that depends on particle size, its orientation within the bed, and slope (Wilson, 1993a); K_s is a seepage parameter that depends on hydraulic gradient, particle density, its orientation within the bed, and slope; f_c is a dimensionless parameter based on cohesion; K_L is the ratio of drag and lift coefficients along with the ratio of velocities, assumed equal to 1 (Wilson, 1993a, 1993b); K_f is the ratio of projected area drag and lift forces; k_r (= k_v/ k_a = 2/3) is the geometry ratio for a spherical particle; k_a (= π/4) is the area constant of a spherical particle; and $S\ (=\tan\alpha)$ is the channel slope.

The particle is detached if the flow characteristic on the left side (F_d) of equation (4.4a) is greater than the right side, $w_s(K_{ls} - K_s + f_c)$, which is primarily a function of seepage, particle, and bed characteristics. Wilson (1993b) suggested that the values of moment lengths for equal radii of spherical particles are l_1 = 0.86 d/2, $l_2 = l_4$ = 0.5 d/2, and l_3 = 1.18 d/2. These moments lengths were computed based on combinations of particles sizes and gaps developed by Wilson (1993b). Accordingly, the new moment length (l_5), which is the moment length of the horizontal component of seepage force, is equal to 0.14 d/2. Similarly, based on combination of particles sizes and gaps, Wilson (1993b) suggested that K_f ranges between 0 to 1 with a value equal to 0.92 for equal radii of a spherical particle.

Wilson (1993a, 1993b) developed the original model assuming a spherical particle, which is more appropriate for non-packed materials. The behavior, arrangement, and shape of the particles of compacted cohesive soils are different than those proposed by Wilson (1993b) and are related to moisture/density relationships. Lambe (1962) presented the effects of compaction on clay soil structure compacted at different water contents as related to the arrangement of soil particles and the electric forces between neighboring particles (Figure 4.2). At low water contents (point *A*), the electric repulsive forces between particles are smaller than the attractive forces. This results in a net attraction between the particles; therefore, the particles tend to flocculate in a disorderly array (Lambe, 1962). A more orderly array of particles can be observed as water content increases until the soil reaches its optimum water content (i.e., point *B*) due to an increase in the repulsive forces between the particles, resulting in the maximum bulk density (Figure 4.2). Beyond point *B* (i.e., wet side of the optimum water content), a parallel arrangement between the soil particles is observed leading to a decrease in the bulk density (Lambe, 1962).

Due to the nature of the sample preparation in this study, the arrangement of particles at optimum water content was of interest. Accordingly using the Lambe (1962) model, Figure (4.3)

shows an assumed average arrangement of particles for a compacted soil at optimum water content. The soil particle is assumed to be a tetragonal shape system (plate) with an angle of 90 degrees at its edges and a square top face. Therefore, the particle volume (V_p) is equal to $k_v l_p d^2$ and the projected area of drag force (A_p) is equal to $k_a d^2$, where $l_p = n_p d$ is the length of a tetragonal particle, and n_p is a particle length factor which depends on soil texture, soil orientation, and compaction degree. Therefore, the volume constant (k_v) of a tetragonal particle is equal to n_p and the area constant (k_a) of a tetragonal particle is equal to unity. Accordingly, the geometry ratio (k_r) for a tetragonal particle is equal to k_r ($= k_v / k_a = n_p$) and the ratio of projected area drag and lift forces (K_f) is equal to (k_a / n_p) for a tetragonal particle (where $K_f = A_p / A_p^* = k_a d^2 / n_p d^2$, and A_p^* is the projected area of the lift force). Based on Figure (4.3), the values of moment lengths for equal tetragonal particles are $l_1 = 0$, $l_2 = l_4 = d/2$, and $l_3 = l_5 = n_p d/2$ (where point *A* is placed in the middle of a tetragonal particle).

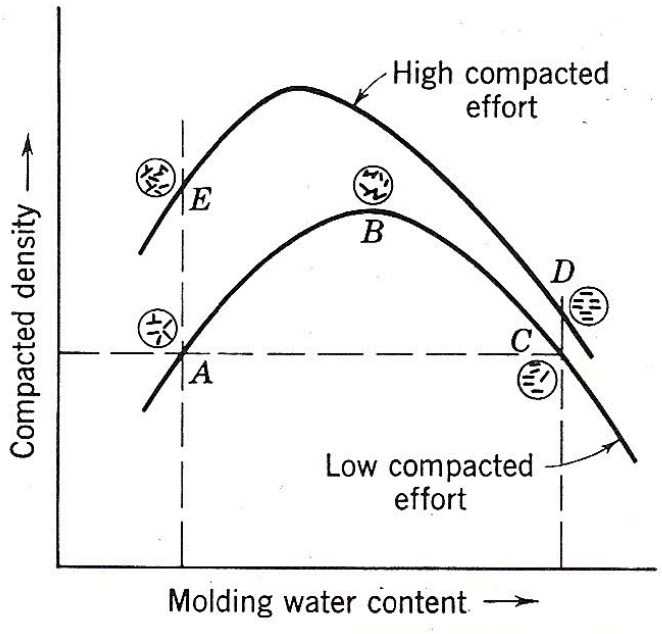

Figure 4.2. Effects of compaction on soil structure (Lambe, 1962).

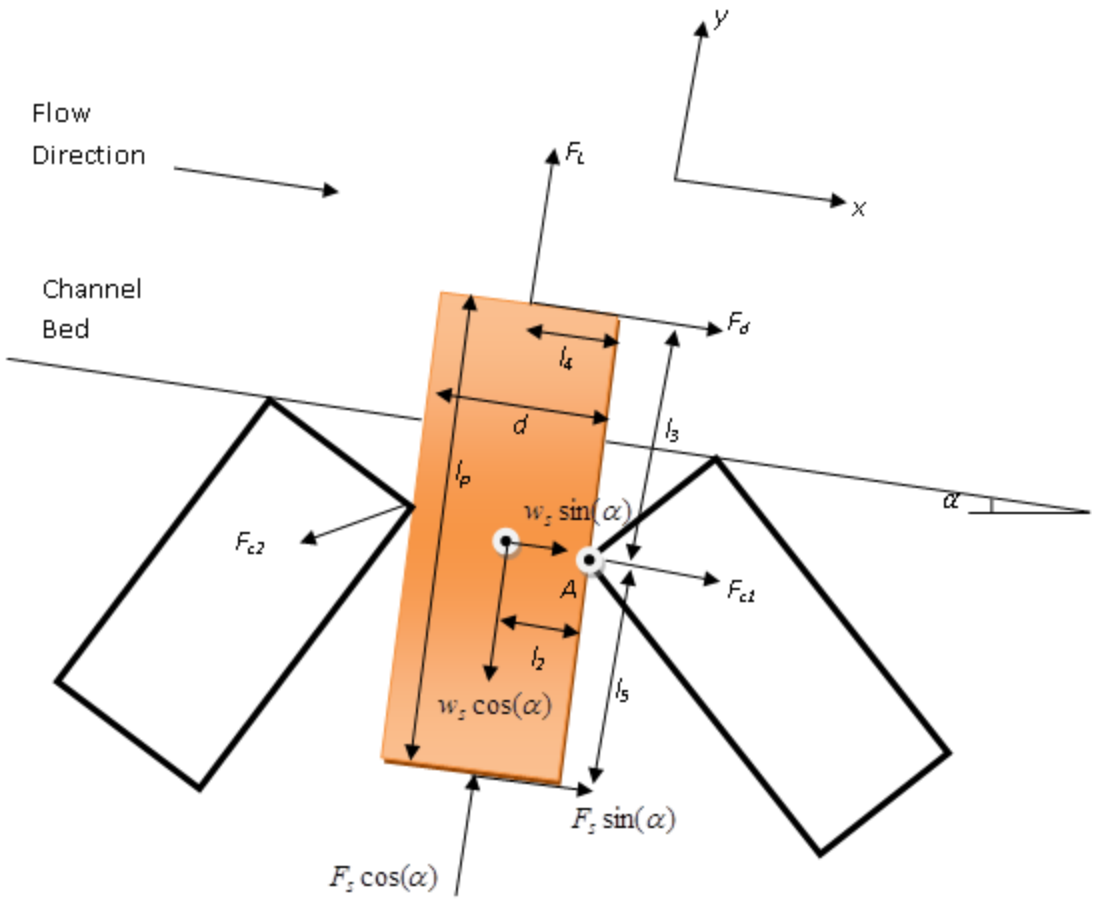

Figure 4.3. The arrangement of a particle for compacted soil as proposed in this study for a horizontal channel (where F_L is the lift force; F_d drag force; w_s is the submerge particle weight; F_{c1}, F_{c2},……, F_{cn} are contact forces between particles; F_s is the seepage force; l_1, l_2, l_3, l_4 and l_5 are lengths of moments for the forces; $l_p = n_p d$ is the length of a tetragonal particle, n_p is a particle length factor; d is an equivalent particle diameter; and α is the channel angle slope).

4.3.1. Flow Characteristics in an Open Channel

The flow in an open channel is always turbulent and the drag force rapidly changes with time and space. Therefore, the mean value is important in characterizing the turbulent flow properties (Wilson, 1993a). Einstein and El-Samni (1949) presented the time averaged forces at the channel bed using the time averaged velocity. The time averaged drag force ($\overline{F}_d$) is expressed as:

$$\overline{F}_d = C_D K_f k_a d^2 \frac{\rho_w U_d^{\,2}}{2} \tag{4.5}$$

where C_D is the drag coefficient and U_d is the time averaged velocity defined by Wilson (1993a):

$$U_d = \frac{u_*}{k}\ln(\phi) + B \tag{4.6a}$$

where k is von Karmon constant equal to 0.4 (Schlichting, 1979); ϕ (= z_d/k_s) is a fraction assumed to be 1.0 by Yang (1973), 0.35 by Einstein and El-Samni (1949), and 0.6 by Wilson (1993b); z_d is a height that the drag velocity is acting upon and it is equal to ($l_3 + y_p$) according to Wilson (1993b); y_p is a pivot point equal to ($k_s - d/2 - l_1$) for a spherical particle and equal to ($k_s - n_p\, d/2 - l_1$) for a tetragonal particle; k_s is a roughness height equal to $d/2\sqrt{3}$ for a spherical particle and equal to ($n_p\, d/2$) for a tetragonal particle; B is a dimensionless term that depends on the laminar sublayer thickness and roughness height defined by the shear Reynolds number, where B ranges from 6.5 to 9.9 (Schlichting, 1979); and u_* is shear velocity expressed as:

$$u_* = \sqrt{\frac{\tau}{\rho_w}} \tag{4.6b}$$

Substituting equations (4.6a) and (4.6b) into equation (4.5) yields:

$$\overline{F}_d = K_o k_a d^2 \tau \tag{4.7a}$$

$$K_o = \frac{[C_D K_f (\frac{1}{k}\ln(\phi) + B)^2]}{2} \tag{4.7b}$$

where K_o is known as a velocity flow parameter in this study.

4.3.2. Incipient Motion

Wilson (1993a) suggested that incipient motion could be estimated using the time averaged values. Then, critical shear stress, τ_c, can be calculated. If the drag force from equation (4.4a) is equal to the time averaged drag force from equation (4.7a), then the critical shear stress to initiate motion (i.e. $\tau_c = \tau$) is determined from:

$$w_s(K_{ls} - K_s + f_c) = K_o k_a d^2 \tau_c \tag{4.8a}$$

$$\tau_c = \frac{k_r}{K_o} g(\rho_s - \rho_w) d(K_{ls} - K_s + f_c) \tag{4.8b}$$

$$\tau_c^* = \frac{\tau_c}{g(\rho_s - \rho_w)d} = \frac{k_r}{K_o}(K_{ls} - K_s + f_c) \tag{4.8c}$$

where τ_c^* is known as the critical Shields parameter. The right side of equations (4.8b) and (4.8c) are related to seepage, soil, and bed characteristics. Wilson (1993b) evaluated his general framework without calibration by calculating the incipient motion of non-cohesive particles (i.e. $f_c = 0$) in the absence of seepage (i.e. $K_s = 0$) and compared them with those obtained from Simons and Senturk (1977). Wilson (1993b) reported that the average predicted detachment rate was 18-22% smaller when using the Wilson Model compared to the excess shear stress model.

4.3.3. Detachment Rate Model

Particle detachment occurs when the drag force in equation (4.4a) is greater than the weight, seepage, and cohesive forces. Wilson (1993a) used a similar probability framework for turbulent forces as developed by Einstein (1950) and Partheniades (1965). Accordingly, the probability of the drag force in the presence of a seepage force (equation 4.4a) is defined as:

$$P = 1 - \int_{-\infty}^{w_s(K_k - K_s + f_c)} f(F_d) d(F_d) \tag{4.9}$$

where P is the exceedance probability of drag force and $f(F_d)$ is a probability density function.

To determine the detachment rate, assume that P is the fraction of the total bed area at a given time. Then the number of particles of diameter d for potential detachment per unit area bed (n_{di}) is expressed as (Wilson, 1993a):

$$n_{di} = \frac{\Delta FF_i P}{k_a d^2} \tag{4.10}$$

where ΔFF_i is the fraction finer value for bed materials and $k_a d^2$ is the projected horizontal area of a single particle. The rate of particle detachment, which is the number of detached particles divided by the time required for those particles to leave other particles, is expressed as (Wilson, 1993a):

$$n_{ri} = \frac{\Delta FF_i P}{k_a d^2 (K_e t_e)} \tag{4.11}$$

where n_{ri} is the particle detachment rate; t_e is the exchange time of a single particle; and K_e is a parameter to account for the additional time to remove surrounding particles such that the underlying particles are no longer protected from the flow. The erosion or detachment rate in units of mass per area per time is determined by multiplying equation (4.11) by the density and volume of each particle and can be expressed as:

$$\varepsilon_{ri} = n_{ri} \rho_s k_v d^3 = \Delta FF_i P \rho_s k_r \left(\frac{d}{K_e t_e}\right) \tag{4.12}$$

The exceedance probability, P, and the exchange time, t_e, can be estimated to determine the erosion or detachment rate. For determining the particle exchange time, Wilson (1993a)

proposed that the particle exchange time was a function of the exit velocity of the particle (V_e) which can be determined from Newton's second law of motion as following:

$$V_e = \frac{F_n}{m} t_e \tag{4.13}$$

where F_n is a time averaged net forces acting in the direction of movement within the exchange time of a particle and $m = (\rho_s - \rho_w) k_v d^3$ is the mass of particle. Wilson (1993a) considered that the vertical of forces (drag force and particle submerged weight) represented the net force for sliding or rolling a particle. Using the same approach proposed by Wilson (1993a), the time averaged net force including seepage can be evaluated as:

$$F_n = K_t \overline{F}_d - \mu_f w_s + \mu_s F_s \tag{4.14}$$

where $\overline{F}_d = K_o k_a d^2 \tau$ is the average drag force; K_t is a factor of cumulating instantaneous fluid forces equal to 2.5 (Chepil, 1959); μ_f is a coefficient of friction; $w_s = g(\rho_s - \rho_w) k_v d^3$ is the submerged particle weight; μ_s is the seepage coefficient which is function of soil and fluid characteristics; and $F_s = i k_v d^3 g \rho_w$ is the seepage force. Substituting equation (4.14) into equation (4.13) yields:

$$V_e = [\frac{K_t K_o k_a d^2 \tau}{(\rho_s - \rho_w) k_v d^3} + \frac{i \mu_s k_v d^3 g \rho_w}{(\rho_s - \rho_w) k_v d^3} - \frac{\mu_f g (\rho_s - \rho_w) k_v d^3}{(\rho_s - \rho_w) k_v d^3}] t_e \tag{4.15}$$

The above equation can be rearranged by introducing τ^* and K_n terms:

$$V_e = [K_n \tau^* + \frac{i \mu_s \rho_w}{(\rho_s - \rho_w)} - \mu_f] g t_e \tag{4.16}$$

where $\tau^* = \frac{\tau}{g(\rho_s - \rho_w)d}$ is the Shields parameter; and $K_n = K_t\ K_o / k_r$ is a combination of particle and fluid factors. Assuming that the particle has to move a distance equivalent to its diameter, the exchange time can be calculated as (Wilson, 1993a):

$$t_e = \frac{k_{dd}}{V_e} d \tag{4.17}$$

where k_{dd} is the detachment distance parameter equal to 2 according to Einstein (1950). Substituting equation (4.16) into equation (4.17) yields:

$$t_e = d \sqrt{\frac{k_{dd}}{gd(K_n\tau^* + \frac{i\mu_s\rho_w}{(\rho_s - \rho_w)} - \mu_f)}} \qquad \text{if } [K_n\tau^* + \frac{i\mu_s\rho_w}{(\rho_s - \rho_w)}] > \mu_f \tag{4.18}$$

In the absence of seepage, the seepage parameter can be neglected (i.e., $\frac{i\mu_s\rho_w}{(\rho_s - \rho_w)} = 0$) and the exchange time of a single particle (equation 4.18) will match that proposed by Wilson (1993a).

Wilson (1993a) used three probability distributions for equation (4.9) to calculate the exceedance probability, *P*: Extreme Value Type I, normal, and log-normal distributions. Wilson (1993a) recommended the Extreme Value Type I because it simplified the detachment model calculations, predicted similar results to the log-normal distribution, and obtained low probabilities for negative drag forces. Therefore, the Extreme Value Type I distribution was also used in this study to represent the exceedance probability of the drag force. By following the same derivation obtained from Wilson (1993a), the Extreme Value Type I distribution in presence of a seepage force is expressed as:

$$P = 1 - \exp[-\exp(-\mu_e)] \tag{4.19a}$$

$$\mu_e = (\frac{\pi}{e_v\sqrt{6}})[\frac{k_r(K_{ls} - K_s + f_c)}{K_o\tau^*} - (1 - \frac{1.365e_v}{\pi})] \quad (4.19b)$$

where μ_e is the upper limit of integration for the Extreme Value Type I distribution and e_v is the coefficient of variation equal to 0.35 according to Einstein and El-Samni (1949). By combining equations (4.12), (4.18), and (4.19), the erosion or detachment rate (ε_{ri} , M/L^2/T) based on turbulent probability in presence of a seepage force is expressed as:

$$\varepsilon_{ri} = \frac{\Delta FF_i}{K_e}\rho_s k_r \sqrt{\frac{gd(K_n\tau^* + \frac{i\mu_s\rho_w}{(\rho_s - \rho_w)} - \mu_f)}{k_{dd}}}\{1 - \exp[-\exp(-\mu_e)]\}$$

$$\text{If } [K_n\tau^* + \frac{i\mu_s\rho_w}{(\rho_s - \rho_w)}] > \mu_f \quad (4.20)$$

Wilson (1993a, 1993b) used a calibration procedure to obtain parameter values including the cohesive parameter, f_c, and the exposure parameter, K_e, because there was a little information available on these parameters. Due to difficulty in determining the interaction between bed particles sizes when the total erosion or detachment rate was determined from equation (4.20), Wilson (1993a, 1993b) developed a single approach to determine the total detachment rate by incorporating the effects of particle sizes indirectly in the calibration procedures. The results of this approach corresponded to those obtained from Einstein and El-Samni (1949). Following the same approach as Wilson (1993a, 1993b), this study assumed that μ_f was small relative to the value of $[K_n\tau^* + \frac{i\mu_s\rho_w}{(\rho_s - \rho_w)}]$ and e_v was 0.36. Therefore, the total erosion or detachment rate, ε_r , in the presence of seepage, is expressed using dimensional parameters b_0 and b_1:

$$\varepsilon_r = b_0\sqrt{\tau}\left[1-\exp\{-\exp(3-\frac{b_1}{\tau})\}\right] \tag{4.21a}$$

$$b_0 = \rho_s \frac{k_r}{K_e}\sqrt{\frac{K_n + K_{st}}{k_{dd}(\rho_s - \rho_w)}} \tag{4.21b}$$

$$b_1 = (\frac{\pi}{e_v\sqrt{6}})\frac{k_r(K_{ls} - K_s + f_c)}{K_o}\, g(\rho_s - \rho_w)d \tag{4.21c}$$

$$K_{st} = \frac{\mu_s gid\rho_w}{\tau} = \mu_{sr} gid\rho_w \tag{4.21d}$$

where b_0 has dimensions of $(M/L^3)^{0.5}$, b_1 has dimensions of F/L^2, K_{st} is the seepage parameter due to exchange time of a particle, and $\mu_{sr} = \frac{\mu_s}{\tau}$ is the seepage coefficient ratio. Note that the τ decreases while μ_s increases as the soil erodes. However, the value of μ_{sr} was found constant and equal to 3.85 based on experimental evidence from flume tests and JETs reported in the Chapter V.

In this study, equations (4.21a)-(4.21c) are referred to as the "Modified Wilson Model". The parameters b_0 and b_1 can be derived from using curve fitting techniques and/or methods that minimize the error of these functions relative to measured erosion data. In the absence of seepage, the seepage parameters can be neglected (i.e., $K_s = 0$ and $K_{st} = 0$) and the developed model will match the set of equations proposed by Wilson (1993a, 1993b). Two common methods for generating data to derive the erodibility parameters of the "Modified Wilson Model" include flume tests and JETs.

4.4. DEFINING FLOW CHARACTERISTICS FOR THE FLUME

For open channel tests conducted in flumes, the erosion data can be used to determine the parameters of the "Modified Wilson Model". The effective stress, τ_e, can be defined by accounting for the channel roughness using the Meyer-Peter and Muller formula for stress partitioning in the same manner as defined by Hanson (1990a):

$$\tau_e = \gamma_w DS(\frac{n}{M_n})^b \tag{4.22}$$

where D is the water depth, n is the Manning's roughness coefficient for the soil grain roughness and assumed to be 0.0156 (Temple et al., 1987; Hanson, 1989), M_n is the Manning's roughness for overall roughness, and b is a variable ranging from 4/3 to 2. A b value of 2 was used by Temple (1980) and Hanson (1989) for bare channels. The value of M_n can be calculated using Manning's formula and the measured discharge and slope for each flume run. The effective shear stress (τ_e) was used instead of the average shear stress (τ) in the "Modified Wilson Model" when applied to flume test data.

4.5. DEFINING FLOW CHARACTERISTICS FOR THE JET DEVICE

The submerged jet has a boundary shear stress equation and velocity distribution profile different than that used in the derivation of the "Modified Wilson Model" (i.e., different velocity flow parameter, K_o) for open channel flow. Hanson and Cook (2004) presented the average shear stress along the boundary, τ_j, in the jet impingement zone as the following:

$$\tau_j = \tau_o \left(\frac{J_p}{J} \right)^2 \tag{4.23}$$

where $\tau_o = C_f \rho_w U_o^2$ is the maximum shear stress due to the jet velocity at the nozzle (Pa); C_f = 0.00416 is the coefficient of friction; $U_o = C\sqrt{2gh}$ is the jet velocity at the orifice (cm/sec); C is discharge coefficient; h is the pressure head (cm); $J_p = C_d d_o$; d_o is the nozzle diameter (cm); C_d = 6.3 is the diffusion constant; and J is the scour depth from jet nozzle height.

Poreh and Cermak (1959) developed an equation for the velocity distribution profile for an unconfined radial jet outside of the boundary layer. Of interest for this study, Al-Madhhachi et al. (2012b, Chapter III) developed the velocity distribution profile for the zone of the diffusion effect, where the maximum boundary reference velocity is at r/J_i equivalent to 0.13, based on the submerged jet velocity profile developed by Poreh and Cermak (1959):

$$V_r = 4.8\sqrt{\frac{K}{J_i^2}}\exp[-100(\frac{z_d}{r})^2] \qquad \text{for } (\frac{r}{J_i} \text{ equivalent to } 0.13) \tag{4.24}$$

where V_r is the velocity profile along jet radius r and $K = 0.153\pi d_0^2 U_0^2$ is a kinematic moment flux (Poreh et al., 1967). By substituting the velocity profile of the submerged jet, equation (4.24) for U_d in equation (4.5), the time averaged drag force for the submerged jet can be expressed as (Al-Madhhachi et al., 2012b):

$$\overline{F}_d = C_D K_f k_a d^2 \frac{\rho_w\left(4.8\sqrt{\frac{K}{J_i^2}}\exp[-100(\frac{z_d}{r})^2]\right)^2}{2} \tag{4.25}$$

where all terms were previously defined. By substituting for K and τ_j, equation (4.25) can be rearranged as the following (Al-Madhhachi et al., 2012b):

$$\overline{F}_d = K_{oj} k_a d^2 \tau_j \tag{4.26a}$$

$$K_{oj} = \frac{11.52 C_D K_f \rho_w K \exp[-200(\frac{z_d}{r})^2]}{J_i^{\,2} \tau_i} = \frac{5.537 C_D K_f \exp[-200(\frac{z_d}{r})^2]}{C_f c_d^{\,2}} \tag{4.26b}$$

where K_{oj} is known as a jet velocity flow parameter. Following the same procedure as above in developing the "Modified Wilson Model" and incorporating equations (4.23) and (4.26), the detachment rate model for JETs under the influence of seepage can be expressed as:

$$\varepsilon_r = b_0 \sqrt{\tau_j} \left[1 - \exp\{-\exp(3 - \frac{b_1}{\tau_j})\} \right] \tag{4.27a}$$

$$b_0 = \rho_s \frac{k_r}{K_e} \sqrt{\frac{K_{nj} + K_{st}}{k_{dd}(\rho_s - \rho_w)}} \tag{4.27b}$$

$$b_1 = (\frac{\pi}{e_v \sqrt{6}}) \frac{k_r (K_{ls} - K_s + f_c)}{K_{oj}} g(\rho_s - \rho_w) d \tag{4.27c}$$

where $K_{nj} = K_t \; K_{oj} / k_r$ is a combination of particle and fluid factors for the JET device, b_0 has dimensions of $(M/L^3)^{0.5}$, and $b_1$has dimensions of F/L^2. By using curve fitting techniques and solver routines, the parameters b_0 and b_1 can be derived from observed erosion data from the JET device in the presence of seepage.

4.6. CRITICAL HYDRAULIC GRADIENT FROM THE "MODIFIED WILSON MODEL"

The general framework for developing a critical hydraulic gradient was based on the dislodging and stabilizing forces and their associated moment lengths for particle detachment during the saturation process in the absence of flow forces (i.e. $F_L = 0$ and $F_d = 0$). Figure (4.1) shows the forces that act to remove a single soil particle during the saturation process including the particle weight, w_s, contact forces between particles (F_{c1}, F_{c2},……, F_{cn}), and seepage force, F_s.

Particle detachment occurs if the driving moment is greater than the resisting moment. Assume that these moments act around point *A*. Then the point of incipient motion due to a seepage force is defined as:

$$w_s \sin(\alpha)(l_1) + F_s \cos\alpha(l_2) = w_s \cos(\alpha)(l_2) + F_s \sin\alpha(l_3) + M_c \quad (4.28)$$

where all terms were previously defined. By incorporating a seepage force ($ik_v d^3 g\rho_w$) and the submerged particle weight formula [$g(\rho_s - \rho_w)k_v d^3$], equation (4.28) can be rewritten as:

$$i_c k_v d^3 g\rho_w\left[\cos(\alpha)(l_2) - \sin(\alpha)(l_3)\right] = g(\rho_s - \rho_w)k_v d^3\left[\cos(\alpha)(l_2) - \sin(\alpha)(l_1)\right] + M_c \quad (4.29)$$

The above equation can be rearranged by dividing both sides by the term $k_v d^3 g\rho_w\left[\cos(\alpha)(l_2) - \sin(\alpha)(l_3)\right]$ and introducing a f_{cs} term, then the critical hydraulic gradient (i_c) can be expressed as:

$$i_c = \frac{(\rho_s - \rho_w)}{\rho_w}\frac{\left[l_2 - Sl_1\right]}{\left[l_2 - Sl_3\right]} + f_{cs} \quad (4.30a)$$

$$f_{cs} = \frac{M_c}{k_v d^3 g\rho_w\left[\cos(\alpha)(l_2) - \sin(\alpha)(l_3)\right]} \quad (4.30b)$$

where f_{cs} is the dimensionless parameter based on cohesion. For non-cohesive soils and horizontal channel slope, the critical hydraulic gradient (i_c) is equal to $\frac{(\rho_s - \rho_w)}{\rho_w}$ which matches the critical hydraulic gradient reported in the literature (Fox and Wilson, 2010).

4.7. EXAMPLE ANALYSIS WITH SEEPAGE

An example is presented in order to demonstrate the influence of seepage on the erodibility of a cohesive soil and on the derived erodibility parameters with seepage forces. The

example is for a silty sand soil (72% sand, 13% silt, and 15% clay). This soil was acquired from disturbed streambank samples along Cow Creek in Stillwater, OK (Al-Madhhachi et al., 2012b; Lovern and Fox, 2012). As discussed below, the erodibility of cohesive soils under the influence of seepage can be theoretically predicted based on observed flume and/or JET data without seepage. Because the parameters of the "Modified Wilson Model" are mechanistically defined, b_1 and b_0 can be determined based on measured or predicted seepage gradients without re-running JETs or flume tests.

To illustrate this concept, previous flume tests were conducted on samples of this soil packed at optimum water content (14%) and at a bulk density of 1.68 Mg/m^3 without seepage forces (Al-Madhhachi et al., 2012b). The "Wilson Model" (without seepage forces) was fit to this data with estimated parameters of b_0 = 12 g/m-s-N$^{0.5}$ and b_1 = 6 Pa.

For flume tests and modified parameter b_1, equation (4.21c) can be rewritten as:

$$b_1 = \left(\frac{\pi}{e_v\sqrt{6}}\right)\frac{k_r(K_{ls}+f_c)}{K_o}g(\rho_s-\rho_w)d - \left(\frac{\pi}{e_v\sqrt{6}}\right)\frac{k_r K_s}{K_o}g(\rho_s-\rho_w)d \qquad (4.31)$$

where the first term $\left(\frac{\pi}{e_v\sqrt{6}}\right)\frac{k_r(K_{ls}+f_c)}{K_o}g(\rho_s-\rho_w)d$ is the "Wilson Model" parameter b_1 from flume data without seepage (i.e., equivalent to 6 Pa). The second term in equation (4.31) can be mathematically calculated by assuming or determining the following: e_v = 0.35 as proposed by Einstein and El-Samni (1949); for a tetragonal particle $k_r = n_p$ (where n_p assumed 2.8 for the silty sand soil); K_s depends on hydraulic gradient i; the moments lengths, l_1 = 0, $l_2 = l_4 = d/2$, and $l_3 = l_5 = n_p\, d/2$ for a tetragonal particle; K_f (=k_a /n_p, where k_a = 1 for a tetragonal particle); ρ_s = 2.65 Mg/m^3; ρ_w = 1 Mg/m^3; d was equal to d_{50} for silty sand (0.16 mm); the open channel flow velocity parameter, K_o, depends on C_D equal to 0.2 according to Einstein and El-Samni (1949); z_d

(= $l_3 + y_p$), where y_p (= 0) for a tetragonal particle; B (=6.5); von Karmon k is equal to 0.4; k_s is a roughness height equal to (n_p d/2) for a tetragonal particle.

Similarly, for JET data, the modified parameter b_1 from equation (27c) can be rewritten as:

$$b_1 = (\frac{\pi}{e_v\sqrt{6}})\frac{k_r(K_{ls}+f_o)}{K_{oj}}g(\rho_s-\rho_w)d - (\frac{\pi}{e_v\sqrt{6}})\frac{k_r K_s}{K_{oj}}g(\rho_s-\rho_w)d \quad (4.32)$$

where the first term $(\frac{\pi}{e_v\sqrt{6}})\frac{k_r(K_{ls}+f_o)}{K_{oj}}g(\rho_s-\rho_w)d$ is the "Wilson Model" parameter b_1 from JET data without seepage (i.e., equivalent to 6 Pa). The second term in equation (4.32) can be mathematically calculated by assuming or determining the following: K_{oj}, which depends on C_D equal to 0.2 according to Einstein and El-Samni (1949); z_d (= $l_3 + y_p$), where y_p (= 0) for a tetragonal particle; C_f (=0.00416); r equal to 0.13J_i; and the other terms as defined above.

The "Modified Wilson Model" parameter b_0 is influenced by seepage forces in the K_{st} terms (see equation 4.21b for flume and equation 4.27b for JET). For the flume, the terms in equation (4.21b) can be mathematically calculated by assuming or determining the following: K_n = K_t K_o / k_r; K_t = 2.5 according to Chepil (1959); k_{dd} = 2 according to Einstein (1950); $K_{st} = \mu_{sr} gid\rho_w$; μ_{sr} is the seepage coefficient ratio (where μ_{sr} was found to equal 3.85 based on experimental evidence from flume tests and JETs reported in the Chapter V); i is hydraulic gradient; and other terms were previously defined. The parameter K_e can be predicted from the observed flume data without seepage:

$$K_e = \rho_s \frac{k_r}{b_0}\sqrt{\frac{K_n}{k_{dd}(\rho_s-\rho_w)}} \quad (4.33)$$

Similarly, to predict parameter b_0 for JETs, the terms in equation (4.27b) can be mathematically calculated in same fashion as explained above. The only differences were in the terms K_{oj}. The

parameter K_e can be also determined from the observed JET data without seepage based on b_0 (b_0 =12 g/m-s-N$^{0.5}$ and equation 4.33).

4.8. RESULTS AND DISCUSSION

For the silty sand case study described above, seepage forces modified the derived "Modified Wilson Model" parameters (b_0 and b_1) (Figure 4.4). Note that b_0 increased (equation 4.21b for flume and equation 4.27b for JET) as K_{st} increased due to an increased seepage gradient for both flume tests and JETs. The parameter value changed approximately an order or magnitude when increasing the seepage gradient to approximately 2 m/m. When the seepage force was increased (K_s increased), b_1 decreased for both flume tests and JETs (Figure 4.4), and similarly, varied by approximately an order of magnitude when increasing the seepage gradient to approximately 2 m/m. The JET methods can be used to predict the flume erosion data as shown in Figure (4.4).

The impact of the seepage gradients was apparent when using the "Modified Wilson Model" parameters to calculate the erosion rate versus shear stress relationship with seepage (Figure 4.5). Again, the JET techniques provided equivalent erosion rates to flume tests based on predicted b_0 and b_1. Note the nonlinear relationship between average shear stress and erosion rate, even for the case without seepage (i=0). The excess shear stress model cannot predict this nonlinear relationship, although a linear relationship seems more plausible to represent the data for smaller seepage gradients (Figure 4.5).

The above analysis illustrates how the "Modified Wilson Model" can be used to predict the influence of seepage on soil erodibility. The following Chapter will evaluate the "Modified Wilson Model" parameters and the derivation of such parameters for various seepage gradients from both flume tests and "mini" JETs on two cohesive soils.

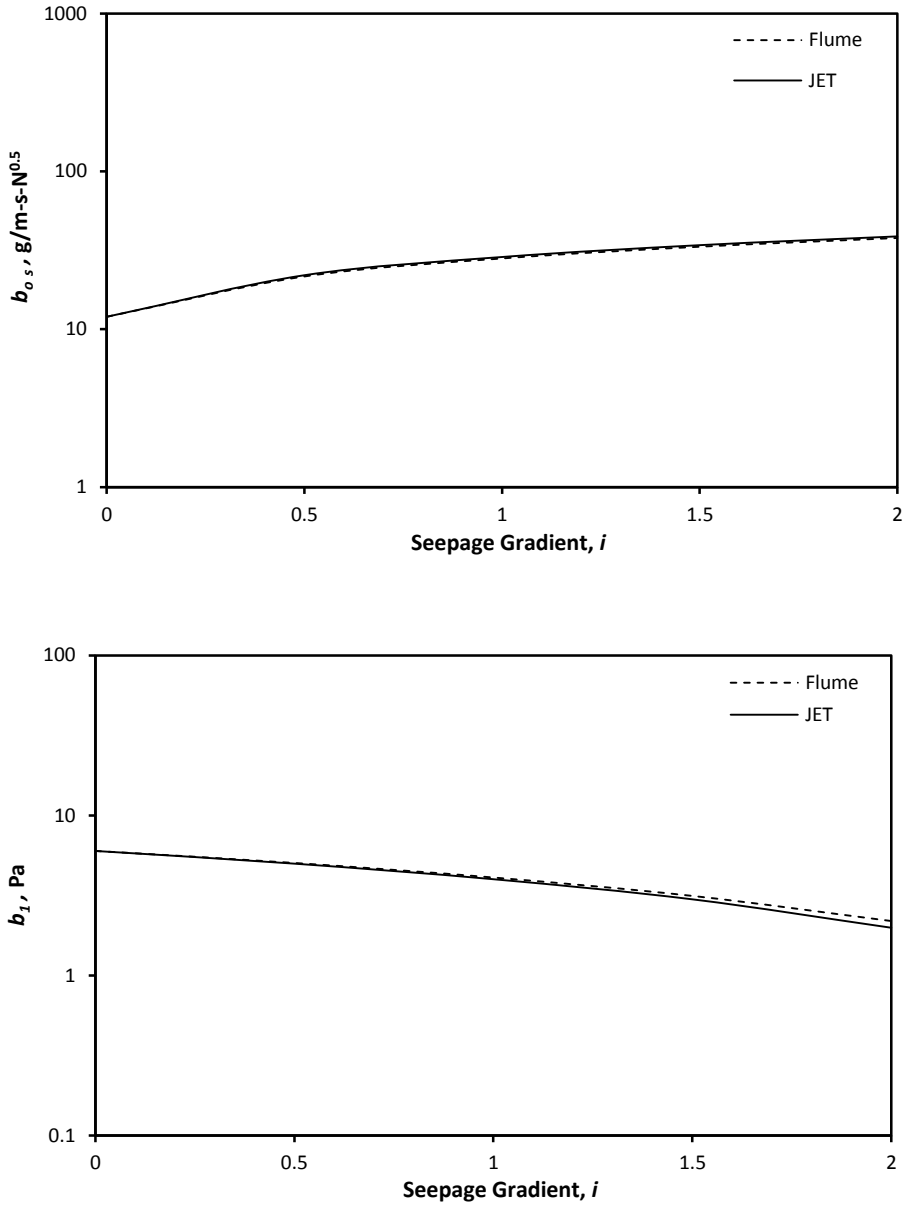

Figure 4.4. Influence of seepage gradients on the "Modified Wilson Model" parameters for a silty sand soil packed at optimum water content and a bulk density of 1.75 Mg/m^3. Values for no seepage gradient are taken from Al-Madhhachi et al. (2012b). Values at the various seepage gradients (*i*) represent predictions of b_0 and b_1 of the proposed model.

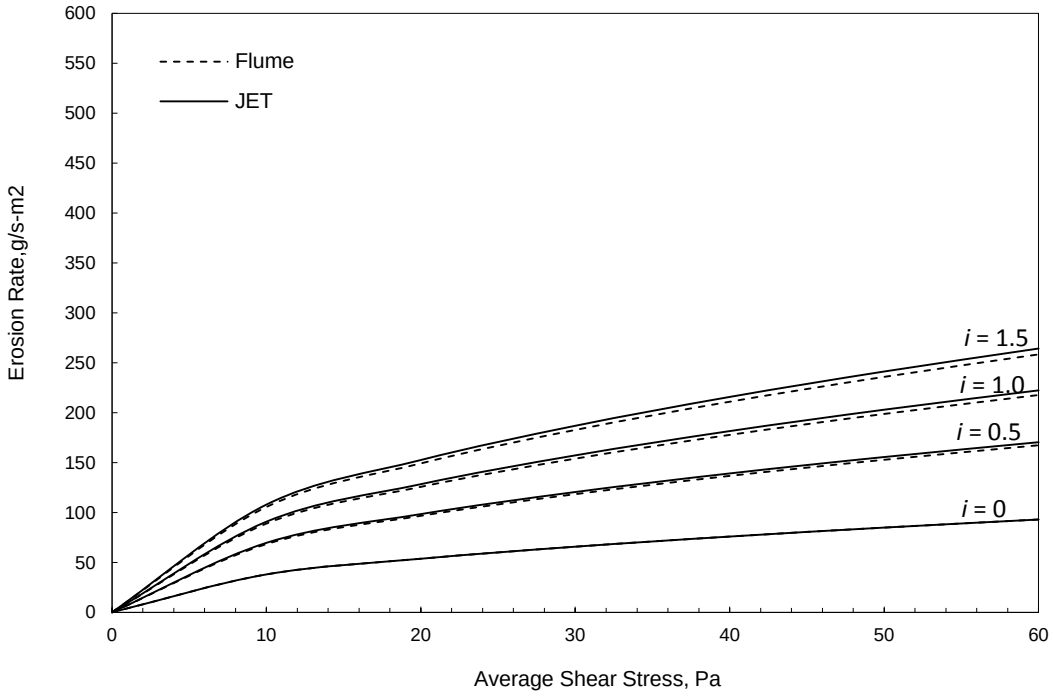

Figure 4.5. Erosion rate versus shear stress of a cohesive soil (silty sand) for a case without seepage (*i* = 0) and cases with different seepage gradients based on the "Modified Wilson Model" parameters for flume and JETs.

4.9. CONCLUSIONS

Seepage forces acting in concert with fluvial forces were incorporated into a fundamental detachment model to predict the erodibility of cohesive soils. The new detachment model, referred to as a "Modified Wilson Model", was based on the general framework developed by Wilson (1993a, 1993b), but also included seepage forces within two primarily soil-based parameters (b_0 and b_1). The proposed model was described along with the definition of the velocity distributions and methods of analysis for the material parameters (b_0 and b_1) for flume and JET techniques. The critical hydraulic gradient equation was developed based on the dislodging and stabilizing forces and their associated moment lengths for particle detachment during the saturation process in the absence of fluvial forces.

In order to investigate the influence of seepage, an example was presented to determine the soil erodibility in cases with and without seepage. Seepage forces influenced the erodibility parameters (b_0 and b_1) and the corresponding predicted erosion rate. As expected, increased seepage forces decreased the predicted "Modified Wilson Model" parameter b_1 but increased the parameter b_0 for both flume tests and JETs. The influence of seepage on erosion can be predicted based on JET techniques using the "Modified Wilson Model" parameters with a priori JET experiments without seepage. In general, the "Modified Wilson Model" is advantageous in being a more mechanistic, fundamentally-based erosion equation that can replace the more commonly used empirical detachment models such as the excess shear stress model.

4.10. ACKNOWLEDGMENTS

This research is based upon work supported by the National Science Foundation under Grant No. 0943491. Any opinions, findings, and conclusions or recommendations expressed in this material are those of the authors and do not necessarily reflect the views of the National Science Foundation.

CHAPTER V

MECHANISTIC DETACHMENT RATE MODEL TO PREDICT SOIL ERODIBILITY DUE TO FLUVIAL AND SEEPAGE FORCES: II. MODEL EVALUATION[4]

5.1. ABSTRACT

This is the second of two chapters that develop and evaluate a mechanistic detachment model to predict soil erodibility due to fluvial and seepage forces. The objective of this study was to evaluate a mechanistic fundamental detachment rate model to improve predictions of the erosion rate of cohesive soils due to both fluvial and seepage forces. The new detachment model, which is referred to as the "Modified Wilson Model", was based on two modified dimensional soil parameters (b_0 and b_1) that included seepage forces. The erodibility of two cohesive soils (silty sand and clayey sand) was measured in flume tests and with a new miniature version of the JET device ("mini" JET). The soils were packed in three equal lifts in a standard mold (for JETs) and in a soil box (for flume tests) at a uniform bulk density (1.5 or 1.6 Mg/m^3) near the soil's optimum water contents, with the tests vertically oriented. A seepage column was utilized to

[4] Submitted to *ASCE, Journal of Hydraulic Engineering*
Al-Madhhachi, A. T., Fox, G. A., Hanson, G. J., Tyagi, A. K., and Bulut, R. 2013b. Mechanistic Detachment Rate Model to Predict Soil Erodibility due to Fluvial and Seepage Forces: II. Model Evaluation. J. Hydraulic Eng., ASCE.

induce a constant hydraulic gradient on the soils tested in the flume or with the "mini" JET. The "Modified Wilson Model" parameters, b_0 and b_1, were derived from the erosion rate data with and without the influence of seepage from flume and JETs. Seepage forces had a non-uniform influence on the derived b_0 and b_1 as functions of the hydraulic gradient and dry density. The proposed model parameters were able to predict the erosion flume test and JET data using JET methods. The more fundamental detachment model can be used in place of the excess shear stress model with parameters that can account for any additional forces using JET techniques.

5.2. INTRODUCTION

When quantifying soil detachment rates, the interaction among fluvial forces and adjacent near-surface seepage forces are typically neglected (Fox and Wilson, 2010). Recent studies have demonstrated the importance of groundwater seepage on erosion and bank or hillslope failure (Fox et al., 2006a; Fox et al., 2007; Wilson et al., 2007; Fox and Wilson, 2010). The intricate linkage between seepage and fluvial forces has recently been emphasized in field seepage experiments (Midgley et al., 2012a). Seepage commonly occurs at the toes on streambanks and hillslopes where bank stored water returns to the streams following storm events. Such locations on a bank are a critical location for creating geotechnical instability due to fluvial undercutting (Midgley et al., 2012a).

The difficulty in addressing such conditions is the lack of a mechanistic approach for incorporating multiple forces in predicting detachment. A more rigorous framework, such as the one proposed by Wilson (1993a, 1993b) and extended by Al-Madhhachi et al. (2013a, Chapter III) and referred to as the "Modified Wilson Model", provides an approach to further advance predictions of the detachment rate process by incorporating multiple forces simultaneously. The fundamental detachment model is based on a simple two-dimensional representation of soil particles or aggregates and can be written as a function of two dimensional soil parameters, b_0

and b_1. Recent research incorporated the hydraulic analysis methods of submerged jet erosion tests (JETs) into the fundamental detachment model, significantly expanding its potential use in soil erosion research (Al-Madhhachi et al., 2012b).

The objectives of this study were (1) evaluate the extended fundamental detachment model developed by Al-Madhhachi et al. (2013a, Chapter III), referred to as the "Modified Wilson Model", using flume tests and JETs, (2) investigate the influence of seepage gradient forces on the model parameters, and (3) demonstrate a procedure for predicting the model parameters under any seepage gradient force using JET techniques.

5.3. GENERAL THEORETICAL FRAMEWORK INCLUDING SEEPAGE

The erosion rate (ε_r, M/L^2/T) predicted by the "Modified Wilson Model" for flume data under the influence of seepage can be expressed as (Al-Madhhachi et al., 2013a, Chapter IV):

$$\varepsilon_r = b_0 \sqrt{\tau_e} \left[1 - \exp\{-\exp(3 - \frac{b_1}{\tau_e})\} \right] \tag{5.1a}$$

$$b_0 = \rho_s \frac{k_r}{K_e} \sqrt{\frac{K_n + K_{st}}{k_{dd}(\rho_s - \rho_w)}} \tag{5.1b}$$

$$b_1 = (\frac{\pi}{e_v \sqrt{6}}) \frac{k_r (K_{ls} - K_s + f_c)}{K_o} g(\rho_s - \rho_w) d \tag{5.1c}$$

where b_0 has dimensions of (M/L^3)$^{0.5}$; b_1 has dimensions of F/L^2; and other key terms and parameters are defined as:

$$\tau_e = \gamma_w DS(\frac{n}{M_n})^b \tag{5.2a}$$

$$K_n = K_t \; K_o / k_r \tag{5.2b}$$

$$K_o = \frac{[C_D K_f (\frac{1}{k}\ln(\phi) + B)^2]}{2} \tag{5.2c}$$

$$K_{st} = \mu_{sr} gid\rho_w \tag{5.2d}$$

$$K_{ls} = \frac{\cos(\alpha)(l_2 - l_1 S)}{l_3 + l_4 \frac{K_L}{K_f}} \tag{5.2e}$$

$$K_s = \frac{i\rho_w}{(\rho_s - \rho_w)} \frac{\cos(\alpha)(l_2 - l_5 S)}{l_3 + l_4 \frac{K_L}{K_f}} \tag{5.2f}$$

$$f_c = \frac{M_c}{w_s(l_3 + l_4 \frac{K_L}{K_f})} \tag{5.2g}$$

where τ_e is the effective shear stress; K_n is a combination of particle and fluid factors; K_o is known as a velocity flow parameter; K_{st} is seepage parameter for exchange particle time; K_{ls} is a dimensionless parameter that depends on particle size, its orientation within the bed, and slope; K_s is a seepage parameter that depends on hydraulic gradient, particle density, its orientation within the bed, and slope; f_c is a dimensionless parameter based on cohesion; M_c is the sum of moments of cohesive and frictional resistance forces as proposed by Wilson (1993a); and other terms are defined in Table (5.1).

Similarly, Al-Madhhachi et al. (2013a, Chapter IV) developed a mechanistic detachment model for JET data under the influence of seepage:

Table 5.1. Definition of parameters in the "Modified Wilson Model".

Symbols	Description	Value or Equation	Reference
B	Log-velocity intercept parameter ranging from 6.5 to 9.8	6.5	Schilichting (1979)
b	Variable ranging from 4/3 to 2	2	Temple (1980) and Hanson (1989)
C	Discharge jet coefficient	0.75	Al-Madhhachi et al. (2012a)
C_D	Drag coefficient	0.2	Einstein and El-Samni (1949)
C_d	Diffusion constant	6.3	Hanson and Cook (2004)
C_f	Coefficient of friction	0.00416	Hanson and Cook (2004)
D	Water depth	Measured from flume tests	Experiments in this study
d	Equivalent particle diameter equivalent to d_{50}	0.16 mm for silty sand and 0.095 mm for clayey sand	Al-Madhhachi et al. (2012a)
d_o	Nozzle diameter	3.18 mm for "mini" JET	Al-Madhhachi et al. (2012a)
e_v	Coefficient of variation	0.35	Einstein and El-Samni (1949)
h	Pressure head for JET	61 cm	Experiments in this study
i	Hydraulic gradient	0.25 to 2.5	Experiments in this study
J_i	Jet nozzle height	34 mm	Experiments in this study
J_p	Potential core of jet nozzle	$C_d\, d_o$	Hanson and Cook (2004)
K	Kinematic moment flux	$0.153\pi d_0^2 U_0^2$	Poreh et al. (1967)
K_e	Exposure of lower particle parameter	-	Wilson (1993a, 1993b)
K_f	Ratio of projected area drag and lift forces	k_a/n_p	Al-Madhhachi et al. (2013a)
K_L	Ratio of drag and lift coefficients along with the ratio of velocities	1	Wilson (1993a, 1993b)
K_t	Factor of cumulating of instantaneous fluid forces	2.5	Chepil (1959)
k	von Karmon constant	0.4	Schilichting (1979)
k_a	Area constant of a tetragonal particle	1	Al-Madhhachi et al. (2013a)
k_{dd}	Detachment distance parameter	2	Einstein (1950)
k_r	Geometry ratio for a tetragonal particle	k_v/k_a	Al-Madhhachi et al. (2013a)
k_s	Roughness height	$n_p\, d/2$	Al-Madhhachi et al. (2013a)
k_v	Volume constant of a tetragonal particle	n_p	Al-Madhhachi et al. (2013a)
l_1	Moment length of gravity downslope	0	Al-Madhhachi et al. (2013a)
l_2	Moment length of gravity into bed	$d/2$	Al-Madhhachi et al. (2013a)
l_3	Moment length of drag force	$n_p\, d/2$	Al-Madhhachi et al. (2013a)
l_4	Moment length of lift force	$d/2$	Al-Madhhachi et al. (2013a)
l_5	Moment length of seepage force	$n_p\, d/2$	Al-Madhhachi et al. (2013a)
M_n	Manning's roughness for overall roughness	Manning's formula	Hanson (1989)
n	Manning's roughness coefficient for the soil grain roughness	0.0156	Temple et al. (1987) and Hanson (1989)

Table 5.1. (Continued).

Symbols	Description	Value or Equation	Reference
n_p	Particle length factor for tetragonal particle	2.8 for silty sand and 4.5 for clyey sand	Experiments in this study
S	Energy slope	Manning's formula	Hanson (1989)
r	Jet radius upon maximum jet velocity works	0.13 J_i	Al-Madhhachi et al. (2012b)
U_o	Velocity of jet at the orifice	$C\sqrt{2gh}$	Hanson and Cook (2004)
w_s	Submerged particle weight	$g(\rho_s - \rho_w)k_v d^3$	Wilson (1993a, 1993b)
y_p	Pivot point a tetragonal particle	k_s - n_p d/2 - l_1	Al-Madhhachi et al. (2013a)
z_d	Height that the drag velocity is acting upon	$l_3 + y_p$	Al-Madhhachi et al. (2013a)
μ_{sr}	Seepage coefficient ratio	3.85	Experiments in this study
ρ_s	Particle density	2.65 Mg/m^3	Freeze and Cherry(1979)
ρ_w	Water density	1 Mg/m^3	-
α	Channel angle slope	0	Experiments in this study

$$\varepsilon_r = b_0\sqrt{\tau_j}\left[1-\exp\{-\exp(3-\frac{b_1}{\tau_j})\}\right] \tag{5.3a}$$

$$b_0 = \rho_s \frac{k_r}{K_e}\sqrt{\frac{K_{nj}+K_{st}}{k_{dd}(\rho_s-\rho_w)}} \tag{5.3b}$$

$$b_1 = (\frac{\pi}{e_v\sqrt{6}})\frac{k_r(K_{ls}-K_s+f_c)}{K_{oj}}g(\rho_s-\rho_w)d \tag{5.3c}$$

where b_0 has dimensions of $(M/L^3)^{0.5}$; b_1 has dimensions of F/L^2; and other key terms and parameters are defined as:

$$\tau_j = \tau_o\left(\frac{J_p}{J}\right)^2 \tag{5.4a}$$

$$K_{nj} = K_t\ K_{oj} / k_r \tag{5.4b}$$

$$K_{oj} = \frac{5.537 C_D K_f \exp[-200(\frac{z_d}{r})^2]}{C_f c_d{}^2} \quad (5.4c)$$

where τ_j is the average shear stress for JET, K_{nj} is a combination of particle and fluid factors for JET, K_{oj} is known as a velocity jet parameter, and other terms are defined in Table (5.1).

The parameters b_0 and b_1 can be derived using curve fitting techniques and/or methods that minimize the error of these functions relative to measured erosion data from flume or/and JETs. In the absence of seepage, the seepage parameters can be neglected (i.e., $K_s = 0$ and $K_{st} = 0$) and the developed model will match the set of equations developed by Al-Madhhachi et al. (2012b).

5.4. DEVELOPING THE CRITICAL HYDRAULIC GRADIENT

The fundamental model can also be used to predict the critical seepage gradient, independent of fluvial forces, necessary for particle mobilization. Al-Madhhachi et al. (2013a, Chapter IV) developed the critical hydraulic gradient for streambeds based on the dislodging and stabilizing forces and their associated moment lengths for particle detachment during the saturation process in absence of flow forces. The critical hydraulic gradient (i_c) was expressed as (Al-Madhhachi et al., 2013a):

$$i_c = \frac{(\rho_s - \rho_w)}{\rho_w} \frac{[l_2 - Sl_1]}{[l_2 - Sl_3]} + f_{cs} \quad (5.5a)$$

$$f_{cs} = \frac{M_c}{k_v d^3 g \rho_w [\cos(\alpha)(l_2) - \sin(\alpha)(l_3)]} \quad (5.5b)$$

where f_{cs} is the dimensionless parameter based on cohesion and other terms were previously defined. For non-cohesive soils and horizontal channel slope (i.e. $S = 0$ and/or $\alpha = 0$), the critical

hydraulic gradient (i_c) is equal to $\frac{(\rho_s - \rho_w)}{\rho_w}$ which matched the critical hydraulic gradient reported in the literature (Fox and Wilson, 2010).

5.5. MATERIALS AND METHODS

5.5.1. Flume Experiments

Open channel erosion tests were conducted in a flume at the USDA Hydraulic Engineering Research Unit in Stillwater, OK. The flume was constructed inside a pre-existing drainage basin 12.2 m long and 3 m wide with 0.75 m side walls. The flume consisted of the following parts: water delivery pipe, upstream water reservoir, flume, soil box, water box, water column, and tailgate (Figure 5.1). The water delivery pipe was 305 mm in diameter and it was attached to the water reservoir to provide the required discharge (maximum discharge was 0.17 m^3/s) from Lake Carl Blackwell. The upstream water reservoir was 1.2 m long, 1.2 m wide, and 1.4 m deep, and served the function of providing a smooth entrance flow condition to the flume. The flume was 4.9 m long and 0.6 m wide with 0.6 m wall sides.

A soil box (1 m long, 61 cm wide, and 25 cm deep) was placed in the middle of the flume (Figure 5.1). Soil was packed at optimum water content (14% to 15.5%) at uniform bulk density (1.5 to 1.6 Mg/m^3) in the soil box prior to testing. A water box (1 m long, 61 cm wide, and 15 cm deep) was placed in the middle of the flume beneath the soil box. A water column (15 cm in diameter) was attached to the water box from the side and could provide up to 300 cm of water head.

A tailgate was placed at the end of the flume with a fixed height of 0.14 m for all tests to provide desired flow conditions during testing. The effective shear stress was varied (ranging from 0.1 to 6.4 Pa) by changing the discharge into the flume (maximum discharge was 0.17 m^3/s). A mechanical jack was attached beneath the flume to provide the desired channel slope (1% to

3%). The design slope for testing was fixed at 1.5% for all tests to provide the desired flow condition.

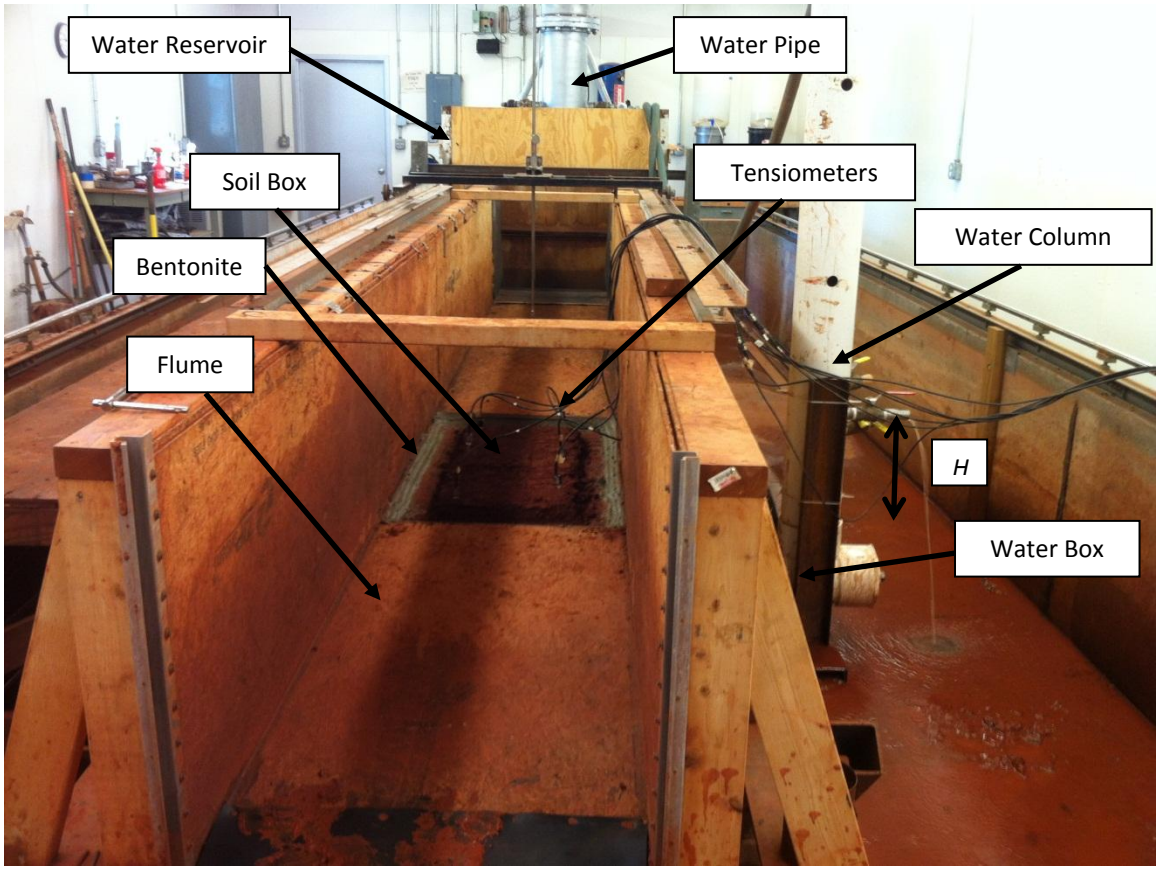

Figure 5.1. Indoor flume with soil box for quantifying soil detachment. The water column was used to provide a constant hydraulic head (*H*) on the soil.

5.5.2. Laboratory Devices

"Mini" JET Device. The "mini" JET apparatus consisted of the following parts (Figure 5.2a): pressure gauge, outlet and inlet water, depth gauge, rotatable plate, submerged tank, foundation ring, valve, and hoses. The adjustable head tank was used for the "mini" JET to provide the desired water head. Scour readings were acquired using the depth gauge. The rotatable plate had a

3.18-mm diameter nozzle. This rotatable plate was used to prevent the water from impinging upon the soil sample at the beginning of testing and during scour depth readings at different times during the test runs. The submerged tank was 70 mm in height and 101.6 mm in diameter with a 6.4-mm wall thickness. The submerged tank did not open from the top. The rotatable plate and depth gauge were attached to the top of the tank. The foundation ring was 180 mm in diameter and was pushed into the soil 51 mm when used in the field (Al-Madhhachi et al., 2012a, 2012b).

(a) "Mini" JET Device

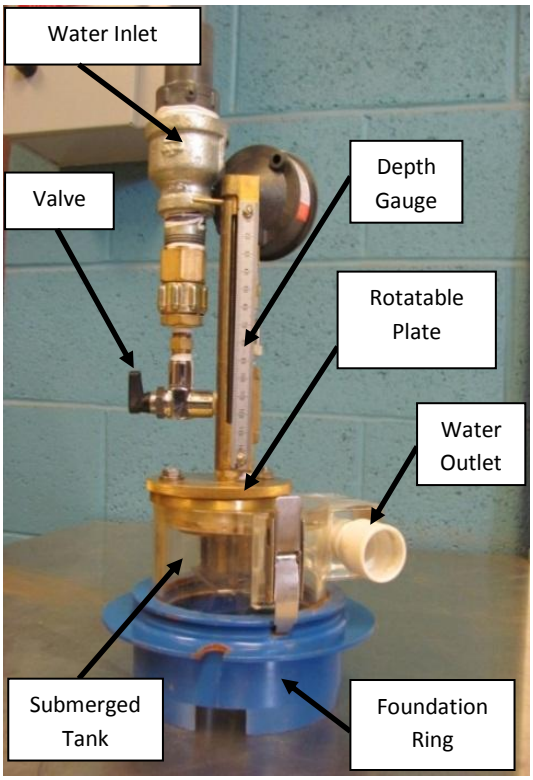

(b) Seepage Column

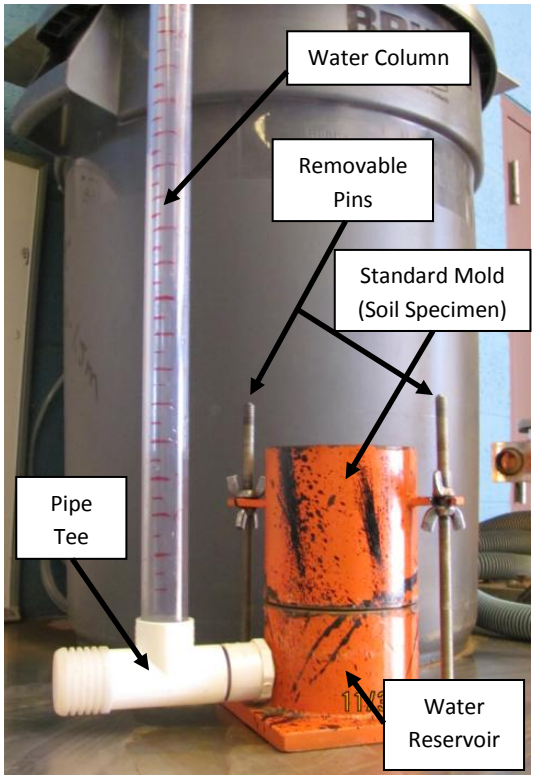

Figure 5.2. Laboratory "mini" JET device and seepage column.

Seepage Column. A seepage column was designed to impose seepage forces on the cohesive soil (Figure 5.2b). The standard mold was 944 cm^3 in volume (101.6 mm in diameter and 116.8 mm in height). The water reservoir was 101.6 mm in diameter and 76.2 mm high. A circular porous

plate was attached to the top of the water reservoir to prevent soil from falling down into the water reservoir. The circular porous plate was 101.6 mm in diameter and had 3.18-mm diameter openings. A removable flexible screen was placed between the standard mold and porous plate to prevent small particles of soil from entering into the water reservoir. The removable flexible screen had 1.6-mm diameter openings. A pipe tee was used to connect the water reservoir and the water column and hold the water column in a vertical position. The water column was 25.4 mm in diameter and it was attached to the water reservoir from the side and could provide up to 180 cm of water head. Removable pins were used to attach the standard mold to the water reservoir and the "mini" JET from the bottom and top, respectively. The "mini" JET provided a downward vertical fluvial force on the streambed while the seepage column provided an upward vertical seepage force (Figure 5.3).

5.5.3. Soil Characteristics

The two soils utilized in the flume and laboratory "mini" JET experiments were classified as silty sand and clayey sand soils (Table 5.2). Soils were tested and analyzed according to ASTM Standards (2006). Sieve analysis and hydrometer tests were conducted according to ASTM Standard D422. Liquid limit and plastic limit tests were performed according to ASTM Standard D4318.

Table 5.2. Properties of the two soils for testing (Al-Madhhachi et al., 2012a).

Soil Location	Grain Size			Plasticity Index, %	Standard Compaction		Soil Classification USCS
	% Sand	% Silt	% Clay		Maximum Density, Mg/m^3	Optimum Water Content, %	
USDA Hydraulic lab	57	18	25	4	2.00	10.8	SC – Clayey Sand
Streambank of Cow Creek	72	13	15	Non-Plastic	1.83	12.9	SM – Silty Sand

(a) Saturation process (b) Testing using “mini” JET

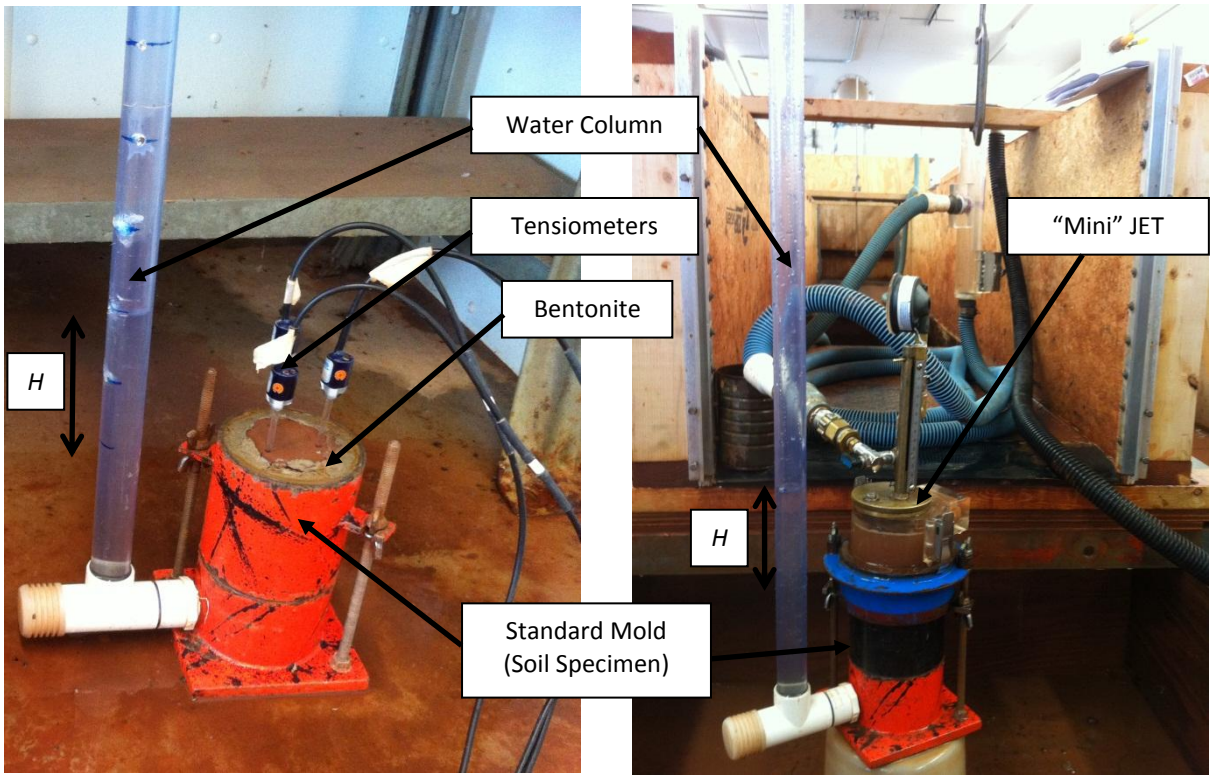

Figure 5.3. Experimental setup of the “mini” JET device and the seepage column during (a) saturation process and (b) testing using “mini” JET.

5.5.4. Experimental Procedure for Flume Tests

The soils were air dried and crushed into small pieces. In order to achieve the optimum desired water content for compaction, the soils were mixed with a pre-defined quantity of water and left for 24 hr in closed buckets to allow for even moisture distribution throughout the sample. The soils were packed at the optimum water content (14.0 % to 15.5 %) based on a compaction effort of 240 kN-m/m^3. Then, the soils were compacted in the flume soil box in three equal lifts at uniform bulk density (1.5 to 1.6 Mg/m^3) using a hand packer (25 cm by 25 cm base plate). In order to investigate the influence of seepage, some samples were tested without seepage (i.e., H =

0) and without saturating the soil sample prior to the test (unsaturated soil sample). Others were tested after inducing a desired constant *H* and saturating the sample prior to the test. For samples tested with seepage, the edges of the soils in the flume soil box were over packed and bentonite was packed along the edge of each layer to prevent water from flowing along the edges during the saturation process (Figure 5.1). Tests were repeated for each set of experimental conditions.

For soil samples tested without seepage, the steps of running the flume and collecting data followed Al-Madhhachi et al. (2012b, Chapter III). For soil samples tested with seepage forces, a pressure was provided to the water box by a constant head water column in order to establish a seepage gradient in the soil bed. The water column was filled with water to a desired water head (*H*) and the setup was left to saturate the soil sample. Tensiometers were placed at different heights (5 and 10 cm) in the soil specimen to monitor pore-water pressures and the saturation process (Figure 5.1).

After the soil box was saturated and the imposed gradient established, the following steps were used for running the flume and collecting data. Before turning flow into the flume, point gage readings were taken to determine the channel bed level and the initial soil surface at time zero for each station. The flume was usually divided into 10 stations with an interval of 30 cm upstream and downstream of the test section and intervals of 15 cm in the test area of the channel bed. Following point gage readings, the water source for establishing open channel flow in the flume was opened to fill the water reservoir and the time of testing was started when the water reached the soil surface in the test section of the flume. The water head was held constant in the water column during the testing. The readings of the scour bed and water depth were taken using the point gage at different time intervals. Usually, the readings were acquired each 2 to 8 minutes with a maximum test period of 95 minutes.

5.5.5. Experimental Procedure for "Mini" JETs

The soils were air dried and then passed through a sieve with openings of 4.75 mm (No. 4 sieve). The soils were packed in three equal lifts in a standard mold at a uniform bulk density (1.5 to 1.6 Mg/m^3) near the soil's optimum water content (14.5% to 16.0%). To achieve this optimum water content, the soils were mixed with required quantities of water and allowed to equilibrate for at least 24 hr in a closed container. Some samples were tested without seepage (i.e., $H = 0$) and without saturating the soil sample prior to the test (unsaturated soil sample). Others were tested using both the "mini" JET device and seepage column by inducing a desired constant H and saturating the sample prior to the test (Figures 5.3a and 5.3b). For samples tested with seepage, the edges of the soils in the standard mold were over packed and bentonite was packed along the edge of each layer to prevent water from flowing along the edges during the saturation process (Figure 5.3a). Tests were repeated for each set of experimental conditions.

For soil samples tested with the "mini" JET device, the set-up procedure was the same with the exception that a series of samples were tested without seepage and a series were tested with seepage. The steps of running the "mini" JET and collecting data (without seepage) followed Al-Madhhachi et al. (2012a, Chapter II).

For soil samples tested with seepage, a pressure was provided to the water reservoir by the constant head water column. The water column was filled with water to a desired water head and the setup was left to saturate the soil sample. Tensiometers were placed at different heights (5 and 7 cm) in the soil to monitor pore-water pressures and the saturation process (Figure 5.3a). After the soil specimen was saturated and the imposed gradient established, the "mini" JET device was placed above the standard mold so that the standard mold was in the center of the submerged tank directly below the jet nozzle (Figure 5.3b). The adjustable head tank was then set at the desired constant head and hoses (including water source) were connected to the JET device.

The steps of running the "mini" JET and collecting data (with seepage) followed Al-Madhhachi et al. (2012a, Chapter II).

5.5.6. Deriving the "Modified Wilson Model" Parameters

Data from the flume and "mini" JET device were used to determine the "Modified Wilson Model" parameters, b_0 and b_1, for both silty sand and clayey sand soils. The "Modified Wilson Model" parameters (b_0 and b_1) were derived from observed JET and flume data using the solver routine in Microsoft Excel which utilized the generalized reduced gradient method to minimize the error between the measured data and the functional solutions of the equations (equation 5.1a for flume data and equation 5.3a for JET data). Constraints were used within the Excel solver routine to limit potential solutions of b_0 and b_1. The maximum allowable change for the parameters b_0 and b_1 was between 50% to 60% from their initial estimated values as recommended by Wilson (1993b) and Al-Madhhachi et al. (2012b).

In order to investigate how the model fit the observed flume and JET data, the normalized objective function (*NOF*) (Pennell et al., 1990; Hession et al., 1994) was calculated to quantify the goodness of fit. The *NOF* is the ratio of the standard deviation (*STDD*) of differences between observed and predicted data to the overall mean (X_a) of the observed data:

$$NOF = \frac{STDD}{X_a} = \frac{\sqrt{\frac{\sum_{i=1}^{N}(x_i - y_i)^2}{N}}}{X_a} \tag{5.6}$$

where x_i and y_i are the observed and predicted data, respectively, and N is the number of observations. In general, 1%, 10%, and 50% deviations from the observed values result in *NOF* values of 0.01, 0.1, and 0.5, respectively (Fox et al., 2006b).

5.6. RESULTS AND DISCUSSION

5.6.1. Established Hydraulic Gradient

The imposed hydraulic gradient (i) was verified from tensiometer readings during the saturation process based on an assumed linear distribution of pressure heads (Table 5.3). Similar values were observed between the imposed and actual established hydraulic gradient in both the flume tests and JETs for both soils (Table 5.3). The critical hydraulic gradient (i_c) determined from equations (5.5a-5.5b) was also reported in Table (5.3). Soil swelling was observed for samples tested with seepage during the saturation process. Piping was also observed for samples prepared for flume tests during the saturation process when the hydraulic gradient was greater than 1.0 m/m; therefore, flume tests were performed with i equal to or less than unity for both soils.

5.6.2. Observed Erosion Data with Seepage

Seepage forces influenced the observed scour depth measurements when flume or "mini" JETs were performed for both soils (Figures 5.4 and 5.5). Higher erosion rates were observed with higher hydraulic gradients increased in both flume tests (Figures 5.4c, 5.4d, 5.5c, and 5.5d) and JETs (Figures 5.4a, 5.4b, 5.5a, and 5.5b) for both soils. Even higher erosion rates were observed for silty sand soil than clayey sand soil. Seepage forces tended to have less influence as the material density increased for both flume and "mini" JETs and for both soils.

Table 5.3. Calculated and established hydraulic gradient (*i*) and calculated critical hydraulic gradient (i_c) from flume and "mini" JETs for both soils.

Soils		Silty Sand			Clayey Sand		
Testing Techniques	Dry Density, Mg/m^3	Imposed *i*	Established *i*	i_c (Eq.5.5)	Imposed *i*	Established *i*	i_c (Eq.5.5)
Flume	1.6	0.50	0.57	4.56	0.50	0.60	4.48
		0.75	0.82		0.75	0.75*	
		1.00	1.05		1.00	1.10	
	1.5	0.25	0.30	2.06	0.25	0.32	3.70
		0.50	0.58		0.50	0.57	
JET	1.6	0.50	0.42	5.82	0.50	0.51	5.85
		1.00	1.04		1.00	1.01	
		1.50	1.35		1.50	1.45	
		2.00	1.99		2.00	2.01	
		2.50	2.57		2.50	2.50*	
	1.5	0.50	0.41	3.89	0.50	0.41	4.84
		0.75	0.75*		0.75	0.68	
		1.00	1.01		1.00	1.00*	

* Not measured for that case.

5.6.3. Seepage and "Modified Wilson Model"

The "Modified Wilson Model", based on deriving the parameters b_0 and b_1, matched the observed scour depth versus time for both flume tests and "mini" JETs (Figures 5.4 and 5.5). The model matched the erosion data without seepage ($i = 0$) and with seepage ($i > 0$). *NOF* values for the observed versus predicted scour depths using the "Modified Wilson Model" of silty sand soil from flume and JETs tests ranged from 0.08 to 0.33 and 0.03 to 0.16, respectively (Table 5.4), and for the clayey sand soil from 0.10 to 0.24 and 0.03 to 0.13, respectively (Table 5.4). Therefore, the "Modified Wilson Model" predicted the observed scour depth data for the "mini" JET data as well as or even better than the flume data. Similar observations were reported by Al-Madhhachi et al. (2012b, Chapter III). This was due to larger soil sample size and greater soil layer depths used in the flume introducing more potential variability in the results comparing to the JETs.

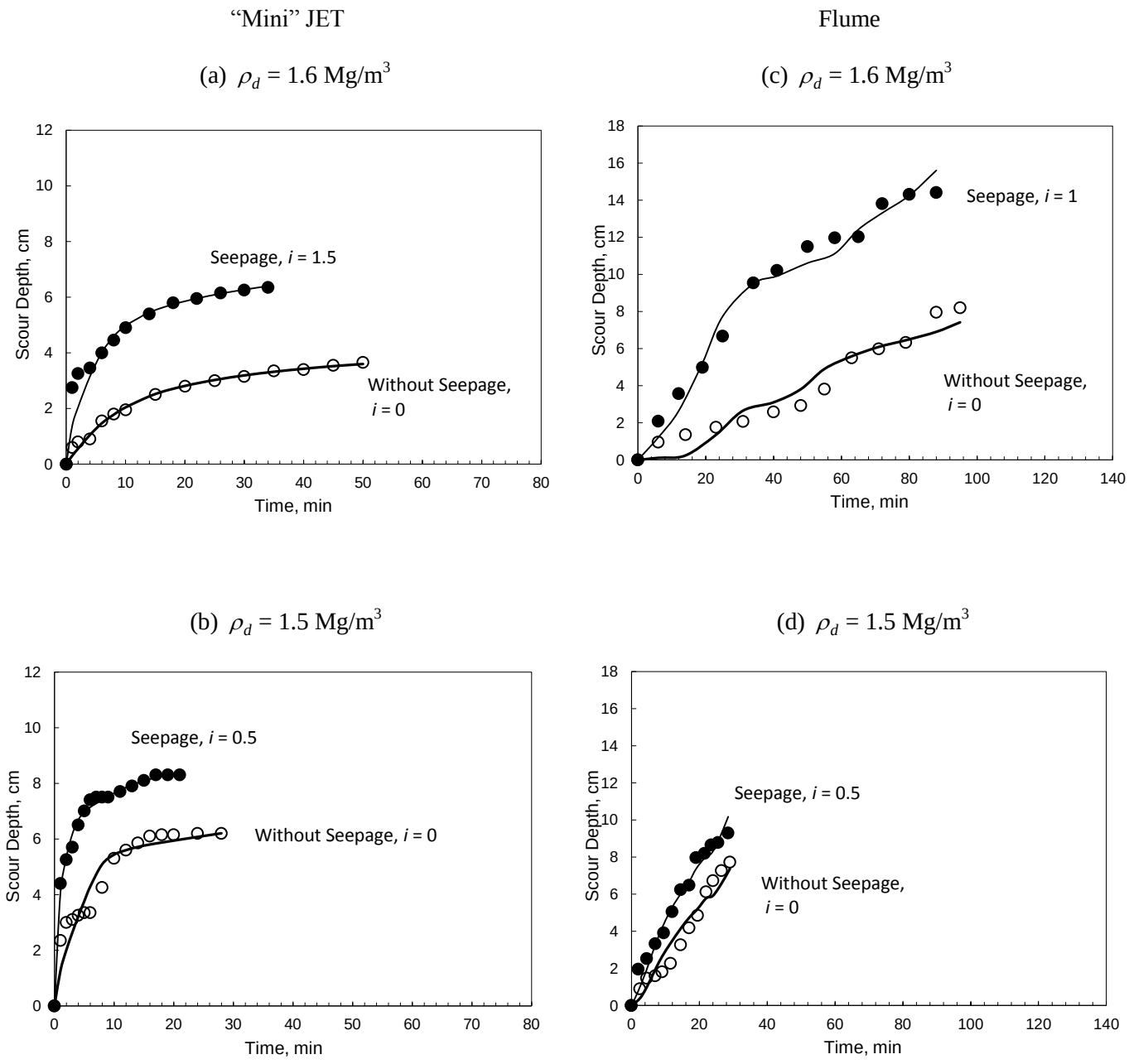

Figure 5.4. Comparison between the observed (circles) and predicted erosion data using the "Modified Wilson Model" (lines) for data without seepage (open circles) and a case with seepage (solid circles). Observed erosion data are from the flume tests and "mini" JETs for the silty sand soil at 1.5 to 1.6 Mg/m^3.

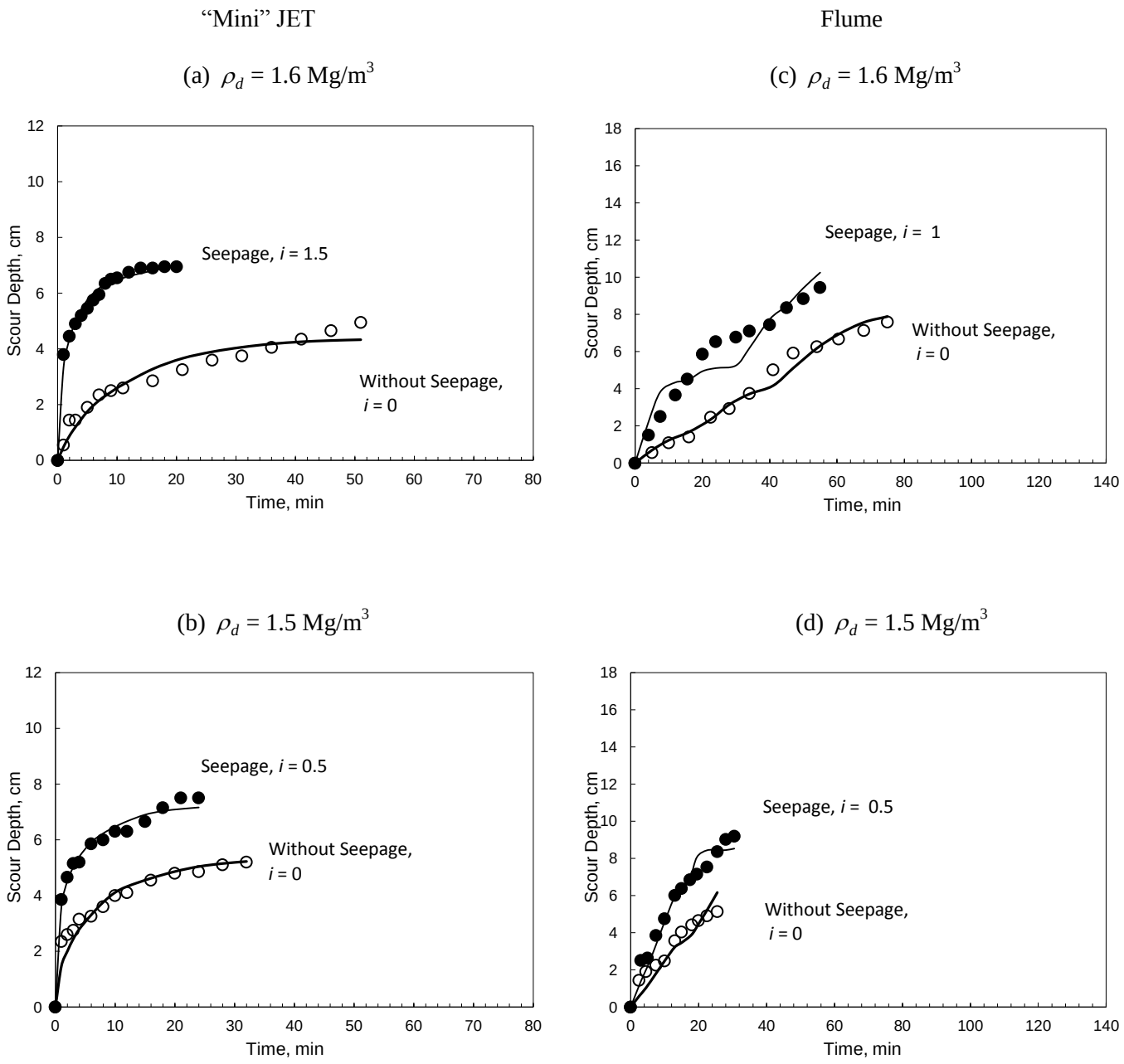

Figure 5.5. Comparison between the observed (circles) and predicted erosion data using the "Modified Wilson Model" (lines) for data without seepage (open circles) and a case with seepage (solid circles). Observed erosion data are from the flume tests and "mini" JETs for the clayey sand soil at 1.5 to 1.6 Mg/m^3.

Table 5.4. *NOF* values for observed versus predicted scour depths by "Modified Wilson Model" for both soils and for flume and "mini" JET tests. All tests were performed with a total number of samples, n = 26 for flume tests and n = 40 for JET tests for both soils.

Soils	Silty Sand						Clayey Sand					
Model	Flume			"Mini" JET			Flume			"Mini" JET		
	Min	Max	Ave	Min	Max	Ave	Min	Max	Ave	Min	Max	Ave
Modified Wilson	0.08	0.33	0.14	0.03	0.16	0.10	0.10	0.24	0.16	0.03	0.13	0.08

The "Modified Wilson Model" parameters are primarily soil material parameters that depend on properties of the soil particle shape and its orientation. As expected, seepage forces influenced the derived "Modified Wilson Model" parameters (b_0 and b_1) in both flume tests and JETs for both soils (Figures 5.6 and 5.7). The parameter b_0 was developed to include the seepage force in its formulation (equations 5.1b for flume and 5.3b for JET) as well as b_1 (equations 5.1c for flume and 5.3c for JET). Note that b_1 decreased as the seepage force (K_s) increased while b_0 increased as K_{st} increased with increased hydraulic gradients (Figures 5.6 and 5.7).

5.6.4. Predicting Seepage Parameters from Data without Seepage

As discussed by Al-Maddhachi et al. (2013), the erodibility of cohesive soils under the influence of seepage can theoretically be predicted based on observed flume and/or JET data without seepage. Flume or "mini" JETs could be performed during conditions without seepage to derive b_0 and b_1. Then, b_1 can be converted to modified b_1 (that included seepage term) and b_0 can be converted to modified b_0 (that included seepage term) based on measured or predicted seepage gradients at any time without re-running JETs or flume tests. The parameters b_0 and b_1 are mechanistically defined.

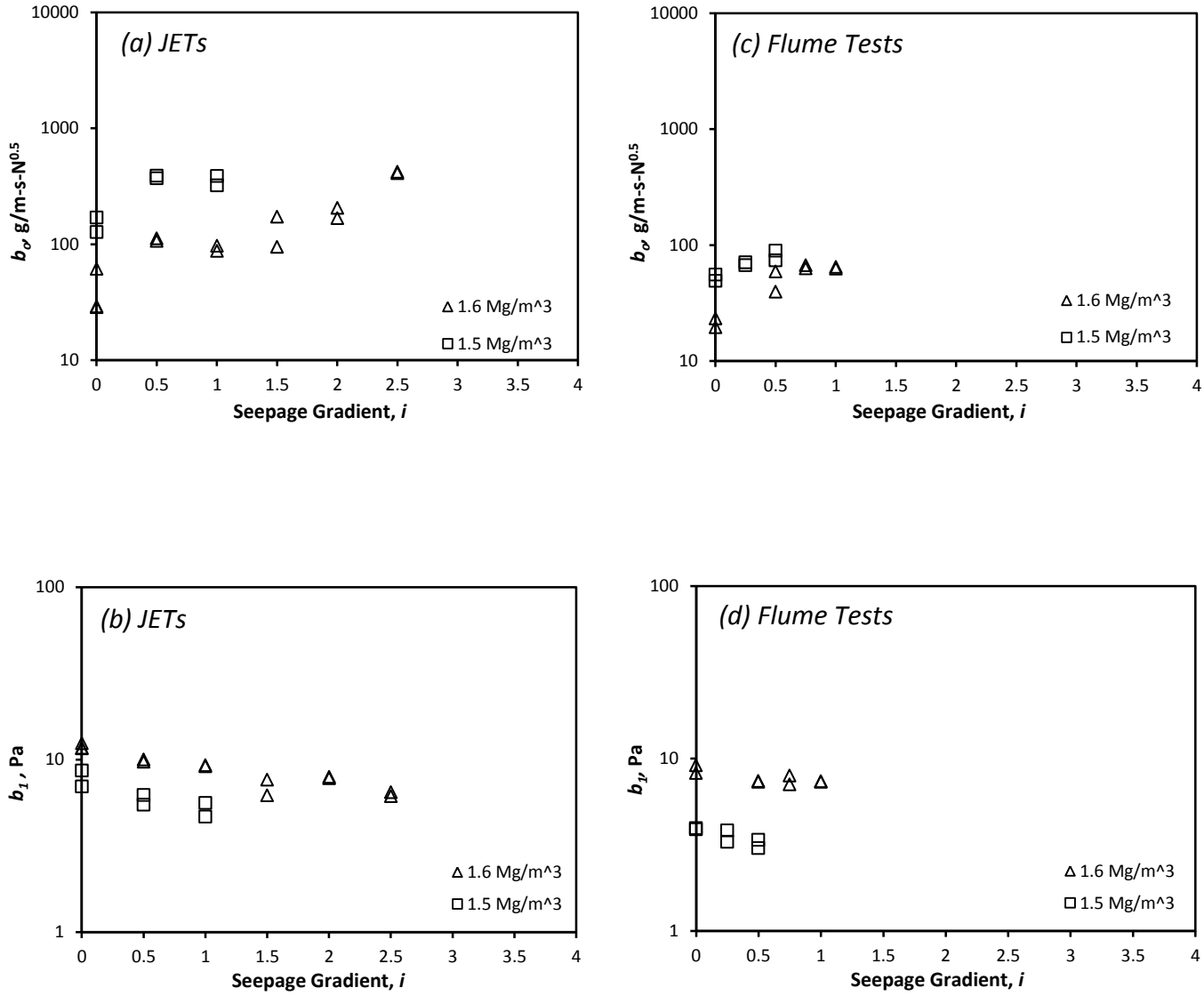

Figure 5.6. Influence of a seepage force on the derived "Modified Wilson Model" parameters (b_0 and b_1) at uniform bulk density (1.5 to 1.6Mg/m^3) from flume tests and "mini" JETs for the silty sand soil.

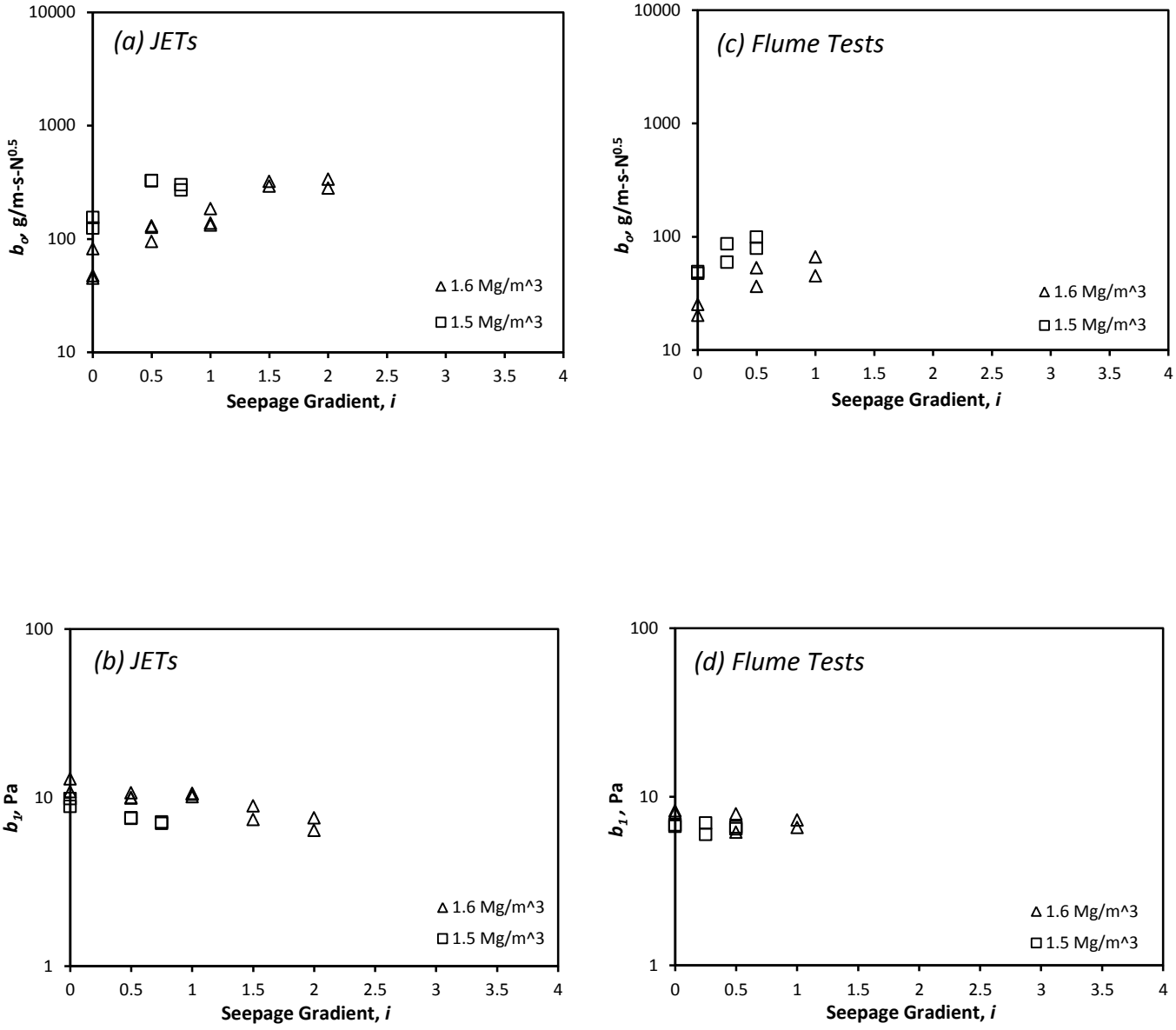

Figure 5.7. Influence of a seepage force on the derived "Modified Wilson Model" parameters (b_0 and b_1) at uniform bulk density (1.5 to 1.6 Mg/m^3) from flume tests and "mini" JETs for the clayey sand soil.

For flume tests and modified b_1, equation (1c) can be rewritten as:

$$b_1 = (\frac{\pi}{e_v\sqrt{6}})\frac{k_r(K_{ls}+f_o)}{K_o}g(\rho_s-\rho_w)d - (\frac{\pi}{e_v\sqrt{6}})\frac{k_rK_s}{K_o}g(\rho_s-\rho_w)d \quad (5.7)$$

where the first term $(\frac{\pi}{e_v\sqrt{6}})\frac{k_r(K_{ls}+f_o)}{K_o}g(\rho_s-\rho_w)d$ is the "Wilson Model" parameter from flume data without seepage (i.e., $K_s = 0$). The second term in equation (5.7) can be mathematically calculated by assuming or determining the following: for a tetragonal particle $k_r = n_p$ (where n_p was 2.8 for silty sand and 4.5 for clayey sand based on observed data) and all other terms given in Table (5.1).

Similarly, for JET data, the parameter b_1 from equation (3c) can be rewritten as:

$$b_1 = (\frac{\pi}{e_v\sqrt{6}})\frac{k_r(K_{ls}+f_o)}{K_{oj}}g(\rho_s-\rho_w)d - (\frac{\pi}{e_v\sqrt{6}})\frac{k_rK_s}{K_{oj}}g(\rho_s-\rho_w)d \quad (5.8)$$

where the first term $(\frac{\pi}{e_v\sqrt{6}})\frac{k_r(K_{ls}+f_o)}{K_{oj}}g(\rho_s-\rho_w)d$ is the "Wilson Model" parameter b_1 from JET data without seepage (i.e., $K_s = 0$). The second term in equation (5.8) can be mathematically calculated from values given in Table (5.1). The values of n_p were based on the particle shape for a specific soil; therefore, additional research is needed to determine n_p for various seepage forces in different soil types.

In the same fashion, the "Modified Wilson Model" parameter b_0 can also be derived based on observed seepage gradients. For flume tests, the terms in equation (5.1b) can be mathematically calculated using the values given in Table (5.1) and K_e, which can be predicted from observed flume data without seepage using the following equation:

$$K_e = \rho_s\frac{k_r}{b_0}\sqrt{\frac{K_n}{k_{dd}(\rho_s-\rho_w)}} \quad (5.9)$$

Similarly, for JET data and modified parameter b_0, the terms in equation (5.3b) can be mathematically calculated in same fashion as explained above. The only differences were in the terms K_{oj}.

The predictive equations for b_0 and b_1 from the parameters without seepage (b_0 and b_1 when seepage terms equivalent to zero) appropriately estimated the derived parameter values from both flume tests and JETs for both soils (Figures 5.8 and 5.9). Prediction of b_1 was based on the seepage force (K_s), the parameter n_p (which was equal to 2.8 for silty sand and 4.5 for clayey sand for both flume tests and JETs), and particle diameter, d (which was equal to 0.16 mm for silty sand and 0.095 mm for clayey sand). Prediction of b_0 was based on hydraulic gradient (K_{st}), the parameter n_p, particle diameter, d, and the seepage coefficient ratio μ_{sr} . Additional research is needed to verify μ_{sr} for various seepage forces in different soil types. The predictive equations for b_0 and b_1 based on JET techniques (equations 5.3b and 5.3c) appropriately estimated the derived parameters from flume erosion data (Figures 5.8c, 5.8d, 5.9c, and 5.9d). This indicted that JET methods can be used to predict the influence of seepage on the soil erodibility from observed erosion streambeds.

5.7. SUMMARY AND CONCLUSIONS

The "Modified Wilson Model" parameters (b_0 and b_1) were evaluated using data from flume experiments and JETs tested with and without seepage forces. A flume and a laboratory "mini" JET device along with a seepage column were utilized to measure the "Modified Wilson Model" parameters (b_0 and b_1) for silty sand and clayey sand soils packed at a uniform bulk density (1.5 to 1.6 Mg/m^3) near the soil's optimum water content at different established seepage gradients. Seepage forces influenced the observed and predicted erosion data and erodibility parameters derived from the "Modified Wilson Model".

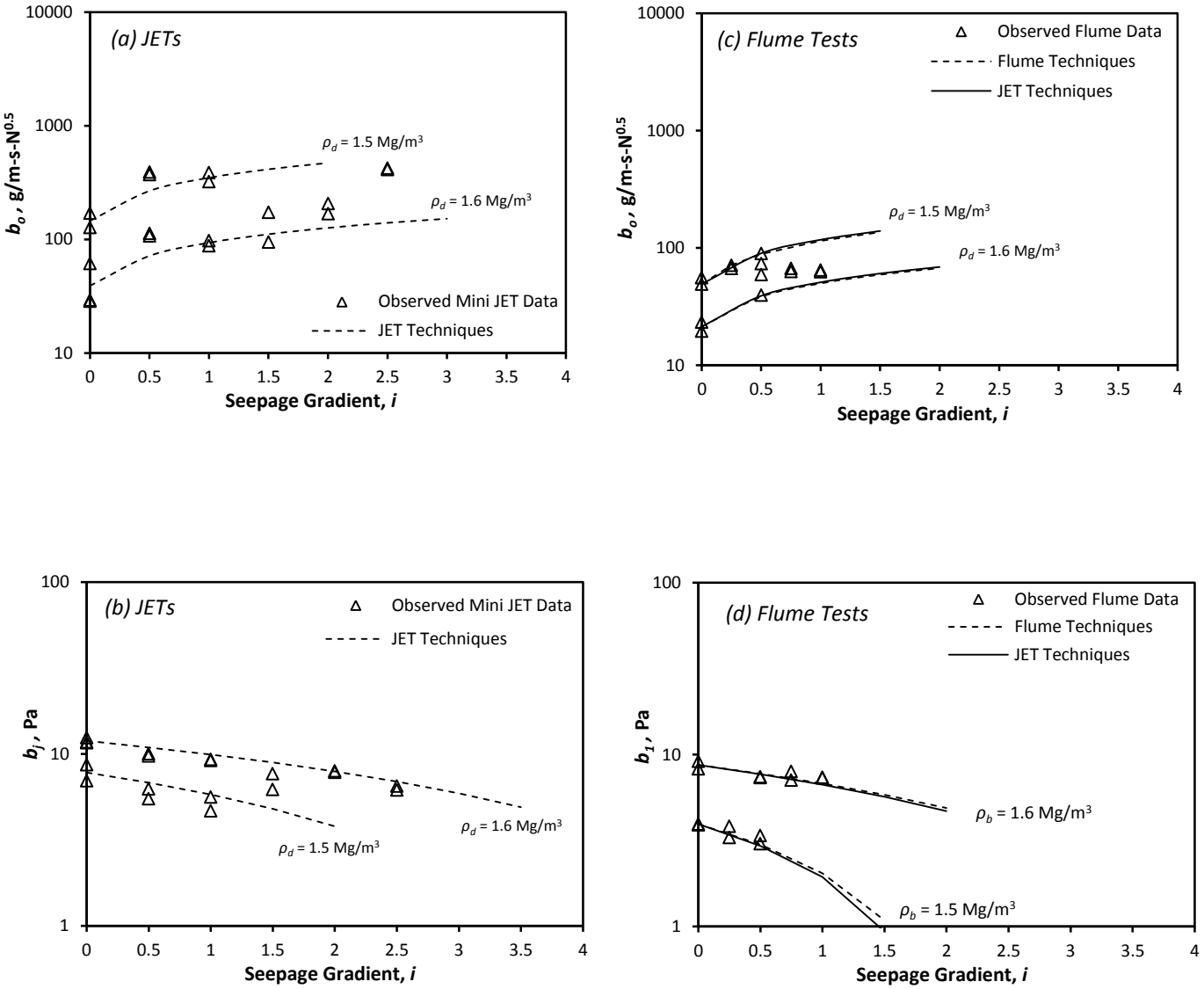

Figure 5.8. Evaluating the ability to predict the "Modified Wilson Model" parameters b_1 and b_0 using data from flume tests and JETs without seepage for the silty sand soil. Symbols represent the derived parameters from flume tests and JETs with seepage. Dashed and solid lines represent the predictions of b_1 and b_0 based on the seepage gradient (*i*).

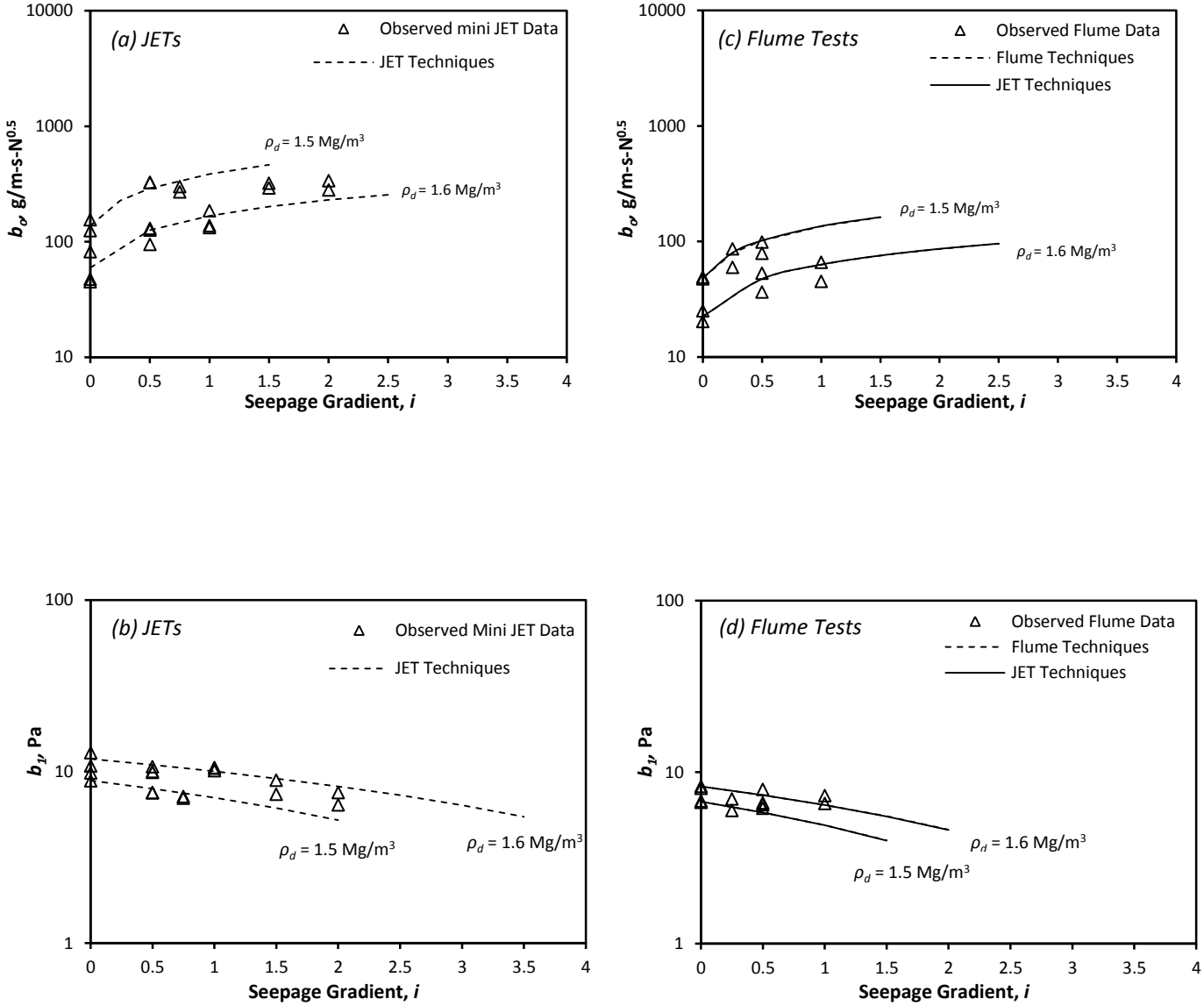

Figure 5.9. Evaluating the ability to predict the "Modified Wilson Model" parameters b_1 and b_0 using data from flume tests and JETs without seepage for the clayey sand soil. Symbols represent the derived parameters from flume tests and JETs with seepage. Dashed and solid lines represent the predictions of b_1 and b_0 based on the seepage gradient (i).

The "Modified Wilson Model" predicted the observed data from "mini" JET as well as or even better than the flume tests. As expected, increased seepage forces decreased the observed

"Modified Wilson Model" parameter b_1 but increased the parameter b_0 for both flume and JETs. The influence of seepage on erosion can be predicted based on JET techniques using the "Modified Wilson Model" parameters with a priori flume or/and JET experiments without seepage. JET techniques can be used to predict the influence of seepage on the soil erodibility from observed erosion of streambeds. In general, the "Modified Wilson Model" is advantageous in being a more mechanistic, fundamentally based erosion equation that can replace more commonly used empirical detachment models such as the excess shear stress model.

5.8. ACKNOWLEDGMENTS

This research is based upon work supported by the National Science Foundation under Grant No. 0943491. Any opinions, findings, and conclusions or recommendations expressed in this material are those of the authors and do not necessarily reflect the views of the National Science Foundation. The authors acknowledge Mohammad Rahi and David Criswell, Oklahoma State University, for assisting with the flume experiments.

CHAPTER VI

PREDICTING THE ERODIBILITY OF STREAMBANKS DUE TO FLUVIAL AND SEEPAGE FORCES[5]

6.1. ABSTRACT

Seepage influences the erodibility of streambanks, streambeds, dams, hillslopes, and embankments. Usually the erosion rate of cohesive soils due to fluvial forces is computed using an excess shear stress model. However, no mechanistic approaches are available for incorporating seepage forces into the excess shear stress model parameters. Recent research was incorporated seepage forces into a mechanistic fundamental detachment rate model to improve predictions of the erosion rate of cohesive streambeds. The new detachment model, which is referred to as a "Modified Wilson Model", was based on two modified dimensional soil parameters (b_0 and b_1) that included seepage forces due to localized groundwater flow. The objective of this study was to modify the "Modified Wilson Model" parameters (b_0 and b_1) to predict the influence of seepage on erodibility of cohesive streambanks and to compare the results to those obtained from tests on

[5] Will be submitted to *Journal of Geomorphology*
Al-Madhhachi, A. T., Fox, G. A., Tyagi, A. K., Hanson, G. J., and Bulut, R. 2014. Predicting the Erodibility of streambanks due to Fluvial and Seepage Forces. Geomorphology.

horizontal beds. A new miniature version of a submerged jet erosion test device ("mini" JET) and a seepage column were utilized to deriving the "Modified Wilson Model" parameters, b_0 and b_1, of a silty sand soil and a clayey sand soil influenced by different seepage gradients. The experimental setup was intended to mimic a streambed and a streambank when the "mini" JET and seepage column were placed in vertical and horizontal directions, respectively. The soils were packed in three equal lifts in a standard mold at a target uniform bulk density (1.5 to 1.6 Mg/m^3) near the soil's optimum water contents. The model was fit to the experimental data to derive b_0 and b_1 with and without the influence of seepage. The "Modified Wilson Model" predicted the observed data for both vertical and horizontal experimental setups. Seepage forces influenced the observed erosion data with a non-uniform influence on b_0 and b_1 as function of the hydraulic gradient and dry density. The influence of seepage forces can be predicted by the "Modified Wilson Model" parameters in both vertical and horizontal experimental setups as well as from field data using JET techniques.

6.2. INTRODUCTION

Hillslope and streambank erosion are important geomorphologic processes throughout the world. In fact, the erosion of streambanks represents a significant component of the total sediment load in some streams (Bull, 1997; Simon and Darby, 1999; Evans et al., 2006). Streambank erosion at the bank toe or at the top of confining layers often leads to undercutting and streambank collapse or failure in cohesive soils (Fox and Wilson, 2010). These locations are also points of considerable interaction between the streamflow and near-streambank groundwater during and immediately after storm events. However, when quantifying fluvial erosion rates, the interaction among the fluvial forces and adjacent near-surface groundwater forces are generally neglected, especially their effect on fluvial erosion (Fox and Wilson, 2010).

Recent studies have demonstrated the importance of ground water seepage on erosion and bank or hillslope failure (Fox et al., 2007; Wilson et al., 2007; Fox and Wilson, 2010). Several studies have investigated erosion specifically due to seepage, including the development of empirical sediment transport models for this process (Fox et al., 2006a; Fox et al., 2007; Wilson et al., 2007; Chu-Agor et al., 2008; Chu-Agor et al., 2009). The intricate linkage between seepage and fluvial forces has recently been emphasized in field seepage experiments (Midgley et al., 2012a). However, more work is needed on understanding the role of groundwater seepage gradients in the fluvial erosion process.

Typically the erosion rate of cohesive streambanks is simulated using excess shear stress models, such as in the Bank Stability and Toe Erosion Model (BSTEM, Midgley et al., 2012b). When considering multiple forces influencing soil erodibility, the disadvantage of using an excess shear stress model is the lack of mechanistic predictions of its parameters for specific soil and hydraulic conditions. A more fundamentally-based, mechanistic detachment model is preferred for modeling the range of environmental conditions experienced during fluvial erosion. A mechanistic detachment model provides the means for incorporating seepage forces directly.

Wilson (1993a, 1993b) developed a mechanistic detachment model to provide a general framework for studying soil and fluid characteristics and their impact on cohesive soil erodibility. The model was developed based on a simple two-dimensional representation of particles. However, the detachment model is not restricted to a single particle and can be applied for aggregates. The model was evaluated using erosion rate data for cohesive soils. The model was calibrated to the observed data based on two dimensional parameters b_0 and b_1.

A new miniature version of a submerged jet erosion test (JET) device, which is referred to as the "mini" JET, was recently developed (Al-Madhhachi et al., 2012a). The "mini" JET device is smaller, lighter, and requires less water compared to the original JET device and can be

more easily used in the field as well as in laboratory. The "mini" JET provides essentially equivalent results to the original JET (Simon et al., 2010; Al-Madhhachi et al., 2012a). Recently Al-Madhhachi et al. (2012b) incorporated the hydraulic analysis of JET devices into the fundamental detachment model (the "Wilson Model") to predict the erodibility of cohesive soils. They used both the original and "mini" JET devices and verified the results with data from flume tests. The "Wilson Model" predicted the observed data for flume and JET devices as well as or better than the excess shear stress model. Al-Madhhachi et al. (2012b) verified the results of using "mini" JET with the flume test results in predicting the erosion rate of cohesive soils using the "Wilson Model" parameters or/and excess shear stress model parameters. They concluded that the more fundamentally-based detachment model can be used in the place of the excess shear stress equation with parameters that can be estimated using existing JET techniques.

Al-Madhhachi et al. (2013a, 2013b) incorporated seepage forces into a mechanistic detachment model to predict the erodibility of cohesive soils. Their model ("Modified Wilson Model") was based on the general framework developed by Wilson (1993a, 1993b), but also included seepage forces with two soil parameters (b_0 and b_1). They performed flume and laboratory "mini" JETs along with a seepage column to measure the "Modified Wilson Model" parameters (b_0 and b_1) for silty sand and clayey sand soils packed at a uniform bulk density (1.5 to 1.6 Mg/m^3) near the soil's optimum water content. They found that the influence of seepage on erosion can be predicted using JET techniques in the "Modified Wilson Model" parameters with a prior JET experiments without seepage. However, their model was limited to predicting the influence of seepage on erodibility of horizontal beds (i.e., cohesive streambeds) only.

The next step is to utilize the "Modified Wilson Model" to analyze the influence of seepage forces on the erodibility of vertically oriented banks and hillslopes such as cohesive streambanks, where material orientations influence the driving and resistance forces of erosion. The objective of this study was to modify the "Modified Wilson Model" parameters to predict the

influence of seepage on erodibility of cohesive streambanks using "mini" JETs and to compare the results to those obtained from tests on horizontal beds (i.e., streambeds).

6.3. GENERAL THEORETICAL FRAMEWORK INCLUDING SEEPAGE IN STREAMBEDS

The general framework for predicting erosion rate was based on the dislodging and stabilizing forces and their associated moment lengths for particle detachment (Figure 6.1). Al-Madhhachi et al. (2013a, 2013b) incorporated seepage forces into a mechanistic detachment model ("Modified Wilson Model") to predict the erodibility of cohesive streambeds. The "Modified Wilson Model" was based on the general framework developed by Wilson (1993a, 1993b), but also included seepage forces with two soil parameters (b_0 and b_1).

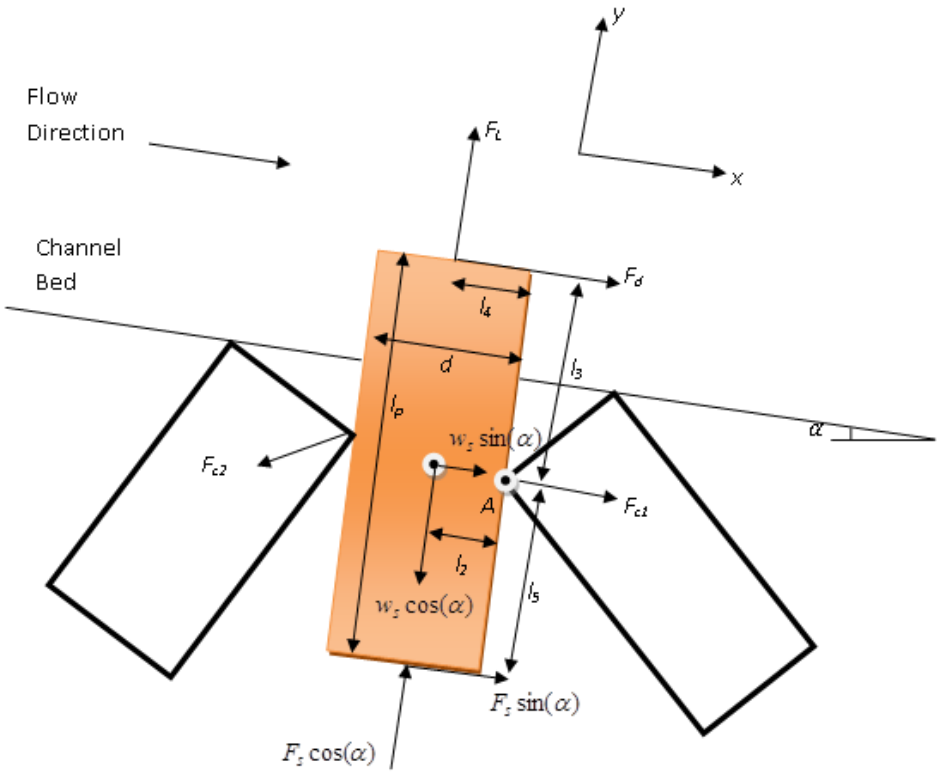

Figure 6.1. The arrangement of a particle for compacted soil as proposed in this study for a horizontal channel (where F_L is the lift force; F_d drag force; w_s is the submerge particle weight; F_{c1}, F_{c2},……, F_{cn} are contact forces between particles; F_s is the seepage force; l_1, l_2, l_3, l_4 and l_5 are lengths of moments for the forces; $l_p = n_p d$ is the length of a tetragonal particle, n_p is a particle length factor; d is an equivalent particle diameter; and α is the channel angle slope) (Al-Madhhachi et al., 2013a).

Al-Madhhachi et al. (2013a) assumed that the soil particle is a tetragonal shape system (plate) with an angle of 90 degrees at its edges and a square top face (Figure 6.1). This was hypothesized due to the nature of the arrangement of particles based on the Lambe (1962) model of sample preparation at optimum water content. The values of parameters according to Al-Madhhachi et al. (2013a) are shown in Table (6.1).

The detachment rate model (ε_r , M/L^2/T) for JET data under the influence of seepage on streambeds can be expressed as (Al-Madhhachi et al., 2013a, 2013b):

$$\varepsilon_r = b_0 \sqrt{\tau_j} \left[1 - \exp\{-\exp(3 - \frac{b_1}{\tau_j})\} \right] \tag{6.1a}$$

$$b_0 = \rho_s \frac{k_r}{K_e} \sqrt{\frac{K_{nj} + K_{st}}{k_{dd}(\rho_s - \rho_w)}} \tag{6.1b}$$

$$b_1 = (\frac{\pi}{e_v \sqrt{6}}) \frac{k_r (K_{ls} - K_s + f_c)}{K_{oj}} g(\rho_s - \rho_w) d \tag{6.1c}$$

where b_0 has dimensions of $(M/L^3)^{0.5}$; b_1 has dimensions of F/L^2; and other key terms and parameters are defined as:

$$\tau_j = \tau_o \left(\frac{J_p}{J} \right)^2 \tag{6.2a}$$

$$K_{nj} = K_t \; K_{oj} / k_r \tag{6.2b}$$

$$K_{oj} = \frac{5.537 C_D K_f \exp[-200(\frac{z_d}{r})^2]}{C_f c_d{}^2} \tag{6.2c}$$

Table 6.1. Definition of parameters in the "Modified Wilson Model".

Symbols	Description	Value or Equation	Reference
C	Discharge jet coefficient	0.75	Al-Madhhachi et al. (2012a)
C_D	Drag coefficient	0.2	Einstein and El-Samni (1949)
C_d	Diffusion constant	6.3	Hanson and Cook (2004)
C_f	Coefficient of friction	0.00416	Hanson and Cook (2004)
d	Equivalent particle diameter equivalent to d_{50}	0.16 mm for silty sand and 0.095 mm for clayey sand	Al-Madhhachi et al. (2013b)
d_o	Nozzle diameter	3.18 mm for "mini" JET	Al-Madhhachi et al. (2012a)
e_v	Coefficient of variation	0.35	Einstein and El-Samni (1949)
h	Pressure head for JET	64 cm	Experiments in this study
i	Hydraulic gradient	0.25 to 2.5	Experiments in this study
J_i	Jet nozzle height	34 mm	Al-Madhhachi et al. (2013b)
J_p	Potential core of jet nozzle	$C_d\, d_o$	Hanson and Cook (2004)
K	Kinematic moment flux	$0.153\pi d_0^2 U_0^2$	Poreh et al. (1967)
K_e	Exposure of lower particle parameter	-	Wilson (1993a, 1993b)
K_f	Ratio of projected area drag and lift forces	k_a/n_p	Al-Madhhachi et al. (2013a)
K_L	Ratio of drag and lift coefficients along with the ratio of velocities	1	Wilson (1993a, 1993b)
K_t	Factor of cumulating of instantaneous fluid forces	2.5	Chepil (1959)
k_a	Area constant of a tetragonal particle	1	Al-Madhhachi et al. (2013a)
k_{dd}	Detachment distance parameter	2	Einstein (1950)
k_r	Geometry ratio for a tetragonal particle	k_v/k_a	Al-Madhhachi et al. (2013a)
k_s	Roughness height	$n_p\, d/2$	Al-Madhhachi et al. (2013a)
k_v	Volume constant of a tetragonal particle	n_p	Al-Madhhachi et al. (2013a)
l_1	Moment length of gravity downslope	0	Al-Madhhachi et al. (2013a)
l_2	Moment length of gravity into bed	$d/2$	Al-Madhhachi et al. (2013a)
l_3	Moment length of drag force	$n_p\, d/2$	Al-Madhhachi et al. (2013a)
l_4	Moment length of lift force	$d/2$	Al-Madhhachi et al. (2013a)
l_5	Moment length of seepage force	$n_p\, d/2$	Al-Madhhachi et al. (2013a)
n_p	Particle length factor for tetragonal particle	2.8 for silty sand and 4.5 for clayey sand	Al-Madhhachi et al. (2013b)
r	Jet radius upon maximum jet velocity works	$0.13\, Ji$	Al-Madhhachi et al.(2012b)
U_o	Velocity of jet at the orifice	$C\sqrt{2gh}$	Hanson and Cook (2004)
w_s	Submerged particle weight	$g(\rho_s - \rho_w)k_v d^3$	Wilson (1993a, 1993b)
y_p	Pivot point a tetragonal particle	$k_s - n_p\, d/2 - l_1$	Al-Madhhachi et al. (2013a)

Table 6.1. (Continued).

Symbols	Description	Value or Equation	Reference
z_d	Height that the drag velocity is acting upon	$l_3 + y_p$	Al-Madhhachi et al. (2013a)
μ_{sr}	Seepage coefficient ratio	3.85	Al-Madhhachi et al. (2013b)
ρ_s	Particle density	2.65 Mg/m^3	Freeze and Cherry(1979)
ρ_w	Water density	1 Mg/m^3	-
α	Bed angle slope	0	Experiments in this study
θ	Bank angle slope	90	Experiments in this study

$$K_{st} = \mu_{sr} g i d \rho_w \tag{6.2d}$$

$$K_{ls} = \frac{\cos(\alpha)(l_2 - l_1 S)}{l_3 + l_4 \frac{K_L}{K_f}} \tag{6.2e}$$

$$K_s = \frac{i \rho_w}{(\rho_s - \rho_w)} \frac{\cos(\alpha)(l_2 - l_5 S)}{l_3 + l_4 \frac{K_L}{K_f}} \tag{6.2f}$$

$$f_c = \frac{M_c}{w_s (l_3 + l_4 \frac{K_L}{K_f})} \tag{6.2g}$$

where τ_j is the average shear stress for JET, K_{nj} is a combination of particle and fluid factors for JET, K_{oj} is known as a velocity jet parameter, K_{st} is seepage parameter for exchange particle time, K_{ls} is a dimensionless parameter that depends on particle size, its orientation within the bed, and slope; K_s is a seepage parameter that depends on hydraulic gradient, particle density, its orientation within the bed, and slope; f_c is a dimensionless parameter based on cohesion; M_c is the sum of moments of cohesive and frictional resistance forces as proposed by Wilson (1993a); and other terms are defined in Table (6.1).

The parameters b_0 and b_1 can be derived from JET data using curve fitting techniques and statistical methods by iteratively minimizing the error of these functions relative to measured erosion data. In the absence of seepage, the seepage parameters can be neglected (i.e. $K_s = 0$ and $K_{st} = 0$) and the developed model (i.e., equations 6.1a-6.1c) will match the set of equations developed by Al-Madhhachi et al. (2012b) (i.e., the "Wilson Model") for JETs.

6.4. GENERAL THEORETICAL FRAMEWORK INCLUDING SEEPAGE IN STREAMBANKS

Equations (6.1a)-(6.1c) can be applied to vertically-oriented JETs, as would be conducted for estimating the erodibility of cohesive streambeds. Similarly, the "Modified Wilson Model" can be also modified for a hillslope or streambank. Forces acting to remove a single soil particle on a streambank including the lift force, F_L, drag force, F_d, particle weight, w_s, contact forces between particles (F_{c1}, F_{c2},……, F_{cn}), and the addition seepage force, F_s are shown in Figure (6.2). The drag force is acting perpendicular to the paper. Particle detachment occurs if the driving moment is greater than the resistive moment. If it is assumed that these moments act around point *A*, then the point of incipient motion with the addition of a seepage force can be defined as:

$$F_d(l_3) + F_L(l_4) + w_s \sin(\theta)(l_1) + F_s \sin(\theta)(l_2) = F_s \cos(\theta)(l_5) + w_s \cos(\theta)(l_2) + M_c \qquad (6.3)$$

where θ is the bank angle and the other terms were defined in Table (6.1). By assuming that the drag force and lift force are proportional (i.e., $K_L/K_f = F_L/F_d$) (Chepil, 1959; Wilson, 1993a) and incorporating the seepage force ($F_s = iVg\rho_w = ik_v d^3 g\rho_w$, where V is the particle volume), equation (6.3) can be rewritten as:

$$F_d = -w_s\left[\frac{\sin(\theta)(l_1)-\cos(\theta)(l_2)}{l_3+l_4\dfrac{K_L}{K_f}}\right]-ik_v d^3 g\rho_w\left[\frac{\sin(\theta)(l_2)-\cos(\theta)(l_5)}{l_3+l_4\dfrac{K_L}{K_f}}\right]+\left[\frac{M_c}{l_3+l_4\dfrac{K_L}{K_f}}\right] \quad (6.4)$$

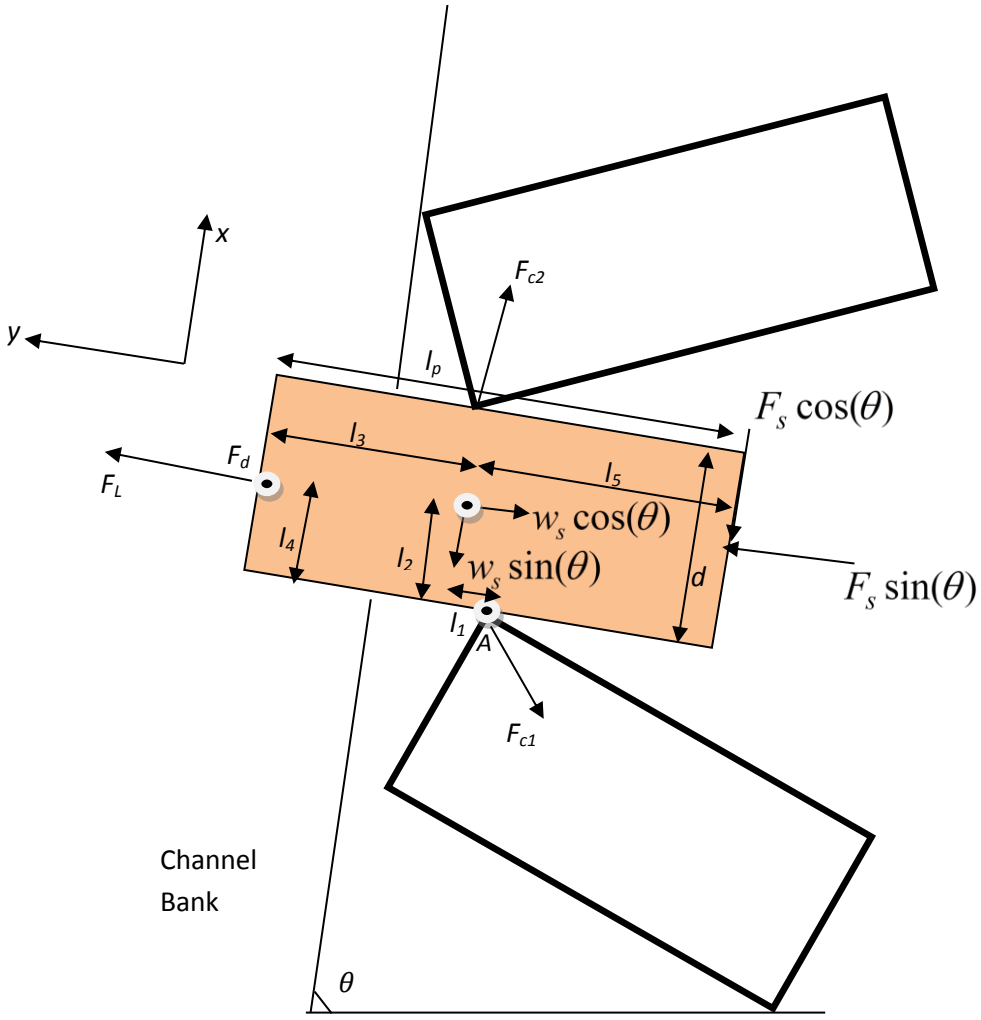

Figure 6.2. Forces and moment lengths acting on a single soil particle in a channel bank in the presence of a seepage force as proposed in this study (where F_L is the lift force; F_d drag force; w_s is the submerge particle weight; F_{c1}, F_{c2},……, F_{cn} are contact forces between particles; F_s is the seepage force; l_1, l_2, l_3, l_4 and l_5 are lengths of moments for the forces; and θ is the bank angle).

The above equation can be rearranged by introducing K_{lsb} and K_{sb} terms:

$$F_d = w_s(f_c - K_{lsb} - K_{sb}) \tag{6.5a}$$

$$K_{lsb} = \frac{\sin(\theta)(l_1) - \cos(\theta)(l_2)}{l_3 + l_4 \frac{K_L}{K_f}} \tag{6.5b}$$

$$K_{sb} = \frac{i\rho_w}{(\rho_s - \rho_w)} \frac{\sin(\theta)(l_2) - \cos(\theta)(l_5)}{l_3 + l_4 \frac{K_L}{K_f}} \tag{6.5c}$$

where K_{lsb} is a dimensionless parameter for the streambanks (K_{lsb} = 0 when l_1 = 0 and θ = 90 degrees); K_{sb} is a seepage parameter for streambanks; and f_c and other parameters were previously defined [K_{sb} is valid only when θ > $\tan^{-1}$ (n_p)]. The particle is detached if the flow characteristics on the left side (F_d) of equation (6.5a) are greater than the right side: $w_s(f_c - K_{lsb} - K_{sb})$, which is due to particle, seepage, and bank characteristics. The values of k_r, K_f, z_d, l_1, l_2, l_3, l_4, and l_5 for streambanks are the same as for streambeds (Table 6.1). By incorporating equations (6.5) and following the same procedure to develop the "Modified Wilson Model" as reported by Al-Madhhachi et al. (2013a), the detachment rate for a streambank in presence of seepage can be expressed as:

$$\varepsilon_r = b_0 \sqrt{\tau_j} \left[1 - \exp\{-\exp(3 - \frac{b_1}{\tau_j})\} \right] \tag{6.6a}$$

$$b_0 = \rho_s \frac{k_r}{K_e} \sqrt{\frac{K_{nj} + K_{st}}{k_{dd}(\rho_s - \rho_w)}} \tag{6.6b}$$

$$b_1 = (\frac{\pi}{e_v \sqrt{6}}) \frac{k_r(f_c - K_{lsb} - K_{sb})}{K_{oj}} g(\rho_s - \rho_w)d \tag{6.6c}$$

where b_0 has dimensions of $(M/L^3)^{0.5}$ and b_1 has dimensions of F/L^2. Similarly, by using curve fitting techniques and solver routines, the parameters b_0 and b_1 can be derived from observed JET erosion data of a streambank under the influence of a seepage force.

6.5. DEVELOPING THE CRITICAL HYDRAULIC GRADIENT FOR STREAMBANKS

Al-Madhhachi et al. (2013a) developed the critical hydraulic gradient for streambeds based on the dislodging and stabilizing forces and their associated moment lengths for particle detachment in the absence of fluvial forces (i.e., $F_L = 0$ and $F_d = 0$). The critical hydraulic gradient (i_c) for streambeds was expressed as (Al-Madhhachi et al., 2013a):

$$i_c = \frac{(\rho_s - \rho_w)}{\rho_w} \frac{[l_2 - Sl_1]}{[l_2 - Sl_3]} + f_{cs} \tag{6.7a}$$

$$f_{cs} = \frac{M_c}{k_v d^3 g \rho_w [\cos(\alpha)(l_2) - \sin(\alpha)(l_3)]} \tag{6.7b}$$

where $S\ (= \tan\alpha)$ is the bed slope, f_{cs} is the dimensionless parameter based on cohesion and other terms were previously defined. For non-cohesive soils and horizontal channel slope (i.e. $S = 0$), the critical hydraulic gradient (i_c) is equal to $\frac{(\rho_s - \rho_w)}{\rho_w}$ which matches the critical hydraulic gradient reported in the literature (Fox and Wilson, 2010).

Similarly, the critical hydraulic gradient can be also derived for a hillslope or streambank. Figure (6.2) shows the forces acting to remove a single soil particle on a streambank during seepage (i.e. no fluvial forces, $F_L = 0$ and $F_d = 0$) including the particle weight, w_s, contact forces between particles (F_{c1}, F_{c2},……, F_{cn}), and seepage force, F_s. Particle detachment occurs if the driving moment is greater than the resisting moment. For particle balance, the theory is assumed

that these moments act around point *A*. Then the point of incipient motion due to the seepage force is defined as:

$$w_s \sin(\theta)(l_1) + F_s \sin(\theta)(l_2) = F_s \cos(\theta)(l_3) + w_s \cos(\theta)(l_2) + M_c \quad (6.8)$$

where all terms were previously defined. By incorporating a seepage force ($ik_v d^3 g\rho_w$) and the submerged particle weight [$g(\rho_s - \rho_w)k_v d^3$], equation (6.8) can be rewritten as:

$$i_c k_v d^3 g\rho_w\left[\sin(\theta)(l_2) - \cos(\theta)(l_3)\right] = g(\rho_b - \rho_w)k_v d^3\left[\cos(\theta)(l_2) - \sin(\theta)(l_1)\right] + M_c \quad (6.9)$$

The above equation can be rearranged by dividing both sides by term $k_v d^3 g\rho_w\left[\sin(\theta)(l_2) - \cos(\theta)(l_3)\right]$ and introducing a f_{csb} term, the critical hydraulic gradient (i_c) for streambanks is expressed as:

$$i_c = \frac{(\rho_s - \rho_w)}{\rho_w}\frac{\left[\cos(\theta)(l_2) - \sin(\theta)(l_1)\right]}{\left[\sin(\theta)(l_2) - \cos(\theta)(l_3)\right]} + f_{csb} \quad (6.10a)$$

$$f_{csb} = \frac{M_c}{k_v d^3 g\rho_w\left[\sin(\theta)(l_2) - \cos(\theta)(l_3)\right]} \quad (6.10b)$$

where f_{csb} is the dimensionless parameter based on streambank cohesion. Equations (6.10a)-(6.10b) are valid for a streambank if $\theta > \tan^{-1}(n_p)$ and l_1 is equal to zero (assuming that point *A* is placed in the middle of a tetragonal particle, Figure 6.2). If $\theta < \tan^{-1}(n_p)$, then equations (6.7a)-(6.7b) are valid to calculate the critical hydraulic gradient (i_c) using the appropriate *S*.

6.6. METHODS AND MATERIALS

6.6.1. Vertical and Horizontal Experimental Devices

The "mini" JET and seepage column devices are illustrated in Figure (6.3a) and Figure (6.3b), respectively. The description, dimensions, functions, and parts of these devices were

reported by Al-Madhhachi et al. (2013b). The experimental setup of the "mini" JET device and the seepage column were intended to mimic a streambed and a streambank when they were placed in vertical and horizontal directions, respectively (Figure 6.4). In mimicking a streambed, the "mini" JET device provided a downward vertical fluvial force on the streambed while the seepage column provided an upward vertical seepage force (Figure 6.4a). In mimicking a streambank, the "mini" JET device provided the perpendicular horizontal fluvial force on the streambank face while the seepage column provided a perpendicular horizontal seepage force in the opposite direction (Figure 6.4b). Therefore, the setup was assumed to represent a conservative estimate of the influence of seepage on erodibility.

(a) "Mini" JET Device

(b) Seepage Column

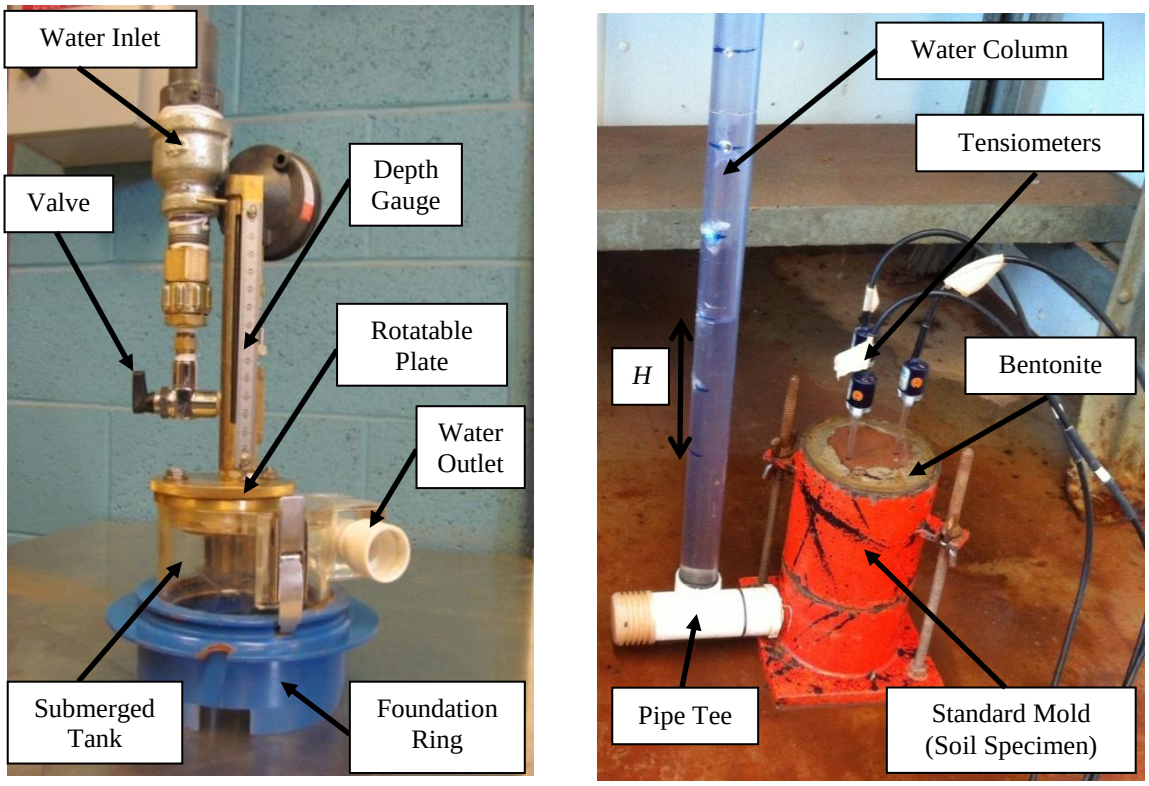

Figure 6.3. Laboratory "mini" JET device and seepage column (where *H* is the seepage head).

(a) Vertical (b) Horizontal

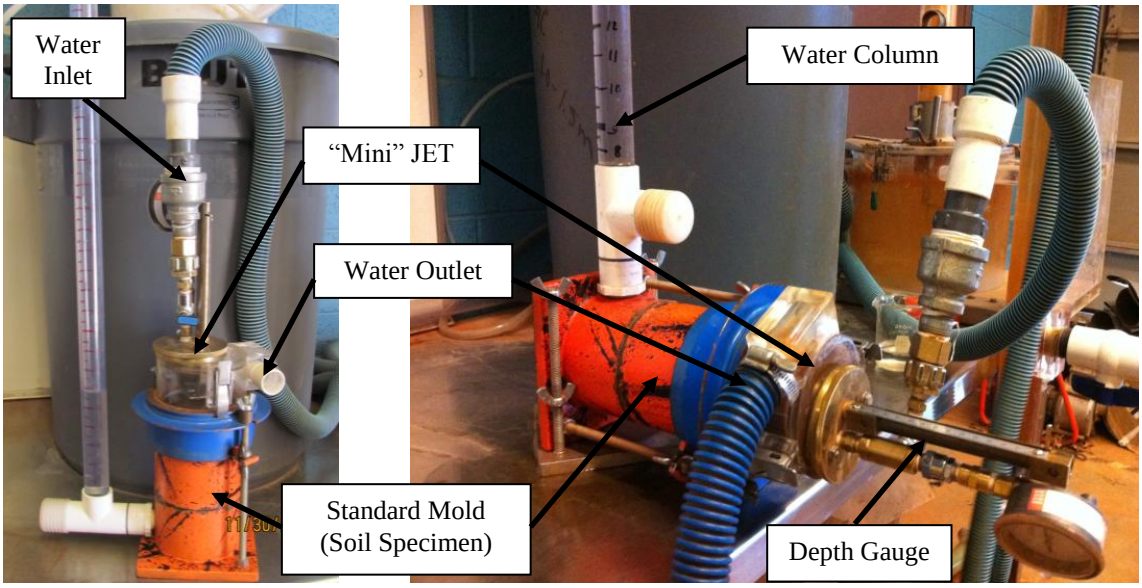

Figure 6.4. The experimental setup of the "mini" JET device and the seepage column when placed (a) vertically simulating a streambed and (b) horizontally simulating a streambank.

6.6.2. Soil Characteristics

The two soils utilized in the laboratory "mini" JET experiments were a silty sand soil and clayey sand soil (Table 6.2). These soils have been tested and analyzed according to ASTM Standards (2006). Sieve analysis and hydrometer tests were conducted according to ASTM Standard D422. Liquid limit and plastic limit tests were performed according to ASTM Standard D4318.

Table 6.2. Properties of the two soils for testing (Al-Madhhachi et al., 2012a).

Soil Location	Grain Size			Plasticity Index, %	Standard Compaction		Soil Classification USCS
	% Sand	% Silt	% Clay		Maximum Density, Mg/m^3	Optimum Water Content, %	
USDA Hydraulic lab	57	18	25	4	2.00	10.8	SC – Clayey Sand
Streambank of Cow Creek	72	13	15	Non- Plastic	1.83	12.9	SM – Silty Sand

6.6.3. Experimental Procedure

The soils were air dried and then passed through a sieve with openings of 4.75 mm (No. 4 sieve). The soils were packed in three equal lifts in a standard mold at a uniform bulk density (1.5 to 1.6 Mg/m^3) near the soil's optimum water content (14.5% to 16.0%). To achieve this optimum water content, the soils were mixed with required quantities of water and allowed to equilibrate for at least 24 hr in a closed container. Some samples were tested without seepage (i.e., $H = 0$) and without saturating the soil sample prior to the test (unsaturated soil sample). Others were tested using both the "mini" JET device and seepage column by inducing a desired constant H and saturating the sample prior to the test (Figure 6.3b). For samples tested with seepage, the edges of the soils in the standard mold were over packed and bentonite was packed along the edge of each layer to prevent water from flowing along the edges during the saturation process (Figure 6.3b). Tests were repeated for each set of experimental conditions.

For soil samples tested without seepage, the standard mold was placed in the center of the submerged tank directly below the jet nozzle for the "mini" JET device. The adjustable head tank was then set at the desired constant head. The steps of running the "mini" JET and collecting data for both vertical and horizontal experiment setups (without seepage) followed Al-Madhhachi et al. (2012a).

For soil samples tested with seepage forces, a pressure was provided to the standard mold by a constant head water column. The water column was filled with water to a desired water head and the setup was left to saturate the soil sample. Tensiometers were placed at different heights (5 and 7 cm) in the soil specimen to monitor pore-water pressures and the saturation process (Figure 6.3b). After the soil specimen was saturated and the imposed gradient established, the "mini" JET device was placed above the standard mold so that the standard mold was in the center of the submerged tank directly below the jet nozzle (Figure 6.4a). The adjustable head tank was then set

at the desired constant head and hoses (including water source) were connected to the JET device. The setup was ready for testing either for a vertical experimental setup or a horizontal experimental setup (Figure 6.4).

Before turning on the water, the depth gauge of the "mini" JET was used to determine the height of the jet nozzle by acquiring the depth gauge readings at the nozzle and the soil specimen surface at the initial time. The jet nozzle and depth gauge are part of a rotatable plate, so that while depth gauge readings were taken the nozzle was rotated away from impinging on the soil specimen. Following depth gauge readings, the jet valve was closed and the water source was opened to fill the head tank, and all air was released from the adjustable head tank. Then, the jet valve was opened to start filling the submerged tank of the "mini" JET. After the submerged tank was filled with water, an initial reading of the water head was taken from the top of the adjustable head tank to the water surface at the submerged tank. This reading was held constant during the test (64 cm for all experiments). The nozzle was then rotated to impinge directly on the soil surface to start the test. The depth gauge was used to acquire scour depth measurements at different time intervals and the water was manually added to the seepage column to apply a constant seepage head (H). Usually, the first reading was acquired after 60 s while the others were acquired every 1 to 5 minutes depending on the degree of scour.

6.6.4. Deriving the "Modified Wilson Model" Parameters

Data from the "mini" JETs for vertical and horizontal experimental setups were used to determine the "Modified Wilson Model" parameters b_o and b_1 for both silty sand and clayey sand soils. The "Modified Wilson Model" parameters b_o and b_1 were derived from observed "mini" JET data. Constraints were used within the Excel solver routine to limit potential solutions of b_o and b_1. The maximum allowable change for the parameters b_o and b_1 was between 50% to 60%

from their initial estimated values as recommended by Wilson (1993b) and Al-Madhhachi et al. (2012b).

In order to investigate how the model fit the observed data from "mini" JETs for both experimental setups, the normalized objective function (*NOF*) (Pennell et al., 1990; Hession et al., 1994) was calculated to quantify the acceptability of the model to fit the observed data. The *NOF* is the ratio of the standard deviation (*STDD*) of differences between observed and predicted data to the overall mean (X_a) of the observed data:

$$NOF = \frac{STDD}{X_a} = \frac{\sqrt{\frac{\sum_{i=1}^{N}(x_i - y_i)^2}{N}}}{X_a} \tag{6.11}$$

where x_i and y_i are the observed and predicted data, respectively, and N is the number of observations. In general, 1%, 10%, and 50% deviations from the observed values result in *NOF* values of 0.01, 0.1, and 0.5, respectively (Fox et al., 2006b).

6.7. APPLIED THE "MODIFIED WILSON MODEL" TO FIELD DATA

6.7.1. Introduction

Streambank restoration and stabilization is widely performed in the United States. However, data are currently lacking on the influence of construction techniques on the resistance of a streambank to geotechnical failure and fluvial erosion. Oklahoma State University constructed a multi-disciplinary riparian and streambank research, education, and demonstration facility along Cow Creek and will monitor and study the site for a minimum of five years. Cow Creek is a typical Oklahoma stream whose natural course has been manipulated and the stream is currently deepening and widening with the formation of associated side-gullies (Figure 6.5).

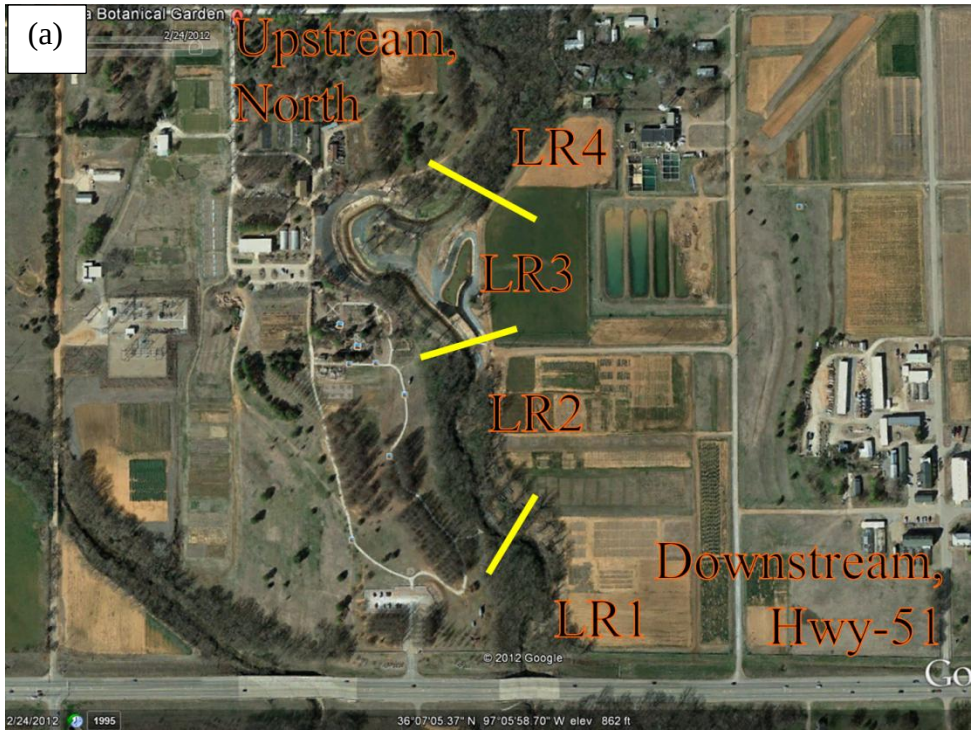

Figure 6.5. (a) Location of the reaches in Cow Creek and (b) In – situ "mini" JET device.

In order to derive the "Wilson Model" parameters (b_o and b_1) from field data, the "mini" JETs were performed on streambanks of Cow Creek, Stillwater, OK (Figure 6.5b). These tests were conducted as a part of stream restoration project along reaches with different levels of streambank modification (LR1, LR2, LR3, and LR4), as shown in Figure 6.5a. The "Modified Wilson Model" parameters b_o and b_1 were derived from JETs at the time without seepage. The soil erodibility of reach LR3 was also investigated for various hypothetical seepage gradients.

6.7.2. Reaches of Cow Creek

Four reaches were utilized on Cow Creek as a part of restoration project. These reaches were compared to one another for impact to erosion characteristics and processes including the interaction with the non-impacted plant assemblage in the control site upstream of the project and interaction with the new growth in the heavily modified reach and two downstream reaches that have rock structures installed.

The first reach (LR1) is located upstream of the highway, at which location a downstream double-step cross-vane was installed on the downstream side of the meander bend and a J-hook was installed on the upstream side of the inner meander bend area. Vegetation was removed for construction access on the inner meander, but no other treatment except seed, straw mulch, and vegetation plantings were used in the disturbed area following construction. The second reach (LR2) has two inner meander bends. Vegetation was removed for construction access on the inner meander, and the inner meander slope was pulled back to approximately a 2H:1V rather than 1H:1V. This area was stabilized with erosion matting, seed underneath. The upper disturbed areas were again treated with seed, straw mulch, and vegetation plantings following construction. The third reach (LR3) is the most heavily modified due to excavation and fill construction of the new stream alignment and stream bank slopes and benches. The downstream half of this reach has no rock structures. Six research plots are located in LR3 each 180 m in

length along the stream with 1H:1V slopes. The last reach (LR4) was not disturbed by construction.

6.7.3. Soil Characteristics of the Reaches

Soil samples were collected and analyzed from each of the reaches (Table 6.3). These samples were tested and analyzed according to ASTM Standards (2006). Sieve analysis and hydrometer tests were conducted according to ASTM Standard D422. Dry densities and water contents were determined for the soil samples (Table 6.3).

Table 6.3. Soil Characteristics of the Reaches.

Soil Properties	Reaches			
	LR4	LR3	LR2	LR1
Sand (%)	53	56	54	46
Silt (%)	21	19	21	26
Clay (%)	26	25	25	28
Water Content (%)	14-28	11-22	15-19	19-23
Dry Density (Mg/m^3)	1.40-1.61	1.59-1.89	1.55-1.73	1.27-1.40
(average values)	(1.57)	(1.73)	(1.59)	(1.35)

6.7.4. Deriving the model parameters from in-situ "mini" JETs

In-situ "mini" JETs were conducted for identifiable soil layers at the upstream control site LR4 and the three treatment sites (LR1, LR2, and LR3). The "Wilson Model" parameters b_o and b_1 were derived based on erosion data from "mini" JETs using an iterative solution aimed at minimizing the error between the measured data and the functional solutions of the equation using the generalized reduced gradient method. The influence of seepage on the soil erodibility of streambanks of the LR3 reach was investigated using the "Modified Wilson Model" parameters (equations 6.6b and 6.6c). Since the silty sand soil utilized in the laboratory experiments of this study were acquired from LR3, a comparison was performed between the

derived "Modified Wilson Model" parameters from laboratory experiments and the derived parameters from the field data.

6.8. RESULTS AND DISCUSSION

6.8.1. Established Hydraulic Gradient

The imposed hydraulic gradient (i) was verified from tensiometer readings from samples prepared for vertical and horizontal experimental setups during the saturation process based on an assumed the linear distribution of pressure heads (Table 6.4). Similar values between calculated and established hydraulic gradient were observed from prepared samples for both setups and both soils (Table 6.4). The critical hydraulic gradient (i_c) determined from equation (6.7a) for streambeds and equation (6.10a) for streambanks were also reported in Table (6.4). Some soil swelling was observed for samples tested with seepage during the saturation process for both experimental setups.

Table 6.4. Calculated and established hydraulic gradient (i) and calculated critical hydraulic gradient (i_c) from streambeds and streambanks of "mini" JETs for both soils.

Soils		Silty Sand			Clayey Sand		
Experimental Setups	Dry Density, Mg/m^3	Imposed i	Established i	i_c	Imposed i	Established i	i_c
Vertical	1.6	0.50	0.42	5.82	0.50	0.51	5.85
		1.00	1.04		1.00	1.01	
		1.50	1.35		1.50	1.45	
		2.00	1.99		2.00	2.01	
		2.50	2.57		2.50	NA*	
	1.5	0.50	0.41	3.89	0.50	0.41	4.84
		0.75	NA		0.75	0.68	
		1.00	1.01		1.00	NA	
Horizontal	1.6	0.50	0.38	7.24	0.50	0.51	5.22
		1.00	0.97		1.00	1.02	
		1.50	1.52		1.50	1.53	
		2.00	2.08		2.00	NA	
	1.5	0.50	0.41	3.47	0.50	0.41	3.36
		1.00	0.98		1.00	NA	

* NA = Not measured for this case.

6.8.2. Observed Erosion Data with Seepage

Seepage forces influenced the observed scour depth measurements when "mini" JETs were performed for both soils and for vertical and horizontal experimental setups (Figure 6.6). Higher erosion rates were observed when hydraulic gradients increased for both soils in both setups. Even higher erosion data were observed when seepage gradient imposed for horizontal experimental setup, especially for clayey sand soil. Seepage forces tended to have less influence as the material density increased for both setups and for both soils.

6.8.3. Seepage and "Modified Wilson Model"

The "Modified Wilson Model", based on derived parameters b_o and b_1, matched the observed scour depth versus time for "mini" JETs of both streambeds and streambanks (Figure 6.6). The model matched the erosion data without seepage ($i = 0$) and with seepage ($i > 0$). *NOF* values for the observed versus predicted scour depths by the "Modified Wilson Model" for the silty sand soil ranged from 0.03 to 0.16 and for the clayey sand soil ranged from 0.00 to 0.20 (Table 6.5) for both experimental setups.

The "Modified Wilson Model" parameters are primarily soil material parameters that depend on properties of the soil particle shape and its orientation. The parameter b_o was developed to include the seepage force in its formulation (equations 6.1b for streambeds and 6.6b for streambanks) as well as to parameter b_1 (equations 6.1c for streambeds and 6.6c for streambanks). Note that b_1 decreased as the seepage force (K_s or K_{sb}) increased while b_o increased as K_{st} increased due to an increased hydraulic gradient (Figure 6.7). Note that b_o for streambeds is theoretically equivalent to the b_o of streambanks. This was verified based on the approximately equivalent values from the experimental data (Figures 6.7a and 6.7c). The values of b_1 were unique from b_1, and again verified by the experimental data (Figure 6.7b and 6.7d). The behavior

of derived the "Modified Wilson Model" parameters followed their formulations relative to soil properties, soil orientation, and soil cohesion.

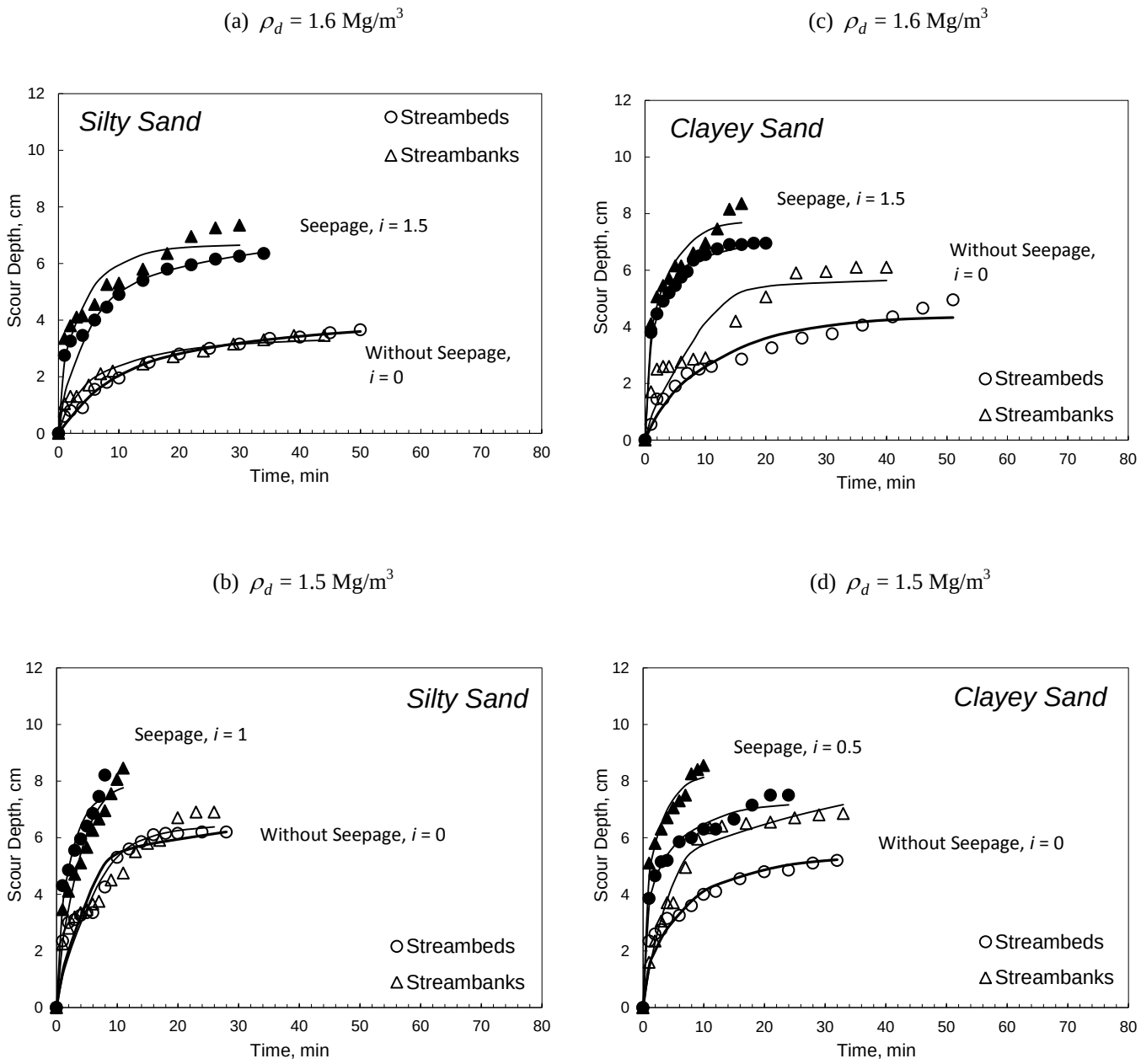

Figure 6.6. Comparison between the observed (circles for streambeds and triangles for streambanks) and predicted erosion data using the "Modified Wilson Model" (lines) for data without seepage (open circles for streambeds and open triangles for streambanks) and a case with seepage (solid circles for streambeds and solid triangles for streambanks). Observed erosion data are from streambeds and streambanks of "mini" JETs for the both soils at 1.5 to 1.6 Mg/m^3.

Table 6.5. *NOF* values for observed versus predicted scour depths by "Modified Wilson Model" for both soils and from "mini" JETs. All tests were performed with a total number of samples, n = 40 for streambeds and n = 30 for streambanks for both soils.

Soils	Silty Sand						Clayey Sand					
Model	Streambeds			Streambanks			Streambeds			Streambanks		
	Min	Max	Ave	Min	Max	Ave	Min	Max	Ave	Min	Max	Ave
Modified Wilson	0.03	0.16	0.10	0.03	0.16	0.09	0.03	0.13	0.08	0.00	0.20	0.08

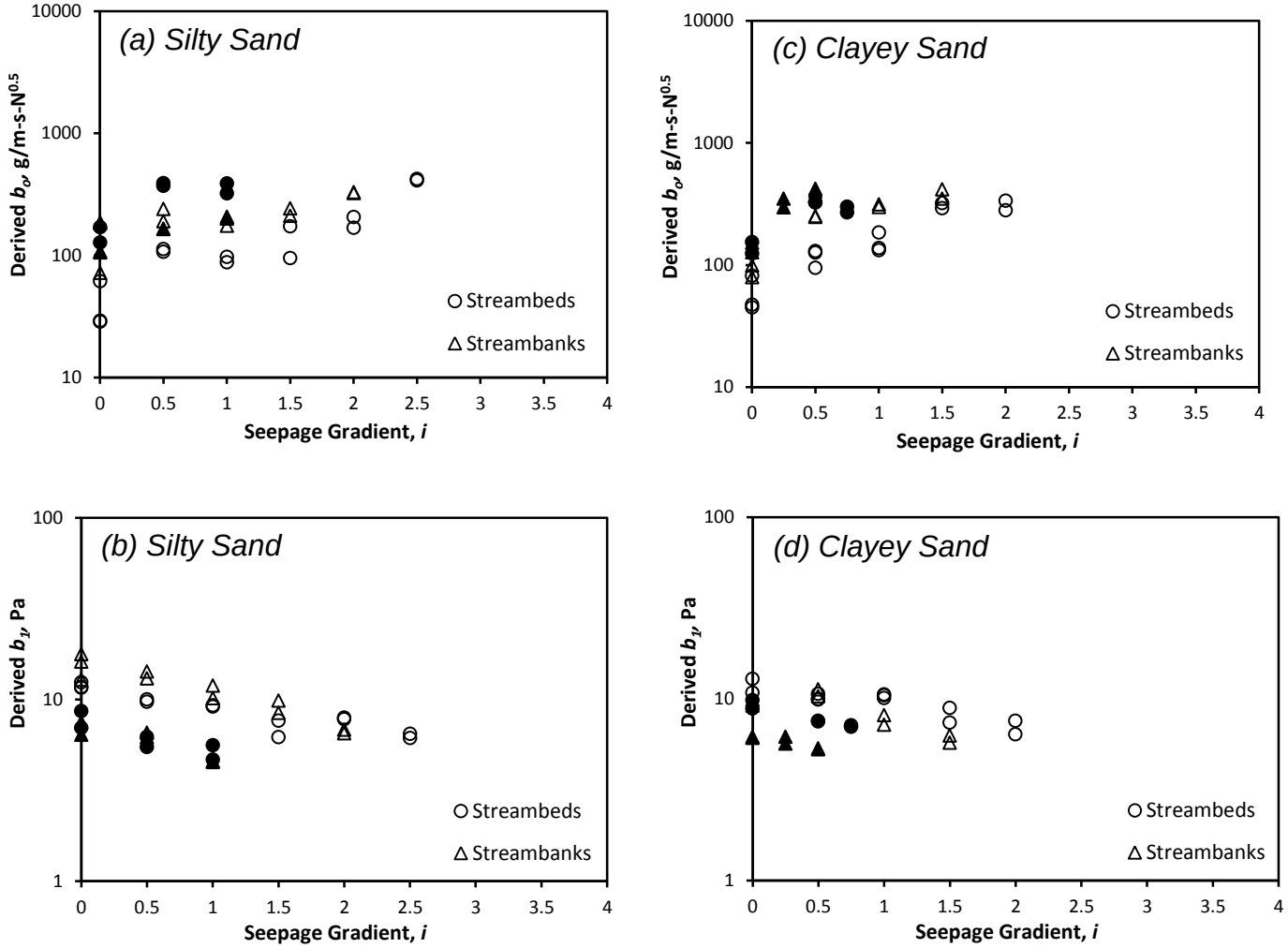

Figure 6.7. Influence of a seepage force on the deriving "Modified Wilson Model" parameters (b_o and b_1) at uniform bulk density (solids symbols represent ρ_d = 1.5 Mg/m^3 and opens symbols represent ρ_d = 1.6 Mg/m^3) from streambeds (circles) and streambanks (triangles) of "mini" JETs.

6.8.4. Predicting Seepage Parameters from laboratory JET Data without Seepage

The erodibility of cohesive soils under the influence of seepage can theoretically be predicted based on observed JET data without seepage for a streambed or/and a streambank. A "mini" JET could be performed on a streambed or/and a streambank at a time without seepage to derive b_o and b_1. Then, b_1 can be converted to modified b_1 (that include seepage) and b_o can be converted to modified b_o (that include seepage) based on measured or predicted seepage gradients at any time without re-running JETs. The parameters b_o and b_1 are mechanistically defined. Accordingly, for streambeds and modified parameter b_1, equation (6.1c) can be rewritten as:

$$b_1 = (\frac{\pi}{e_v\sqrt{6}})\frac{k_r(K_{ls}+f_c)}{K_{oj}}g(\rho_s-\rho_w)d - (\frac{\pi}{e_v\sqrt{6}})\frac{k_r K_s}{K_{oj}}g(\rho_s-\rho_w)d \qquad (6.12)$$

where the first term $(\frac{\pi}{e_v\sqrt{6}})\frac{k_r(K_{ls}+f_c)}{K_{oj}}g(\rho_s-\rho_w)d$ is the "Wilson Model" parameter b_1 for a streambed from JET data without seepage (i.e., $K_s = 0$). The second term in equation (6.12) can be mathematically calculated by using the parameters from Table (6.1). Similar procedure could be conducted to obtain the parameter b_1 of streambanks (equation 6.6c).

In the same fashion, the "Modified Wilson Model" parameter b_0 is also influenced by seepage forces and in particular in the K_{st} term (see equations 6.1b and 6.2d). The terms in equation (6.1b) can be mathematically calculated by using the values in Table (6.1). The parameter K_e can be predicted from observed JET data for a streambed without seepage:

$$K_e = \rho_s \frac{k_r}{b_0}\sqrt{\frac{K_{nj}}{k_{dd}(\rho_s-\rho_w)}} \qquad (6.13)$$

where b_0 is the "Wilson Model" parameter in $(M/L^3)^{0.5}$ and other terms were defined in Table (6.1). Similarly, the parameter b_0 for a streambank can be mathematically calculated from JET data without seepage (see equation 6.6b) based on values reported in Table (6.1) and equation (6.13).

The predictive equations for b_o and b_1 (with seepage) from derived parameters b_o and b_1 (without seepage) appropriately estimated the observed parameter values from JETs and for both soils (Figures 6.8 and 6.9). Prediction of b_1 was based on the seepage gradient, the parameter n_p (2.8 for silty sand and 4.5 for clayey sand), and particle diameter, d. Prediction of b_o was based on hydraulic gradient (K_{st}), the parameter n_p, soil particle diameter, d, and the seepage coefficient ratio, μ_{sr} . Additional researches are needed to determine n_p and μ_{sr} for various seepage forces in different soil types.

6.8.5. Predicting Seepage Parameters from Field Data

As expected, differences were observed in the derived the "Wilson Model" parameters b_o and b_1 for tests performed at the four reaches of Cow Creek streambanks using in-situ "mini" JET as shown in Figure (6.10). It appeared that streambank modification, even excavation and reconstruction of the streambank, resulted in no apparent differences in the reaches. There was a general increasing trend in b_1 moving in the upstream direction, but no correlation to streambank modification type.

As stated previously, the erodibility of cohesive soils under the influence of seepage can theoretically be predicted based on observed JET data without seepage for a streambank (equations 6.6b and 6.6c). For reach LR3, the average value of b_1 was 14.22 Pa for nine tests performed on streambank of LR3. The other terms in equation (6.6c) can be mathematically calculated by using the parameters from Table (6.1). In the same fashion, the parameter b_0 is also influenced by seepage forces and in particular in the K_{st} term (see equations 6.6b). The terms in equation (6.6b) can be mathematically calculated by using the values in Table (6.1). The parameter K_e can be predicted from observed JET data performed on LR3 streambanks without seepage (using equation 6.13 and average b_0 = 76.55 g/m-s-N$^{0.5}$ for nine tests).

The predictive equations for b_o and b_1 from derived field data parameters appropriately estimated the observed parameter values from laboratory JETs performed on a vertical setup for the silty sand soil (Figures 6.11). The results from laboratory and field data experiments indicted that the "Modified Wilson Model" can be simulated in any erosion model such as the Bank Stability and Toe Erosion Model (BSTEM, Midgley et al., 2012b) to predict the soil erodibility due to fluvial forces and any additional forces such as the seepage.

6.9. SUMMARY AND CONCLUSIONS

Seepage forces acting in concert with fluvial forces were incorporated into a fundamental detachment model to predict the erodibility of cohesive streambanks. The "Modified Wilson Model" was based on the general framework developed by Wilson (1993a, 1993b), but also included seepage forces with two soil parameters (b_0 and b_1) that extended by Al-Madhhachi et al. (2013a). A laboratory "mini" JET device and a seepage column were utilized to derive the "Modified Wilson Model" parameters (b_0 and b_1) for silty sand and clayey sand soils packed at a uniform bulk density (1.5 to 1.6 Mg/m^3) near the soil's optimum water content. The experimental setup was intended to mimic a streambed and a streambank when the devices were placed in vertical and horizontal directions, respectively. Seepage forces influenced the observed and predicted scour depth data when using the "Modified Wilson Model" parameters. The "Modified Wilson Model" predicted the observed data across a range of seepage gradients imposed on the both soils and for vertical and horizontal experimental setups. As expected, increased seepage forces decreased the observed "Modified Wilson Model" parameter (b_1) but increased the parameter b_0. The influence of seepage on erosion can be predicted using the "Modified Wilson Model" parameters (b_0 and b_1) with a priori JET experiments on streambeds or/and streambanks without seepage. In general, the "Modified Wilson Model" is advantageous in being a more

mechanistic, fundamentally based erosion equation as compared to the other models such as the excess shear stress model.

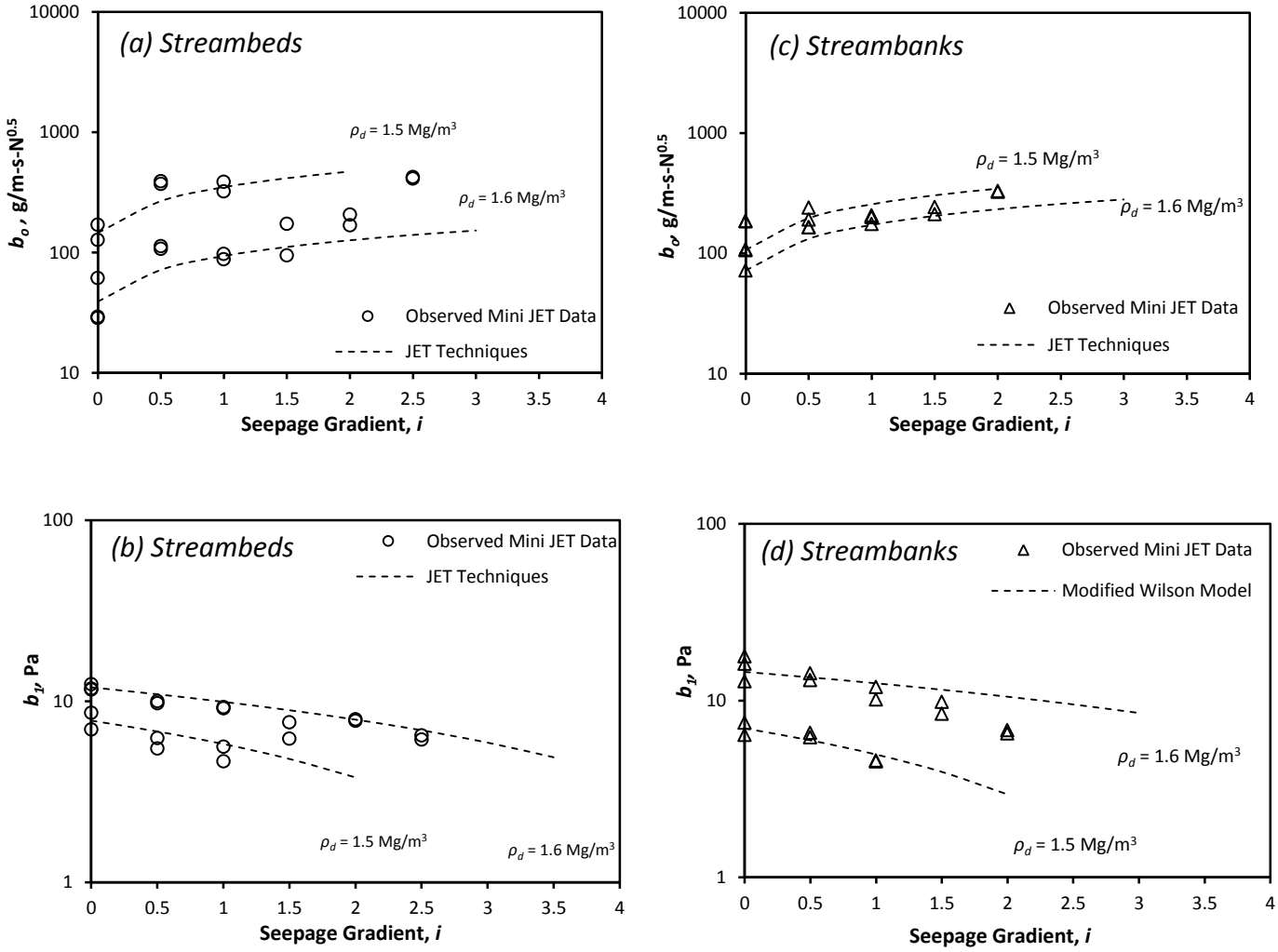

Figure 6.8. Evaluating the ability to predict the "Modified Wilson Model" parameters b_0 and b_1 from derived parameters for without seepage case using data JETs for streambeds and streambanks of the silty sand soil. Symbols represent the deriving parameters from "mini" JET experiments with seepage. Dashed lines represent the predictions of b_0 and b_1 based on the seepage gradient (i).

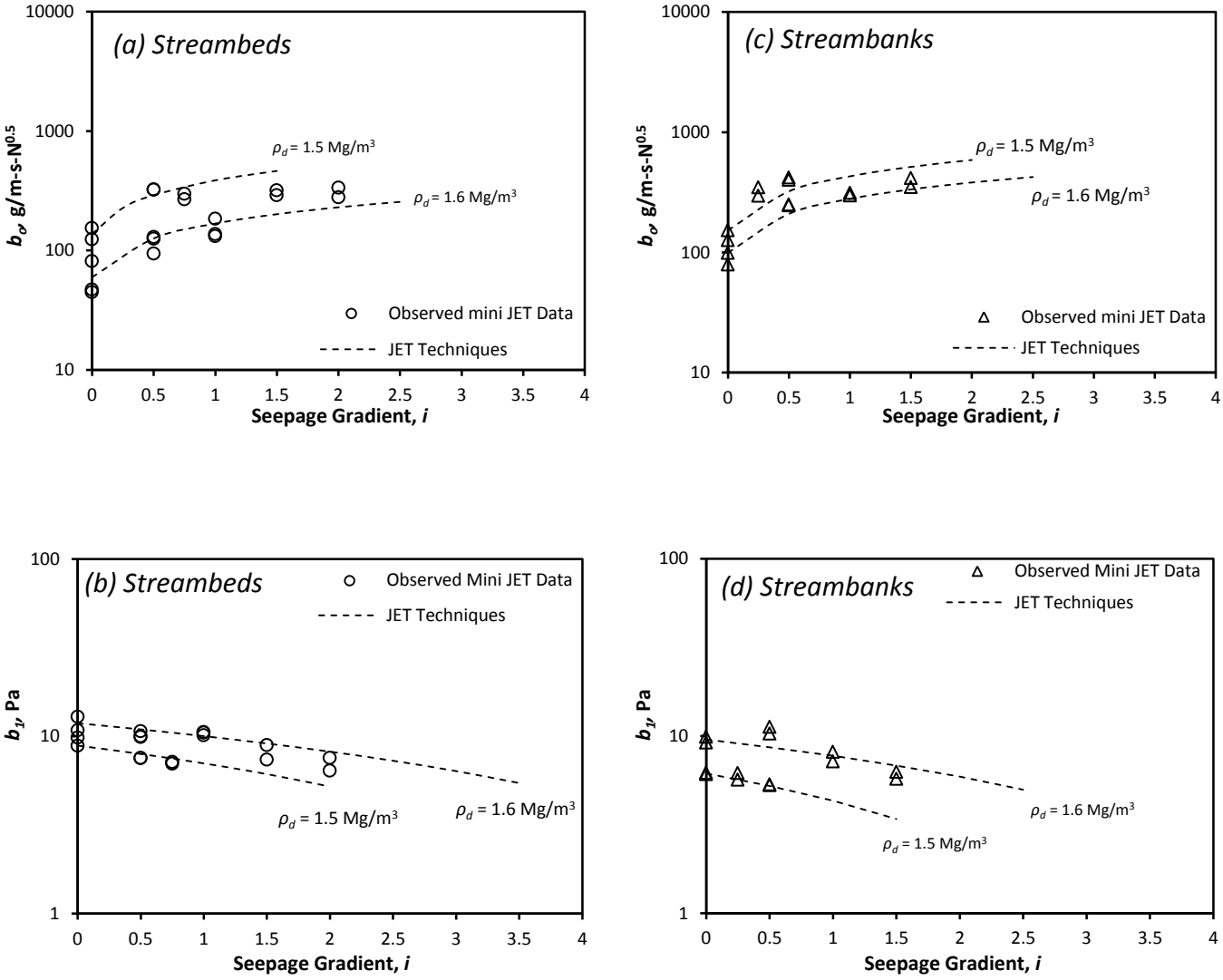

Figure 6.9. Evaluating the ability to predict the "Modified Wilson Model" parameters b_0 and b_1 from derived parameters for without seepage case using data JETs for streambeds and streambanks of the clayey sand soil. Symbols represent the deriving parameters from "mini" JET experiments with seepage. Dashed lines represent the predictions of b_0 and b_1 based on the seepage gradient (*i*).

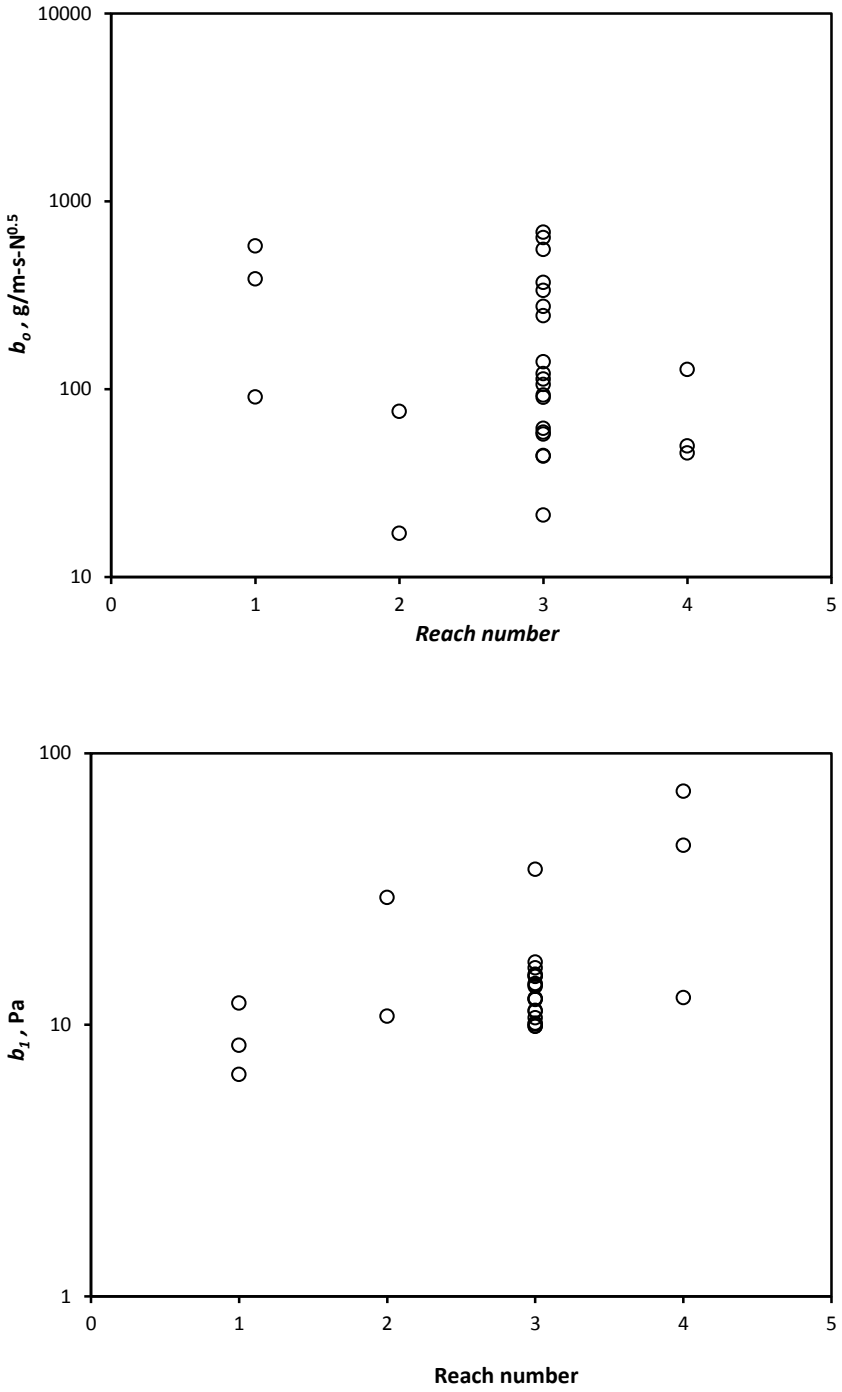

Figure 6.10. Deriving the "Wilson Model" parameters b_o and b_1 from in-situ JETs conducted at four reaches on streambanks of Cow Creek, OK.

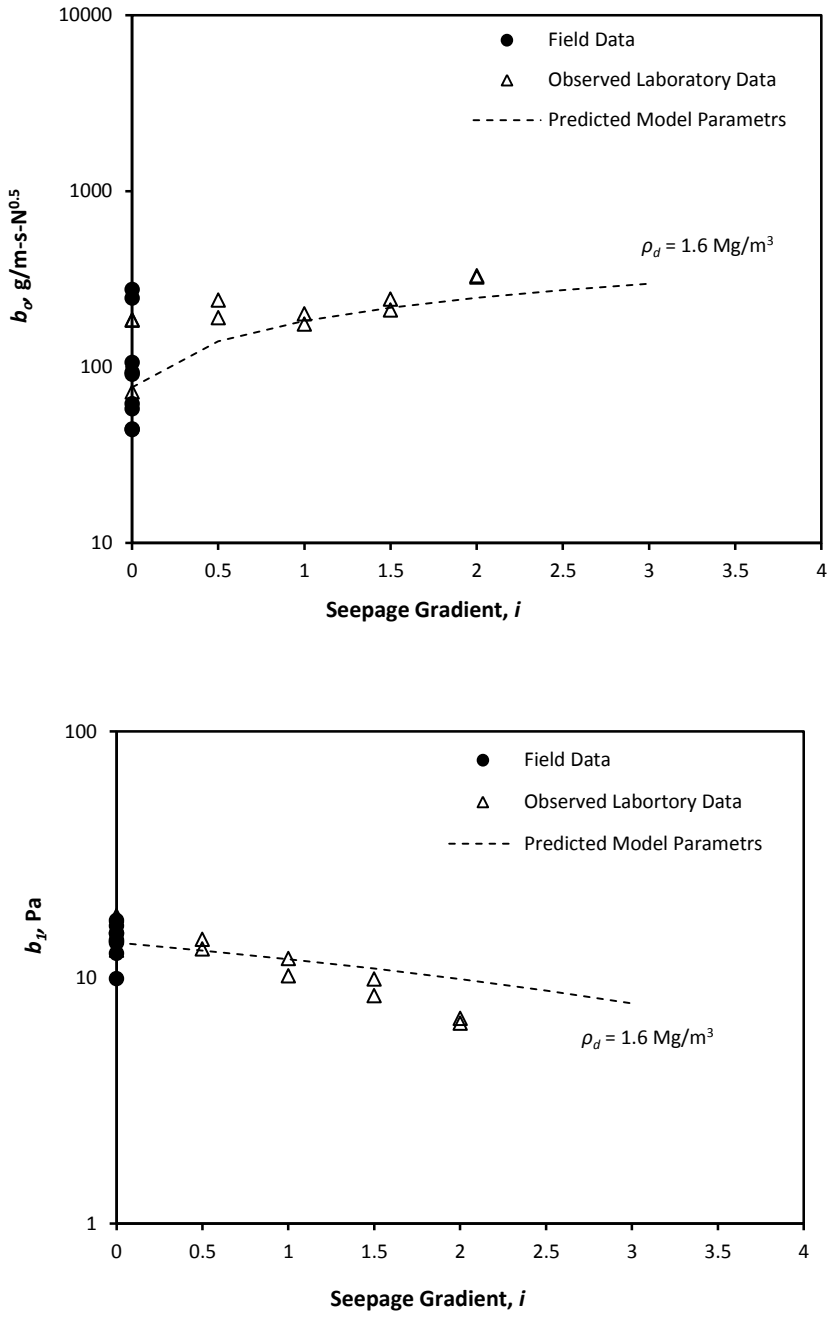

Figure 6.11. Evaluating the ability to predict the "Modified Wilson Model" parameters b_0 and b_1 from derived field parameters using in-situ JETs without seepage for the LR3 of Cow Creek, OK. Triangle symbols represent the deriving parameters from laboratory "mini" JET experiments with seepage on vertical setup. Solid circle symbols represent the deriving parameters from in -situ "mini" JETs on LR3 of Cow Creek for a case without seepage. Dashed lines represent the predictions of b_0 and b_1 from derived field parameters based on the different seepage gradients (i).

6.10. ACKNOWLEDGEMENTS

This research is based upon work supported by the National Science Foundation under Grant No. 0943491. Any opinions, findings, and conclusions or recommendations expressed in this material are those of the authors and do not necessarily reflect the views of the National Science Foundation.

CHAPTER VII

CONCLUSION AND RECOMMENDATIONS

7.1. CONCLUSIONS

The overall objectives of this research were 1) to predict the erodibility of cohesive streambeds and streambanks due to fluvial and seepage forces, and 2) to develop a mechanistic fundamental-based detachment model to predict the soil erodibility due to fluvial and seepage forces using JET techniques. In this study, a more mechanistically based detachment model, the "Wilson Model," was proposed for modeling the erosion rate of soils using the hydraulic analysis of a JET (JET – Jet Erosion Test). Seepage forces were incorporated into a mechanistic fundamental detachment rate model to improve predictions of the erosion rate of cohesive soils using JET techniques. A new miniature version of the JET device ("mini" JET) and flume tests were conducted on the two cohesive soils (silty sand and clayey sand) to derive the model parameters (b_0 and b_1) in order to investigate the influence of seepage on the soil erodibility of streambeds and streambanks. The following conclusions are obtained from this dissertation:

1. The “mini” JET has advantages of being smaller, easier and more convenient to use in many settings, and requires a smaller water supply compare to the larger original JET. The “mini” JET device provided equivalent erosion rate predictions to the laboratory original JET device based on measured the excess shear stress model parameters (k_d and τ_c).
2. A mechanistic erosion model, which is referred to as the “Wilson Model”, was described along with the definition of the velocity distributions and methods of analysis for the material parameters b_0 and b_1 for flume and JET data.
3. The “Wilson Model” predicted the observed data for the two cohesive soils for flume and the JET data as well as or better than the excess shear stress model.
4. The “Wilson Model” parameters b_o and b_1 have similar relationship but different magnitude as the excess shear stress model parameters k_d and τ_c relative to the gravimetric water content of the packed sample.
5. The original and “mini’ JET devices can provide equivalent results to flume experiments for deriving the “Wilson Model” parameters as well as the excess shear model parameters.
6. Seepage forces were incorporated to the new modified detachment model, which is referred to as the “Modified Wilson Model”, based on two modified dimensional soil parameters (b_0 and b_1) that included seepage gradients.
7. The influence of seepage on erosion can be predicted based on JET techniques using the “Modified Wilson Model” parameters with a priori JET experiments without seepage on streambeds or streambanks.
8. The “Wilson Model” or “Modified Wilson Model” is advantageous in being a more mechanistic, fundamentally based erosion equation as compared to the excess shear stress model; the proposed model can be used in the place of the excess shear stress model with

parameters that can be estimated using existing JET techniques; the proposed model can be used to predict and account any additional forces or factors such as turbulence, roughness, seepage forces, material soil orientation (i.e. streambed versus streambank), root effects, negative pore water pressure effects, etc.

7.2. RECOMMENDATIONS FOR FUTURE RESEARCH

Additional research advances are required to verify some parameters and assumptions that are proposed in this study for different soil types. For instance, future research should be conducted using laboratory "mini" and original JET devices to validate the adjustment coefficient of equilibrium depth, C_{je}, proposed in this study for different soil types. Research should be conducted using the "mini" JET with different seepage gradients to obtain relationships with the particle length factor, n_p, and to validate the seepage coefficient ratio value, μ_{sr}, for different soils.

Other research advances include incorporating the "Wilson Model" parameters into a more general streambank erosion and stability model such as the Bank Stability and Toe Erosion Model (BSTEM, Midgley et al., 2012b) to predict the soil erodibility due to fluvial and seepage forces. Research should also be conducted on how to modify the "Wilson Model" parameters to predict soil erodibility due to fluvial forces and other additional forces such as root effects, negative pore water pressure, etc. The impact of assuming a single particle detachment versus aggregate detachment on the model parameters, and the effect of the soil's temperature, soil swelling, and water/soil chemistry on the model parameters b_o and b_1 should also be investigated.

REFERENCES

Al-Madhhachi, A.T., G. J. Hanson, G. A. Fox, A. K. Tyagi, and R. Bulut. 2012a. Measuring erodibility of cohesive soils using laboratory "mini" JET tests. *T. ASABE* (in review).

Al-Madhhachi, A.T., G. J. Hanson, G. A. Fox, A. K. Tyagi, and R. Bulut. 2012b. Deriving parameters of a fundamental detachment model for cohesive soils from flume and jet erosion tests. *T. ASABE* (in review).

Al-Madhhachi, A.T., G. A. Fox, G. J. Hanson, A. K. Tyagi, and R. Bulut. 2013a. Mechanistic detachment rate model to predict soil erodibility due to fluvial and seepage forces: I. model development. *J. Hydraulic Eng., ASCE* (in review).

Al-Madhhachi, A.T., G. A. Fox, G. J. Hanson, A. K. Tyagi, and R. Bulut. 2013b. Mechanistic detachment rate model to predict soil erodibility due to fluvial and seepage forces: II. model evaluation. *J. Hydraulic Eng., ASCE* (in review).

Al-Madhhachi, A. T., G. A. Fox, A. K. Tyagi, G. J. Hanson, and R. Bulut. 2014. Predicting the erodibility of streambanks due to fluvial and seepage Forces. *Geomorphology* (in review).

ASTM. 2006. *Annual Book of ASTM Standards, Section 4: Construction*. Philadelphia, PA, ASTM.

Blaisdell, F. W., L.A. Clayton, and C. G. Hebaus. 1981. Ultimate dimension of local scour. *J. Hydraulics Division, ASCE*, 107(HY3): 327-337.

Briaud, J. L., C. K. Ting, H. C. Chen, S. W. Han, K. W. Kwak. 2001. Erosion function apparatus for scour rate predictions. J. Geotech. and Geoenviron. *Eng. Division, ASCE* 127(2): 105-113.

Bull, L.J. 1997. Magnitude and variation in the contribution of bank erosion to the suspended sediment load of River Severn, UK. *Earth Surf. Proc. Land*, 23(9):773-789.

Chepil, W. S. 1959. Equilibrium of soil grains at threshold of movement by wind. *Soil Science America Proceedings*, 23(6): 422-428.

Chu-Agor, M.L., G.A. Fox, R. Cancienne, and G.V. Wilson. 2008. Seepage caused tension failure and erosion undercutting of hillslopes. *J. Hydrol.* 359:247-259.

Chu-Agor, M.L., G.A. Fox, R. Cancienne, and G.V. Wilson. 2009. Empirical sediment transport function predicting seepage erosion undercutting for cohesive bank failure prediction. *J. Hydrol.* 377:155-164.

Clark, L. A., and T. M. Wynn. 2007. Methods for determining streambank critical shear stress and soil erodibility: implications for erosion rate predictions. *Transactions of the ASAE*, 50(1), 95-106.

Cleaver, J. W., and B. Yates. 1973. Mechanism of detachment of colloidal particles from a flat substrate in a turbulent flow. *J. Colloid Interface Sci.* 44(3): 464-474.

Einstein, H. A. and E. A. El-Samni. 1949. Hydrodynamic forces acting on a rough wall. *Reviews Modern Physics*, 21(3): 520-524.

Einstein, H. A. 1950. *The bed-load function for sediment transport in open channel flows.* SCS Technical Bulletin No. 1026. Washington, DC: USDA.

Evans, D.J., C.E. Gibson, R.S. Rossell. 2006. Sediment loads and sources in heavily modified Irish catchments: a move towards informed management strategies. *Geomorphology*, 79(1/2):93-113.

Fox, G. A., and G. V. Wilson. 2010. The role of subsurface flow in hillslope and streambank erosion: A review. *Soil Sci. Soc. Am. J.* 74(3): 717-733.

Fox, G. A., G. J. Sabbagh, W. Chen, and M. Russell. 2006a. Comparison of uncalibrated Tier II ground water screening models based on conservative tracer and pesticide leaching. *Pest Management Science*, 62(6): 537-550.

Fox, G.A., G.V. Wilson, R. K. Periketi, and , R. F. Cullum. 2006b. Sediment transport model for seepage erosion of streambank sediment. *J. Hydrol. Eng.*, 11(6):603-611.

Fox, G.A., G.V. Wilson, A. Simon, E. J. Langendoen, O. Akay , and J. W. Fuchs. 2007. Measuring streambank erosion due to ground water seepage: correlation to bank pore water pressure, precipitation and stream stage. *Earth Surf. Proc. Land.*, 32:1558-1573.

Freeze, R.A., and Cherry, J.A. (1979). *Groundwater*. Hemel Hempstead: Prentice-Hall International.

Hanson, G. J. 1989. Channel erosion study of two compacted soils. *Transactions of the ASAE*, 32(2), 485-490.

Hanson, G. J. 1990a. Surface erodibility of earthen channels at high stresses. I: Open channels testing. *T. ASAE*, 33(1): 127-131.

Hanson, G. J. 1990b. Surface erodibility of earthen channels at high stresses. II: Developing an in situ testing device. *T. ASAE*, 33(1): 132-137.

Hanson, G. J. 1991. Development of a jet index to characterize erosion resistance of soils in earthen spillways. *Transactions of the ASAE*, 34(5), 2015-2020.

Hanson, G. J. 2001. Field and laboratory jet test testing method for determining cohesive material erodibility. Proc. Of Federal Interagency Sedimentation Conference, Reno, Nevada.

Hanson, G. J., and K. R. Cook. 1997. Development of excess shear stress parameters for circular jet testing. ASAE Paper No. 97 – 2227, ASABE: St. Joseph, MI.

Hanson, G. J., and K. R. Cook. 1999. Procedure to estimate soil erodibility for water management purposes. *ASAE Paper* No. 99 – 2133.

Hanson, G. J., and K. R. Cook. 2004. Apparatus, test procedures, and analytical methods to measure soil erodibility in situ. *Appl. Eng. Agricul.*, 20(4): 455-462.

Hanson, G. J., and S. L. Hunt. 2007. Lessons learned using laboratory jet method to measure soil erodibility of compaction soils. *T. ASABE*, 23(3): 305-312.

Hanson, G. J., and K. M. Robinson. 1993. The influence of soil moisture and compaction on spillway erosion. *T. ASAE*, 36(5): 1349-1352.

Hanson, G. J., K. M. Robinson, and K. R. Cook. 2002a. Scour below an overfall: part II. Prediction. *T. ASAE*, 45(4): 957-964.

Hanson, G. J., and A. Simon. 2001. Erodibility of cohesive streambeds in the loess area of the Midwestern USA. *J. Hydrol. Proc.*, 15(1): 23-38.

Hanson, G. J., K. R. Cook, and A. Simon. 2002b. Non-vertical jet testing of coehsive streambank materials. ASABE Paper No. 022119, ASABE: St. Joseph, MI.

Hanson, G.J., D. M. Temple, S. L. Hunt, and R. D. Tejral. 2011. Development and characterization of soil material parameters for embankment breach. ASABE Applied Engineering in Agriculture, 27(4):1-9.

Hession, W. C., V. O. Shanholtz, S. Mostaghimi, and T. A. Dillaha. 1994. Uncalibrated performance of the finite element storm hydrograph model. *Trans. ASAE*, 37(3): 777-783.

Lambe, T. W. 1962. *Soil Stabilization*. Chap. 4 of Foundation Engineering, G. A. Leonards, Ed., McGraw-Hill, New York.

Lobkovsky, A. E., B. Jensen, A. Kurdrolli, and D. H. Rothman. 2004. Threshold phenomena in erosion driven by subsurface flow. *J. Geophys. Res.*, 109(F4).

Lovern, S. B., and G. A. Fox. 2012. The streambank research facility at Oklahoma State University. *Resource*, 19(2), SP10-SP11.

Mann, H.B., and D. R. Whitney. 1947. On a test of whether one of two random variables is stochastically larger than the other. Annals of Mathematical Statistics, 18, 50-60.

Marot, D., P.L. Regazzoni, and T. Wahl. 2011. An energy based method for providing soil surface erodibility. *J. of Geotech. & Geoenviron. Eng. ASCE,* (posted ahead of print, March 14th, 2011).

Mazurek, K. A. 2010. Erodibility of a cohesive soil using a submerged circular turbulent impinging jet test. 2nd Joint Federal Interagency Conference, Las Vegas, NV, June 27-July 1, 2010.

Midgley, T. L., G. A. Fox, G. V. Wilson, D. M. Heeren, E. J. Langendoen, and A. Simon. 2012a. Streambank erosion and instability induced by seepage: In-situ injection experiments. *J. Hydrol. Eng.* (in press).

Midgley, T., G. A. Fox, D. M. Heeren. 2012b. Evaluation of the Bank Stability and Toe Erosion Model (BSTEM) for predicting lateral streambank retreat on composite streambanks. *Geomorphology* 145-146, 107-114, doi:10.1016/j.geomorph.2011.12.044.

Nearing, M. A. 1991. A probability model of soil detachment by shallow turbulent flow. *Trans. ASAE* 34: 81-85.

Osman, A. M. and C. R. Thorne. 1988. Riverbank stability analysis: I. Theory. *J. Hydraulic Eng.*, 114(2): 134-150.

Owoputi, L. O. and W. J. Stolte. 2001. The role of seepage in erodibility. *Hydrology Processes*, 15, 13-22.

Parchure, T. M. and A. J. Mehta. 1985. Erosion of soft cohesive sediment deposits. *J. Hydraulic Eng., ASCE* 111(10): 1308-1326.

Partheniades, E. 1965. Erosion and deposition of cohesive soils. *J. Hydraulics Div. ASCE*, 91(HY1): 105-139.

Pennell, K. D., A. G. Hornsby, R. E. Jessup, and P. S. C. Rao. 1990. Evaluation of five simulation models for predicting aldicarb and bromide behavior under field conditions. *Water Resour. Res.*, 26(11): 2679-2693.

Poreh, M. and J. E. Cermak. 1959. Flow characteristics of a circular submerged jet impinging normally on a smooth boundary. Proceeding of the Sixth Midwestern Conference on Fluid Mechanics, University of Texas, Austin, Tex., 198-212.

Poreh, M., Tsuel, Y. G., and J. E. Cermak. 1967. Investigation of a turbulent radial wall jet. *J. Appl. Mech.*, 34(2):457-463.

Rajaratnam, N. 1976. *Turbulent Jets*. Amsterdam; New York: Elsevier Scientific Pub. Co.

Regazzoni, P. L., G. J. Hanson, T. Wahl, D. Marot, and J. R. Courivaud. 2008. The influence of some engineering parameters on the erosion of soils. Fourth International Conference on Scour and Erosion (ICSE-4), Tokyo, Japan, November 5-7, 2008.

Rockwell, D. L. 2002. The influence of groundwater on surface flow erosion processes. *Earth Surf. Processes Landforms,* 27(5), 495-514.

Sanford, L. and J. P. Y. Maa. 2001. A unified erosion formulation for fine sediments. *Mar. Geol.*, 179(1-2): 9-23.

Schlichting, H. 1979. *Boundary-layer theory*. New York: McGraw-Hill Book Company.

Sharif, A. R. and J. F. Atkinson. 2012. Model for surface erosion of cohesive soils. *J. Hydraulic Eng., ASCE*, 138(7): 581- 590.

Shugar, D., R. Kostaschuk, P. Ashmore, J. Desloges, and L. Burge. 2007. In situ jet-testing of the erosional resistance of cohesive streambeds. *J. of Civil Engineering*, Canada, Vol. 34, 1192-1195.

Simon, A., R. E. Thomas, and L. Klimetz. 2010. Comparison and experiences with field techniques to measure critical shear stress and erodibility of cohesive deposits. 2nd Joint Federal Interagency Conference, Las Vegas, NV, June 27 - July 1, 2010.

Simon, A. and S.E. Darby. 1999. *The nature and significance of incised river channels*. Incised river channels: Processes, forms, engineering and management, S. E. Darby and A. Simon, eds, Wiley, New York.

Simons, D. B. and F. Senturk. 1977. Sediment transport technology. Fort Collins, CO: Water Resources Publications.

Stein, O. R., and D. D. Nett. 1997. Impinging jet calibration of excess shear sediment detachment parameters. *T. ASAE*, 40(6): 1573-1580.

Temple, D. M. 1980. Tractive force design of vegetated channels. *Transactions of the ASAE*, 23(4):884-890.

Temple, D. M., K. M. Robinson, R. M. Ahring, and A. G. Davis. 1987. *Stability design of grass-lined open channels*. USDA, Agricultural Handbook, No. 667:167, Washington, D. C.

Thoman, R. W. and S. L. Niezgoda. 2008. Determining Erodibility, critical shear stress, and allowable discharge estimates for cohesive channels: case study in the Powder River Basin of Wyoming. *J. of Hydraulic Eng., ASCE,* 134(12), 1677-1687.

Wan, C. F., and R. Fell. 2004. Investigation of rate of erosion of soils in embankment dams. *J. Geotech. & Geoenviron. Eng.*, 130(4):373-380.

Weidner, K., J. Petrie, P. Diplas, S. Nam, M. Gutierrez, and M. Ellenberg. 2012. Numerical Simulation of Jet Test and Associated Soil Erosion. *ICSE6*, Paris.

Wilson, B. N. 1993a. Development of a fundamental based detachment model. *Transaction of ASAE*, 36(4): 1105-1114.

Wilson, B. N. 1993b. Evaluation of a fundamental based detachment model. *Transaction of ASAE*, 36(4): 1115-1122.

Wilson, G.V., R. Periketi, G.A. Fox, S. Dabney, D. Shields, and R.F. Cullum. 2007. Seepage erosion properties contributing to streambank failure. *Earth Surf. Proc. Land.*, 32(3):447-459.

Wynn, T. M., and S. Mostaghimi. 2006. The effects of vegetation and soil type on Streambank erosion, Southwestern Virginia, USA. *Journal of the American Water Resources Association*, 42, 69-82.

Wynn, T. M., M. B. Henderson, and D. H. Vaughan. 2008. Changes in streambank erodibility and critical shear stress due to subaeriel processes along a headwater stream, southwest Virginia, USA. *Geomorphology*, 97(1), 69-82.

Yang, C. T. 1973. Incipient motion and sediment transport. *Proc. ASCE, J. of Hydraulic Division*, 99(HY10): 1805-1826.

VITA

Abdul-Sahib Taufeeq Al-Madhhachi

Candidate for the Degree of

Doctor of Philosophy

Thesis: PREDICTING ERODIBILITY OF COHESIVE STREAMBEDS AND STREAMBANKS DUE TO FLUVIAL AND SEEPAGE FORCES

Major Field: Civil and Environmental Engineering

Biographical:

Education:

Completed the requirements for the Doctor of Philosophy in Civil and Environmental Engineering at Oklahoma State University, Stillwater, Oklahoma in December, 2012.

Completed the requirements for the Master of Science in Water Resources Engineering at Baghdad University, Baghdad, Iraq in 1999.

Completed the requirements for the Master of Science in Water Resources Engineering at Baghdad University, Baghdad, Iraq in 1996.

Experience:

2008 – 2012: Graduate Research Assistant, Oklahoma State University
2003 – 2007: Engineer Consult and Designer, Survey several surveying projects and design Four Small Dams, Northern Iraq and Baghdad, Iraq
2000 – 2007: Instructor (Faculty member), Environmental Engineering, Al-Mustansiriya University, Baghdad, Iraq (Teaching Hydraulic and Mathematics Courses)
1999 – 2007: Hydraulic Laboratory Supervisor, Al-Mustansiriya University, Baghdad, Iraq
1996 – 1999: Graduate Research Assistant, Baghdad University, Baghdad, Iraq

Professional Memberships:

American Society of Civil Engineers
American Society of Agricultural and Biological Engineers
The Honor Society of Phi Kappa Phi